The Dissertation Committee for Nicholas Alexander Maskalenko certifies that this is the approved version of the following dissertation:

The Role of DISC1 in the Organization of the T-Cell Immunological Synapse

Committee:

Martin Poenie, Supervisor

Arturo De Lozanne

Clarence S Chan

Ning Jiang

Haley O Tucker

Lauren I Ehrlich

The Role of DISC1 in the Organization of the T-Cell Immunological Synapse

by

Nicholas Alexander Maskalenko

Dissertation

Presented to the Faculty of the Graduate School of

The University of Texas at Austin

in Partial Fulfillment

of the Requirements

for the Degree of

Doctor of Philosophy

The University of Texas at Austin

August 2019

Dedication

I would like to dedicate this dissertation to my wife Jessica, our family, and our friends. No man that stands alone stands for long, and I owe everything to those who have helped me walk this road through held hands or locked arms.

Acknowledgements

This work would not be what it is without the mentorship of Dr. Martin Poenie. I have been lucky to learn from his vast knowledge and experience, as well as benefit from his support and thoughtfulness. I would also like to thank my committee members, Drs. Clarence Chang, Arturo De Lozanne, Lauren Ehrlich, Jenny Jiang, and Haley Tucker for their guidance. I would especially like to thank Dr. Jessica Lancaster from the Ehrlich lab for providing me mouse cells and troubleshooting advice. I would also like to thank Dr. Yuri Sykulev from Thomas Jefferson University, for time and resources spent in his lab, as well as for his insight. In addition, I would like to thank Drs. Nadezhda Anikeyeva and Maria Steblyanko for their time and experience in the preparation of lipid bilayers and microscopy. Special thanks go to Dr. Shubhankar Nath, who laid the foundations for this work and helped me in my nascent years in the Poenie lab, as well as Dr. Jeffery Kuhn, as his guidance was sought throughout this project. I want to also thank many of my undergraduates, Robin, Adarsh, Jiayu, and Marcheta for their help in my experiments. I would like to also thank Dr. Jennifer Moon for resources and time exchanged with her Cell Biology classroom during the duration of the project. Finally, I would like to acknowledge Richard Salinas at the core facility for helping me sort all of my fluorescent cell lines, and Anna Webb for helping me with confocal imaging.

Abstract

The Role of DISC1 in the Organization of the T-Cell Immunological Synapse

Nicholas Alexander Maskalenko, Ph.D.

The University of Texas at Austin, 2019

Supervisor: Martin Poenie

When T-cells contact an antigenic target or antigen-presenting cell, signaling through the T-cell receptor triggers formation of a specialized junction known as the immunological synapse (IS). In a previous study, DISC1 (Disrupted in Schizophrenia 1) was identified as a component of the IS in T-cells, where it forms a complex with dynein, Nde1, and Lis1. Here we show that there are two isoforms of DISC1 expressed in T-cells, one (DISC1 Lv) that colocalizes with mitochondria and the other (DISC1 L) that accumulates at the IS. The accumulation of DISC1 at the IS is also observed in OT-1 CTLs and NK cells.

Additionally, we show that disrupting DISC1 using CRISPR/Cas9 technology leads to many changes at the synapse. Each isoform upon reintroduction restores specific changes. The translocation of mitochondria was dependent on the Lv isoform. Loss of the L isoform results in a defect in MTOC translocation, failure of Nde1 to move from the center of the IS to the pSMAC, and greatly reduced actin accumulation at the IS. This last effect depends on the association of DISC1 with Girdin, such that loss of expression of

either protein gives the same phenotype. Girdin is involved in cytoskeletal remodeling in other cells but its function in T cells has not been previously described.

The results of this work contribute to the understanding of MTOC translocation and mitochondrial movements, but they also generate new questions about the role and regulation of actin at the synapse. The loss of actin in Girdin or DISC1 deletions does not have a severe effect on MTOC translocation as is seen in cells treated with actin inhibitors. However, these treatments lead to a complete loss of Nde1, Lis1, and dynein from the synapse, suggesting that the dynein complex is ultimately linked to actin. These results point to DISC1 and Girdin functioning in a novel actin signaling pathway working at the IS.

Table of Contents

List of Tables

List of Figures

Chapter 1: Introduction

The ability for an organism to trigger a defense against pathogens, parasites, and toxins is one of the most fundamental functions of life. While host defense mechanisms exist even in prokaryotes such as the CRISPR/Cas9 system (Marraffini, 2015), and many basic mechanisms to immune response are shared among both vertebrates and invertebrates (Litman & Cooper, 2007), jawed vertebrates have developed a diverse combinatory immune system that consists of specialized cells dedicated to the task. In humans, the immune system can be roughly divided into two broad categories: the innate and adaptive immune response. The innate immune system is made up of cells such as macrophages, neutrophils, and dendritic cells that recognize and respond to pathogens through broad patterned recognition of features common to invaders, such as the bacterial endotoxin lipopolysaccharide (LPS). Conversely, the adaptive immune system's humoral and cell-mediated responses are more specific in the recognition of pathogens, abnormalities, and foreign molecules. In the humoral immune response, B lymphocytes (B-cells) produce antibodies that are secreted into the blood. Cell-mediated immunity is characterized by T lymphocytes (T-cells) that interact with antigens bound to Class I or Class II Major Histocompatibility Complex (MHC) molecules. The immune system is adaptive insofar as antibody or T-cell receptors (TcR) are generated by a combinatory mechanism (VDJ recombination) that creates a huge complement of diverse binding sites that are then selected for their binding to an antigen.

For B-cells to amplify and secrete antibodies, the antigen must first bind to an antibody (the B-cell receptor complex; BCR) displayed on the surface of a naïve B-cell. The signaling pathways generated through this process trigger B-cells to proliferate and differentiate into memory cells and plasma cells that secrete antibody. T-cells are activated

by binding to antigens attached to the MHC proteins on the surface of target cells. Of the two classes of MHC, class I is expressed by all nucleated cells, and class II is displayed on the surface of professional Antigen Presenting Cells (APCs). MHC I displays internal peptides derived from infectious agents such as viruses and are recognized by cytotoxic T-cells. MHC II displays peptides from extracellular antigens that have been internalized and processed for recognition by helper T-cells.

There are two major subsets of T-cells: CD4+ and CD8+ (Golubovskaya & Lu, 2016). Both T-cell types express TcR and become activated through the binding of TcR to an antigen presented on the surface of a target cell. Additionally, both T-cell subsets can differentiate into effector or memory T-cells. Effector T-cells can migrate into peripheral tissues and carry out immune functions through TcR-mediated binding to targets. Memory T-cells are functionally quiescent until re-exposed to an activating antigen, at which point they can rapidly proliferate.

The T-cell subsets are distinguished from each other through the expression of different co-receptors (CD4, CD8) in addition to the TcR. These coreceptors trigger different internal signaling molecules that lead to different effector functions. The CD8+ cells that recognize peptide-MHC I are cytotoxic T-cells (CTLs) that kill virally infected or dysfunctional target cells. They do this by either secreting cytotoxins, including perforin and granzymes stored in secretory lysosomes, or by activating the Fas death receptor on the target cell surface and subsequent triggering of the extrinsic pathway of apoptosis.

The CD4+ cells include helper (TH) and regulatory T-cells (T-reg), both of which recognize peptide-MHC II. TH cells signal to other parts of the immune system by helping co-activate other types of T-cells, stimulating B cells into making and secreting antibodies, and mediating the activity of cells of the innate immune system. T-regs function to suppress the immune response by secreting cytokines that downregulate other immune cells.

SIGNALING IN T-CELLS

Engagement of TcR with peptide-MHC triggers a signaling cascade that leads to T-cell activation. TcR binding recruits the Src family kinases Lck and Fyn (Courtney et al., 2018). These kinases phosphorylate Immune Receptor Tyrosine-based Activation Motifs (ITAMs) of the CD3 and ξ chain of the TcR complex. This leads to the recruitment of the tyrosine kinase ZAP70 and phosphorylation of LAT. Phospho-tyrosines on LAT (phospho-LAT) then recruit the multimolecular proximal signaling complex (PSC) around the TcR. Several different pathways are triggered as a result of the formation of PSC, including three transcription factors involved in T-cell activation; Activating Protein 1 (AP-1), Nuclear Factor for Activation of T-cells (NFAT), and Nuclear Factor Kappa B (NFκB) (Figure 1.1).

The G protein Ras becomes activated by the recruitment of its Guanine Nucleotide Exchange Factor (GEF) SoS to phospho-LAT (Courtney et al., 2018). Ras activation triggers the MAPK pathway, which promotes the formation of AP-1. Additionally, phospho-LAT binds to SLP76 and recruits Phospholipase C γ (PLCγ) to the membrane. PLCγ cleaves membrane phospholipids into IP3, which is an activator of CRAC calcium channels. Calcium influx into the cell triggers the calcium-dependent activation and nuclear translocation of NFAT. Finally, phospholipid cleavage by PLCγ leads to the accumulation of diacyl-glycerol around the PSC, which recruits Protein Kinase C θ (PKCθ). PKCθ phosphorylates and activates NFκB (Brownlie and Zamoyska, 2013). Activation of all three of these transcription factors leads to the increased expression of genes for cytokine production and T-cell proliferation.

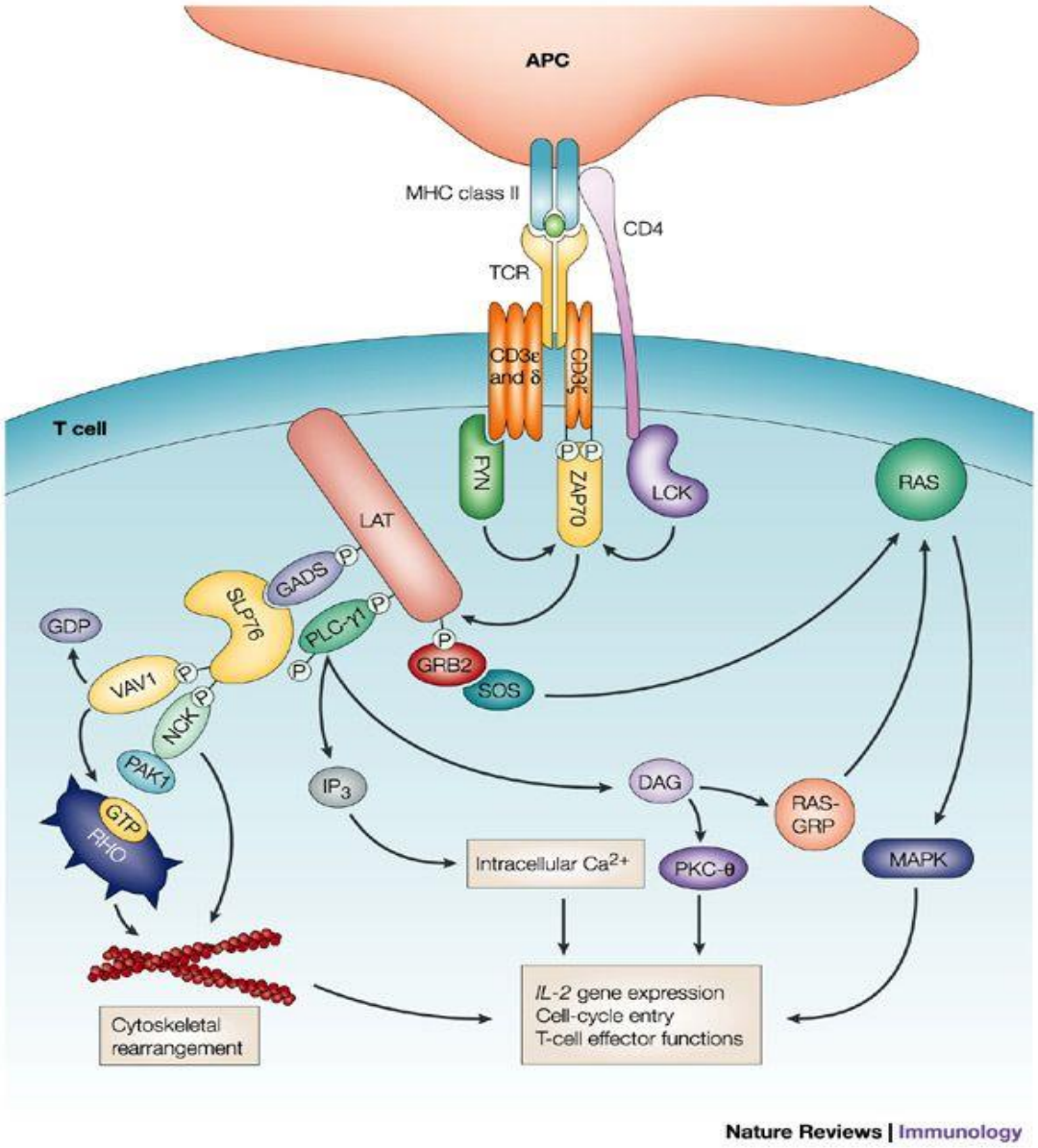

Figure 1.1: Signaling in T-cells

An illustration outlining a summary of TcR signaling is presented. Following TcR engagement with MHC-peptide, Lck and Fyn activate the kinase ZAP70. LAT is phosphorylated by ZAP70, and several SH2-containing proteins are subsequently recruited. PLCγ cleaves phosphoinositide PIP2 into IP3 and DAG, increasing intracellular Ca^{2+} as well as activating PKCθ and Ras. These factors promote activation and gene expression leading to proliferation and interleukin production. SLP76 recruits Vav and other actin signaling factors, which activate several actin-effectors needed for IS signaling and increased T-cell motility, including RhoA, Cdc42, and Rac-1 (Adapted from Abraham, 2004) (Abraham & Weissen, 2004).

CELL SURFACE RECEPTORS AND THE IMMUNOLOGICAL SYNAPSE

When T-cells contact antigenic targets or antigen presenting cells, they form a specialized signaling junction known as the immunological synapse (IS). Early IS formation on the T-cell involves activation and subsequent clustering of TcR on the cell surface. Initially, TcR is often associated with patches of ordered membrane domains known as lipid rafts. Rafts are thicker sections of membrane with high concentrations of sphingolipids, cholesterol, and a unique assortment of embedded and anchored proteins including glycosylphosphotidylinositol-linked (GPI-linked) proteins. Previous research has demonstrated that lipid rafts contain TcR prior to T-cell activation and become aggregated into microcluster domains upon TcR signaling (Dinic et al., 2015).

IS formation is further organized through zones of heavy receptor concentration on the cell surface known as Supramolecular Activation Clusters (SMACs). In the classic IS, three different SMACs are arranged in concentric rings that form a "bullseye" pattern at the contact site. These are the central SMAC or cSMAC, the peripheral SMAC or pSMAC and the distal SMAC, or dSMAC. Alternative arrangements of synapse formation have been observed, including multifocal synapses. These have been seen in synapses formed between T-cells and dendritic cells, and specifically in TH2 CD4+ cells (Dustin et al., 2014).

Each SMAC of the IS appears to be composed of unique proteins and are distinct in function. The cSMAC consists of high concentrations of the TcR complex, CD4/8, CD28, and PKCθ (Monks et al., 2015; Dustin, 2014). T-cell activation requires both TcR signaling and CD28 co-stimulation. After initial contact, TcR signaling rapidly recruits CTLA4 to the cSMAC from exocytic vesicles, which outcompetes CD28 for its ligand (Bour-Jordan et al., 2011). This binding stabilizes CTLA4 at the synapse, which inhibits signaling by controlling phosphorylation of the TcR and disrupting the MAPK pathway.

CD28 and CTLA4 are also important in positive and negative control of attachment between a T-cell and its cognate target cell. This is seen when CD28 antagonists break contact between T-cells and target cells, which can be restored with addition of CTLA4 antagonist (Dilek et al., 2013).

The pSMAC consists mostly of adhesion receptors such as the integrin Lymphocyte Function-Associated Antigen 1 (LFA-1) and Talin, which links LFA-1 to the actin cytoskeleton (Monks et al., 2015). At the beginning of synapse formation, LFA-1 forms the central region of the synapse but is displaced as TcR begins clustering at the cSMAC (Dustin, 2008). LFA-1 also plays a primary role in creating prolonged T-cell contacts with target cells. LFA-1 deficient CD4+ and CD8+ T-cells both exhibit defects in priming and effector functions, respectively (Hogg et al., 2011). Intermediate affinity binding of LFA-1 to its target ligand keeps the two cells in close proximity during initial contact. Through generation of the IS and the linkage of Talin to actin, LFA-1 undergoes a conformational change that converts it to a high affinity receptor (Comrie et al., 2015; Schürpf et al., 2011). High affinity LFA-1 is dense at the border between the pSMAC and cSMAC, where it forms a "gasket" seal between the T-cell and its target (Hammer, Wang, Saeed, & Pedrosa, 2018). This creates an isolate "diffusion zone" at the extracellular side of the cSMAC, where exocytic signals and cytolytic factors can be efficiently diffused to the target cell.

The dSMAC consists primarily of CD45 and microclusters of TcR (Dustin, 2014). Immunofluorescence live imaging shows that in T-cells attached to planar bilayers covered in MHCp, TcR microclusters are the first contact points where MHCp is bound (Alarcón et al., 2011). Through the dynamic cycling of receptors in the pSMAC and dSMAC, these TcR microclusters are moved to the center of the synapse where the cSMAC is formed.

ACTIN SIGNALING IN IMMUNOLOGICAL SYNAPSE FORMATION

The clustering of receptors into a mature immunological synapse necessitates a dynamic rearrangement of cytoskeletal components. The dynamics of actin at the IS can be summarized as a leading edge pushing out radially while old actin filaments are pulled inwards to be broken down and recycled (Kumari et al., 2018). These dynamics are carried out across three separate actin signaling zones, which each have their own independent effectors. A summary of how these zones are arranged is given in Figure 1.2.

Actin foci dependent on actin related proteins 2 and 3 (Arp2/3) form within the pSMAC and dSMAC. These generate a dense lamellipodia of branched actin filaments that extend across the dSMAC (Hivroz & Saitakis, 2016). Formins are actived at the dSMAC/pSMAC border and form concentric arcs of straight actin filaments that are pulled inwards towards the cSMAC through the contractile force of myosin (Murugesan et al., 2016). The flow of the actin network and the force of traction has been shown to organize LFA-1 at the pSMAC while facilitating the high-affinity conformation of LFA-1 (Comrie et al., 2015). TcR microclusters translocate from the dSMAC to the cSMAC by connecting to this actin flow, forming denser clusters of TcR as they move inwards (Yuanqing et al., 2017). The actin flow is then abruptly broken down at the pSMAC/cSMAC border (Yi, Wu, Crites, & Hammer, 2012). Beyond this border, the cSMAC is a loose "hypodense" network of actin (Hammer, Wang, Saeed, & Pedrosa, 2018). While initial TcR engagement triggers a filipodia-like protrusion at the center of the nascent synapse, the cSMAC is cleared of actin in the mature IS. This actin clearance is important in establishing the cSMAC as a zone for secretion (Carisey et al., 2018; Ritter et al., 2017).

Inhibiting actin dynamics at the immunological synapse through actin inhibitors has been shown to affect the ability of a T-cell to spread across the bound target cell (Jankowska & Burkhardt, 2018). Treatment with Latrunculin, an actin inhibitor which

binds to actin monomers and prevents F-actin polymerization, has been shown to eliminate actin from the IS (Comrie et al., 2015). Cytochalasin, which inhibits actin polymerization by binding to the fast-growing plus ends of actin, was shown to not completely disrupt actin at the IS, but instead broke up actin at the synapse up into a series of disordered patches. Neither drug was shown to affect TcR localization (tracked with a tagged MHC) but did inhibit the tight ring formation of LFA-1 (tracked with a tagged LFA-1 ligand, ICAM-1).

There are several different Guanine Nucleotide Exchange Factors (GEFs) involved in actin polymerization that are recruited to the synapse following initial TcR signaling: Vav1, Dock 2/8, and SLAT. Phospho-LAT brings SLP76 to the PSC, which in turn recruits Vav1 to the synapse. Vav1 has scaffolding function, and has been shown to interact with PLCγ, facilitating Ca^{2+} influx (Braiman et al., 2006). Additionally, Vav1 activates Rho family GTPases Cdc42 and Rac-1, which are both effectors for actin polymerization. SLAT is also an activator of Cdc42 and Rac-1 (Feau et al., 2013), and becomes recruited to the PSC when SLAT is phosphorylated by Lck (Bécart and Altman, 2009). Dock 2 is specifically a Rac-1 activator and becomes recruited to the synapse through a member of the ELMO family (Harada et al., 2012). Disruption of Dock 2 has been shown to interfere with accumulation of TcR and lipid rafts (Sanui et al., 2003). Dock 8 on the other hand is specifically a Cdc42 activator (Harada et al., 2012). Disruption of Dock 8 has been shown to interfere with LFA-1 polarization at the synapse (Randall et al., 2011).

Cdc42 and Rac-1 both promote F-actin polymerization by inducing actin nucleation through activation of Wiskott-Aldrich syndrome protein family members WASp and WAVE2, followed by subsequent activation of Arp2/3 (Kumari et al., 2015). Silencing either Arp 2 or Arp 3 directly interferes with the accumulation of actin at the IS (Gomez et al., 2007). Disrupting WAVE2 leads to a near complete depletion of actin at the dSMAC,

which induces defects in calcium signaling, adhesion, and T-cell spreading across targets (Jankowska et al., 2018; Nolz et al., 2006; Nolz et al., 2007). Disruption of WASp comparatively results in few morphological changes in the actin architecture but induces defects in synapse stability that has led to the idea that WASp repairs and maintains the dSMAC (Kumari, Curado, Mayya, & Dustin, 2014; Kumari et al., 2015; Sims et al., 2007). Interestingly, the initial formation of filipodia at the cSMAC still occurs independent of Arp 2/3 or Formin silencing, suggesting that other actin nucleators are present (Gomez et al., 2007).

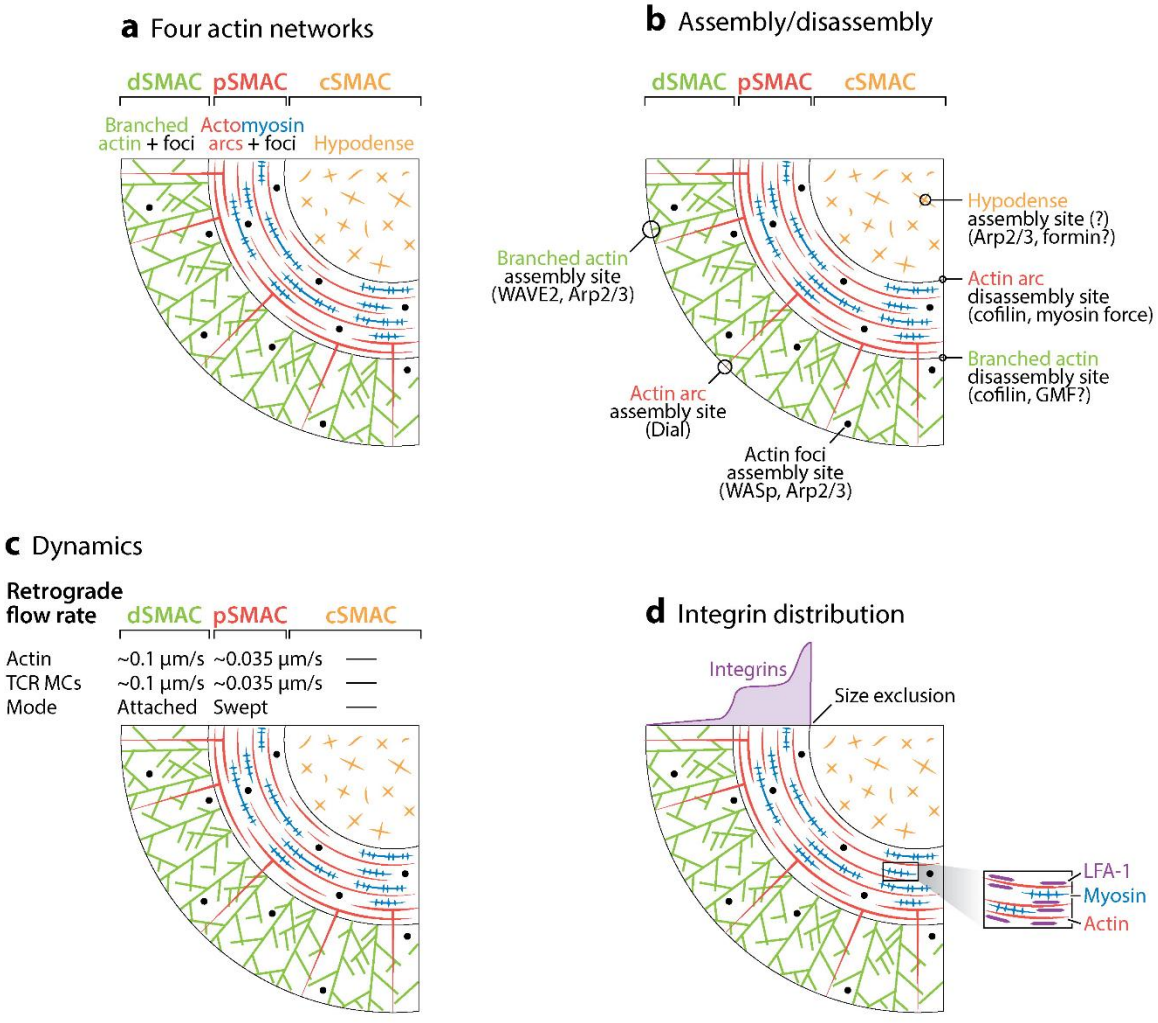

Figure 1.2: Actin Morphology at the Immunological Synapse

Actin at the synapse is a complex network divided into several distinct zones. **(A)** In a mature synapse the cSMAC is mostly barren of actin and is described as “hypodense”. It is surrounded by rings of concentric arcs of straight filaments that form the pSMAC. Beyond that, the dSMAC is rich in branched actin chains. **(B-C)** The dSMAC extends out as a lamellipodia while the actin arcs of the pSMAC are pulled by myosin to the pSMAC/cSMAC boundary where they are disassembled. **(D)** The integrin LFA-1 is most heavily concentrated at this pSMAC/cSMAC boundary. (Adapted from Hammer, 2018) (Hammer, Wang, Saeed, & Pedrosa, 2018).

MOLECULAR MOTORS AND THE MICROTUBULE ORGANIZING CENTER

IS formation is accompanied by the translocation of internal cellular elements such as mitochondria, the Golgi apparatus, and secretory granules required for effector function. This trafficking of organelles and vesicles takes place on microtubules and is carried out through the molecular motors kinesin and dynein, as well as their associated adapter proteins.

The typical kinesin motor (eg, Kinesin 2) is a complex made up of two heavy chains and two light chains, although there are many different variants within the kinesin superfamily (Hirokawa et al., 2010). Dynein is a multimeric protein made up of two heavy chains, two intermediate chains, and several light and intermediate-light chains. Both motor proteins utilize ATP hydrolysis to cycle through binding and unbinding with microtubules in order to move towards a polar end. Both are mechanically different, as kinesin is thought to "walk" across the microtubule in processive steps while dynein makes short "hops." Cargo can be attached to either motor protein through a complex of one or more adapter proteins, enabling intracellular transport along microtubules. Classically, kinesins are involved in anterograde (plus end) directed traffic across microtubules, while dynein is involved in retrograde (minus end) directed traffic.

Central to molecular trafficking within the cell is the Microtubule Organizing Center (MTOC), which creates a "hub" for all the microtubule minus ends within the cell. The directionality of transport along motors is therefore set by the MTOC, with dynein moving towards the MTOC and kinesin moving away from it. During T-cell activation, the MTOC is translocated to the IS where it oscillates within the bounds of the cSMAC (Kuhn & Poenie, 2002). As the MTOC moves towards the synapse, secretory vesicles move towards the MTOC (Martín-Cófreces et al., 2014). This allows for localized secretion to occur directly between a T-cell and the target cell.

While the exact mechanisms by which MTOC translocates toward the synapse is still not fully understood, two primary models have been proposed. In the first model, MTOC translocation is reliant on actin at the synapse. This hypothesis suggests that microtubules are connected to actin early on in IS formation. The MTOC is then pulled to the synapse when actin at the cSMAC of the nascent synapse is reorganized into a ring as the IS matures. Stinchcombe et al. (2006) and Banerjee et al. (2007) have previously suggested that Cdc42 plays a central role in anchoring microtubules to F-actin accumulated at the synapse. Combined with studies that showed Cdc42 depletion had a minimum effect on MTOC translocation (Tskvitaria-Fuller et al., 2006), Gomez et al. (2007) questioned whether the role Cdc42 had on MTOC translocation was a pleiotropic effect unrelated to the actin model. They showed instead that Formins were necessary. It should be noted that Formins play a role in acetylating microtubules, stabilizing them (Thurston et al., 2012). The necessity of Formins in MTOC translocation may not therefore be in promoting actin polymerization but rather by acetylating microtubules.

The second model of MTOC translocation proposes that dynein is the linker that connects microtubules to the pSMAC. Further, as anchored dynein tries to move towards the minus end of the microtubule, it pulls the MTOC up to the synapse (Nath et al, 2016). Supporting this model, dynein has been shown to accumulate at the synapse in T-cells (Combs et al., 2006). Studies in our lab by Laura Christian have shown that sequestering dynein through molecular traps blocks MTOC translocation. Further studies by Shubhanker Nath have shown that the dynein adapter proteins Neurodevelopment Protein 1 (Nde1) and Lissencephaly 1 (Lis1) link dynein to the synapse. Knockdown of Nde1 leads to a complete block of MTOC translocation (Nath et al., 2016). Secretion at the IS is also inhibited, reducing CTL-mediated target cell lysis by ~80%. It is therefore clear that dynein

plays a central role in MTOC translocation, although the role that actin may play still needs to be resolved.

SIMILARITIES BETWEEN NEURO AND IMMUNE SYNAPSES

Both neurons and immune cells form specialized signaling interfaces with other cells, also known as a synapse. The term immunological synapse was originally coined by Michael Norcross due to its likeness in morphology and function to the neuronal synapse (Norcross, 1984). To highlight this, Michael Dustin outlined four characteristics of the neuronal synapse that are also true of the IS (Dustin & Colman, 2002). In both synapses, cells remain physically separated by a fluid filled space known as the synaptic cleft (Papa & Vinuesa, 2018), adhesion molecules like integrin regulate target connections (Lilja & Ivaska, 2018; Urlaub, Höfer, Müller, & Watzl, 2017), signals regulate positional stability of the pre- and post- synaptic zones (Dustin, Bromley, Kan, Peterson, & Unanue, 1997), and areas of the synapse serve as a target for directed secretion (Britt, Farías, Guardia, & Bonifacino, 2016; Martín-Cófreces, Baixauli, & Sánchez-Madrid, 2014).

Originally the IS was only described in terms of being a "functional analogy" to neuronal synapses, but it was noted that both synapses shared some proteins such as the murine Thy-1 (Haeryfar & Hoskin, 2004; Norcross, 1984). With time, more shared molecules have been discovered. For example, the proteoglycan Agrin is concentrated at the synaptic cleft between neurons and muscle cells and is important in the formation of neuromuscular junctions through the clustering of acetylcholine receptors (Bezakova & Ruegg, 2003). Khan et al discovered that Agrin also accumulates at T-cell immunological synapses. In a process like the one found at the neuromuscular junction, they found that Agrin lowers the threshold of T-cell activation by clustering IS surface receptors like TcR (Khan, Bose, Yam, Soloski, & Rupp, 2001).

Beyond their role at the IS, the Nde1/Lis1 complex is well known as being essential for proper neurogenesis, with mutations in Nde1 leading to smaller brain size (microcephaly) and mutations in Lis1 causing a loss of brain sulci and gyri giving rise to lissencephaly (smooth brain) (Di Donato et al., 2017; Wynshaw-Boris, 2007). In neurons the Nde1/Lis1 complex has been shown to be involved in several dynein-dependent processes including the organization of the Golgi (Lam et al., 2010), spindle pole focusing (Moon et al., 2014), and linking dynein to kinetochores (Ye et al., 2017). Through its function in neurons, the Nde1/Lis1 complex is said to promote a "persistent force dynein state" that is required for dynein-based transport under high-load conditions (McKenney, Vershinin, Kunwar, Vallee, & Gross, 2010).

In neurons Nde1/Lis1 often forms a complex with Disrupted in Schizophrenia 1 (DISC1), a protein genetically linked to the development of schizophrenia (Burdick et al., 2008; Soares et al., 2011). Together the DISC1/Nde1/Lis1 complex is involved in intracellular transport and mitosis (Bradshaw et al., 2009: Burdick et al., 2008). Through this complex, DISC1 is known to regulate the localization and function of Nde1/Lis1. DISC1 recruits PDE4 and modulates the PKA-dependent phosphorylation of Nde1, which regulates Nde1 binding to Lis1 (Bradshaw et al., 2011). Disruption of DISC1 prevents Nde1 from localizing to the kinetochores in mitotic cells, partially depleting dynein from those sites and leading to stalling in the metaphase-anaphase transition (Ye et al., 2017).

To perhaps extend the parallels between T-cells and neurons beyond what is already known, our lab has discovered that DISC1 is a component of the T-cell Nde1/Lis1 complex (Nath et al, 2016). Our work here shows that DISC1, which to our knowledge has not been studied before in T-cells, plays an important role in organizing elements of the immunological synapse during T-cell activation.

Although there are no direct studies linking DISC1 to immune function, researchers have long noted a link between schizophrenia and immune dysfunction. Patients suffering from schizophrenia exhibit higher levels of activated lymphocytes in their cerebrospinal fluid (Nikkilä et al., 2001) and elevated levels of IFN-gamma and IL-4, two cytokines primarily linked with TH cells (Kim et al., 2004; Mittleman et al., 1999). Some studies have even suggested that immune dysfunction might cause schizophrenia due to an abnormal array of cytokines during brain development. Autoimmunity has a genetic link to schizophrenia (Pandarakalam, 2014), and may be an etiological basis for the disease. There are also mouse models for DISC1 disruption which report many immune abnormalities, including auto-immune disorders (Haran-Ghera, Ben-Yaakov, Peled, & Bentwich, 1973; Hutchings, Varey, & Cooke, 1986; Jane-wit et al., 2002; Owens & Bonavida, 1976; Rajan, Asensio, Campbell, & Brosnan, 2000; Ritchie & Clapcote, 2013). It is possible then that through DISC1 a link might be established between immune cells and schizophrenia.

JURKAT CELLS AS A MODEL FOR STUDYING T-CELLS

In this study we primarily use the E6.1 Jurkat cell line in order to study the components of the immunological synapse and the movement of cellular organelles during T-cell activation. Jurkat cells are human T lymphocytes derived from acute lymphoblastic leukemia, commonly used as an in vitro model for CD4+ cells (Gioia et al., 2018). In the past, a great deal was learned about TcR signaling by using Jurkat cells as a model, including the characterization of ZAP70, the identification of ITAM domains, and the role of PLCγ in TcR-based signaling to name but a few (Abraham & Weiss, 2004). Although research done with Jurkat cells has tapered somewhat, it is still widely used as a model for a variety of different molecular studies of T-cell biology. Jurkat cells have been used in the

last few years to study HIV infection of T-cells (Hain et al., 2018, Campestrini et al., 2018), calcium signaling in T-cells (Caretta et al., 2018; Cherizova et al., 2018), T-cell adhesions and cytoskeletal dynamics (Bashour et al., 2014; Hui et al., 2015), and are used in the development of CRISPR/Cas9 gene editing tools to study T-cell signaling (Bray et al., 2018; Liu et al., 2017).

Despite this, for all the benefits that Jurkat cells have in being a reliable workhorse cell line for studying T-cells, several abnormalities have been identified which present potential challenges in comparing Jurkat cells to other T-cells. With relevance to TcR signaling, Jurkat cells lack PTEN, a regulator of the PI3K pathway, and shows aberrant signaling in that pathway as a result (Gioia et al., 2018). Older studies had suggested that Jurkat cells lacked expression of CTLA4 (Lindsten et al., 1993), but there have been conflicting findings in later years that suggest Jurkat cells express CTLA4 normally (Pistollo et al., 2002), or that Jurkat cells may express CTLA4 at reduced levels compared to other T-cells due to a mutation present in the CTLA4 gene (Gioia et al., 2018).

Many experiments in our study also utilize the superantigen Staphylococcus Enterotoxin E (SEE) bound to MHC II on a target cell in order to activate Jurkat cells and induce the formation of an immunological synapse. Studies conducted early in the investigation of superantigen effects on T-cell activation found that viral superantigens showed diminished signaling for Ca^{2+} influx and a failure to trigger lytic effector functions in CD8+ cells (Webb & Gascoigne, 1994). While these signaling abnormalities were not observed with bacterial superantigens such as SEE, the use of MHC-SEE over peptide-MHC stimulation may affect Jurkat signaling, synapse formation, and synapse dissipation in so far undiscovered ways. While this model is still a powerful tool in studying T-cell biology, understanding the potential limitations of using Jurkat cells is an important consideration when discussing the findings of research done primarily with them.

SUMMARY OF FINDINGS

In this study, we have shown that DISC1 is critical in the proper organization of the IS during T-cell activation. In Chapter 2, we showed that two DISC1 isoforms are expressed in Jurkat cells, DISC1 isoform L and Lv. Cloning these isoforms into an EGFP construct to express fusion proteins showed that they have distinct localizations in Jurkat cells. DISC1 isoform L-GFP localized to the IS, while DISC1 Lv-GFP localized to mitochondria. Through knockout of DISC1 and the reintroduction DISC1 L and Lv we showed that these individual isoforms were needed in the complete translocation of the MTOC and mitochondria, respectively. In the case of MTOC translocation, we found that disruption of DISC1 affected the proper organization of Nde1/Lis1 and dynein at the IS. In Chapter 3, we showed that knockout of DISC1 disrupts actin polymerization at the IS, which could be restored with DISC1 L. Furthering this connection, we also showed that DISC1 is connected to LFA-1 and to Girdin, an actin effector protein and crosslinker as yet not reported in T-cell signaling. Finally, we show that the actin network at the IS is needed for the recruitment of the Nde1/Lis1/dynein complex, as well as for MTOC translocation. Together, this study establishes a connection through DISC1 between microtubule-based polarization in the activating T-cell and actin dynamics at the IS.

Chapter 2: Characterizing DISC1 in T-cell Polarization

INTRODUCTION

One of the major hallmarks to T-cell function is the focused secretion of effector molecules (Huse et al., 2008; Stinchcombe et al., 2011; Ueda et al., 2015). The process of focused secretion typically happens in a series of steps beginning with the formation of the immunological synapse (IS) (Grakoui et al., 1999; Monks et al., 1998). Formation of the IS is accompanied by the large-scale polarization of organelles and vesicles facilitated by cytoskeletal rearrangement. Many of these processes are microtubule dependent, carried out by the molecular motors dynein and kinesin (Dustin & Choudhuri, 2016; Mentlik et al., 2010; Nath et al., 2016; Schwindling et al., 2010). Classically, dynein and kinesin move cargo in different directions, towards either the microtubule minus or plus ends respectively. While there are isoforms of the kinesin motor that can account for movement of a variety of cargo, in humans only one cytoplasmic dynein is used (Reck-Peterson et al., 2018). Linkage of dynein to various cargos is possible through the mediation of specific adapter proteins.

Dynein-bound cargo is directed towards the IS through the repositioning of the microtubule organizing center (MTOC). Following contact with a target cell, the MTOC is translocated to the IS, where it has been shown to oscillate along the contact site (Kuhn & Poenie, 2002). The reorientation of the MTOC has been shown to be dependent on the accumulation of dynein at the IS (Combs et al., 2006) in association with the adapter proteins Neurodevelopment Protein 1 (Nde1) and Lissencephaly 1 (Lis1) (Nath et al., 2016). A study by Nath et al (2016) presented a model which shows that dynein becomes anchored to the IS through Nde1/Lis1 and “pulls” on microtubules, causing the MTOC to be “reeled in” to the IS.

The Nde1/Lis1 complex is reportedly used for moving heavy cargo like the MTOC, whereas a second dynein complex known as Dynactin is used as an adaptor for moving smaller cargo (Nath et al., 2016). The dynein-Dynactin complex has been shown to transport of a wide variety of targets including secretory vesicles (Matanis et al., 2002), mitochondria (van Spronsen et al., 2013), the Golgi (Short et al., 2002), and endosomes (Schroeder & Vale, 2016). Both Dynactin and Nde1/Lis1 are connected to dynein through the dynein intermediate chain (DIC) and binding of dynein to either complex is mutually exclusive (Nath et al., 2016; Vallee et al., 2012).

The potential role of DISC1 in T-cell activation

Previous work in our lab has shown that another dynein binding protein called DISC1 is present in T-cell dynein complexes. While DISC1 has been studied in neurons, virtually nothing is known of its function in T-cells. In neurons, DISC1 has been shown to be involved in neurite outgrowth and synapse formation (Kamiya et al., 2006; Mao et al., 2009), transport of cargo such as mitochondria (Norkett et al., 2016), and the proper positioning of the centrosome (Bradshaw et al., 2008). The association of DISC1 with Nde1/Lis1 is well established and has been shown to participate in intracellular transport (Bradshaw et al. 2008; Brandon et al. 2005; Miyoshi et al. 2004; Morris et al. 2003; Ozeki et al. 2003, Wang & Brandon, 2011). Yet while some functions of DISC1 are known, understanding its function is complicated by the fact that several isoforms are known and the DISC1 interactome includes over 127 different binding partners in the cell (Lipina & Roder, 2014).

In this study we use Jurkat cells and OT-1 transgenic mouse CTLs to show that DISC1 is recruited to the immunological synapse where it colocalizes with Nde1, Lis1, and

dynein. We identified two known isoforms of DISC1 in Jurkat cells, L and Lv, and show that isoform L accumulates at the IS while isoform Lv is associated with mitochondria. Using CRISPR/Cas9 knockout techniques, we show that disrupting DISC1 in T-cells affects both MTOC and mitochondrial translocation to the synapse. We also show that the localization of Nde1/Lis1 and dynein at the synapse is dependent on DISC1. Furthermore, normal functions are restored when individual isoforms are re-expressed in the CRISPR/Cas9 knockout cells.

MATERIALS AND METHODS

Cell Lines and Reagents

The Jurkat (E6.1), Raji, and EL-4 cell lines were obtained from the American Type Central Collection. OT-1 splenocytes were obtained from Dr. Lauren Ehrlich. These C57BL/6-Tg(TcraTcrb)1100Mjb/J (OT-I) mice were sourced from Jackson Laboratories and bred in house. All strains were bred and maintained under specific pathogen-free conditions in the University of Texas at Austin animal facility. Experiments were performed using mice 1-3 months of age of mixed sex. Mouse maintenance and experimental procedures were carried out with approval from the Institutional Animal Care and Use at the University of Texas at Austin.

RPMI 1640 (Cat # 31800022), Opti-MEM (Cat # 31985062), and DMEM media (Cat # 12100046) were obtained from Gibco Thermo-Fisher. Heat-inactivated fetal bovine serum (FBS) was obtained from Atlas Biologicals (Cat # F-0500-D). The 4 mm gap transfection cuvettes were obtained from Fisher Scientific (Cat # FB104). Goat serum (Cat # G2093), poly-l-lysine (Cat # P2636), mitomycin C (Cat # M4287), and primers were obtained from Sigma-Aldrich. SuperSignal West Pico chemiluminescent substrate solution

(Cat # 34580) and X-ray film (Cat # 34090) were obtained from Thermo Scientific. G418 Sulfate was purchased from Gold Biotechnology (Cat # G-418-5). MMLV reverse transcriptase kit was obtained from Epicentre (Cat # RT80110K). RNeasy Midi Kit was obtained from Qiagen (Cat # 75144). Mini Plasmid and Midi Fast Ion Plasmid Kits were obtained from IBI Scientific (Cat # IB47111, IB47111). All restriction enzymes were obtained from New England Biolabs. Xfect transfection reagent was obtained from Clonetech (Cat # 631318). ProLong Gold Anti-Fade Mounting Reagent was obtained from Life Technologies (Cat # P36930). The Cas9 and DISC1 sgRNA plasmids were obtained from Genecopoeia (Cat # CP-LvC9NU-02-B, HCP268459-LvSG03-1-B). Partially purified Staphylococcus Enterotoxin E (SEE) was obtained from Toxin Technologies (Cat # ET404). OVA fragment peptide (chicken, 257–264 aa, SIINKEKL-OH) was obtained from New England Peptide (Cat # BP10-915).

Rabbit anti-DISC1 antibody (Cat # PA2023) and mouse anti-Talin antibody (Cat # MA1092) were obtained from Boster Biological. Rabbit anti-Nde1 antibody was obtained from Proteintech Group (Cat # 10233-1-AP). Mouse anti-Lis1 antibody (Cat # L7391), rabbit anti-GFP antibody (Cat # G1544), and mouse beta-tubulin antibody (Cat # T8328) were obtained from Sigma-Aldrich. Vβ8 anti-TcR antibody was obtained from BD Biosciences (Cat # 555604). Goat anti-rabbit AlexaFluor 594 conjugated antibody (Cat # A11037) and goat anti-mouse FITC conjugated antibody (Cat # F2012) were obtained from Invitrogen. Goat anti-mouse horse radish peroxidase (HRP) conjugated antibody (Cat # A9917) and goat anti-rabbit HRP conjugated antibody (Cat # A0545) were obtained from Sigma-Aldrich.

Cell Tracker Blue (CTB; Cat # C2110), MitoTracker CMXRos (Cat # M7512) and Rhodamine B Isothiocyanate (Cat # 283924) were obtained from Invitrogen. Propidium

Iodide was obtained from Sigma Aldrich (Cat # P4170). Indo-1 AM was obtained from Molecular Probes (Cat # I1223).

Cell culture

Jurkat cells and Raji cells were grown in RPMI 1640 supplemented with 24 mM sodium bicarbonate, 1 mM sodium pyruvate, 2 mM l-glutamine, 50 µM beta-mercaptoethanol, 10,000 U/mL penicillin, 10 mg/mL streptomycin, and 10% (v/v) FBS (ACC growth media). Gryphon cells were grown in DMEM supplemented with 44mM sodium bicarbonate, 1 mM sodium pyruvate, 2 mM l-glutamine, 50 µM beta-mercaptoethanol, 10,000 U/mL penicillin, 10 mg/mL streptomycin, and 10% (v/v) FBS. All cells were cultured at 37°C in 5% CO2.

For expansion and stimulation of OT-1 cells, EL-4 cells were treated with 50µg/ml mitomycin C for 2 hours, washed thoroughly, and then treated with 1µM Ova peptide. These EL-4 cells were then mixed with OT-1 splenocytes, activated OT-1 cytotoxic T-lymphocytes (CTLs), or used as targets in immunostaining experiments. OT-1 CTLs were maintained in ACC growth media supplemented with 20 U/ml IL-2.

DISC1 identification and cloning

We began identifying possible DISC1 isoforms expressed in Jurkat cells by adapting an RT-PCR method used by Nakata et al (2009). First, total Jurkat mRNA was isolated using the RNeasy Midi Kit. This mRNA was converted into a cDNA library using a MMLV reverse transcriptase kit. Using eight different sets of primers, DISC1 exon fragments were identified from this cDNA library through PCR (Table 2.1).

Primer Number	Sequence	Target Isoform
Forward Primer 1 Reverse Primer 1	5’ ATGCCAGGCGGGGGTCCTCA 3’ 5’ GCGAGAGCCGAATAAAGCTA 3’	DISC1 L and Lv
Forward Primer 2 Reverse Primer 2	5’ TGGCTCTCACAGTGCCTTTA 3’ 5’ TGCATCTTCCTGAAGTTTCTGA 3’	DISC1 L and Lv
Forward Primer 3 Reverse Primer 3	5’ GACACCCTGCTCAGGAAATG 3’ 5’ GCTTCCAGCACAAACATCCT 3’	DISC1 L and Lv
Forward Primer 4 Reverse Primer 4	5’ TCCATCACGAGACGAGACTG 3’ 5’ TCCCAGCTTTTTGACATTCC 3’	DISC1 L and Lv
Forward Primer 5 Reverse Primer 5	5’ CAGCACCCTGAGGAAGAAAG 3’ 5’ GGGATGAGGTGAGTCTTCCA 3’	DISC1 L and Lv for Forward; L for Reverse
Forward Primer 6 Reverse Primer 6	5’ GGAAAGTGTGGGAAGCTGAC 3’ 5’ TCAGGCTTGTGCTTCGTGGA 3’	DISC1 L and Lv
Forward Primer 7 Reverse Primer 7	5’ AAGCAATGCATGCTCATTACAG 3’ 5’ TGTCCAGGACTCTGCATCAC 3’	DISC1 S
Forward Primer 8 Reverse Primer 8	5’ TGGTATCCGTTGGTGAATGTG 3’ 5’ AGTTTGGTTCAGGATGTCGAG 3’	DISC1 Es

Table 2.1: Primers for DISC1 Isoform Identification

Derived from Nakata et al., 2009.

Through this method, DISC1 L and Lv isoforms were identified and verified through Sanger sequencing on an Applied Biosystems 3730 DNA Analyzer (UT ICMB Core Facilities).

Full sized DNA fragments for DISC1 isoform L and Lv were synthesized through PCR of Jurkat cDNA. Primers containing restriction sites were used to place SalI or XhoI at the 5' end and XmaI at the 3' end of DISC1 DNA fragments. These DNA fragments were then subcloned into the monomeric GFP vectors (pmeGFP) which expressed the GFP tag either C terminal (pmeGFP-N1) or N terminal (pmeGFP-C1) to the cloned sequence. The end products were pmeGFP-N1-DISC1-L, pmeGFP-N1-DISC1-Lv, pmeGFP-C1-DISC1-L and pmeGFP-C1-DISC1-Lv. Descriptions of these constructs are explained further in Figure 2.2.

The Nde1-mCherry construct was made by creating DNA fragments of the Nde1 coding sequence through PCR amplification of a pmeGFP-N1-Nde1 template, as described in Nath et al (2016). DNA fragments contained AgeI and XbaI restriction sites on their 5' and 3' ends, which were used to insert the sequence into the pIRES-PURO3-mCherry vector. The pIRES-PURO3-mCherry vector was obtained from Dr. Roger Tsien, and subsequently modified using a standard PCR protocol to insert several additional restriction sites into the multicloning site.

Tetracysteine tagged dynein was generated by first creating DNA fragments of the dynein intermediate chain (DIC) through PCR amplification of a Jurkat cDNA library, which was prepared as described previously in the section. These DNA fragments contained the NsiI and NotI restriction sites on their 5' and 3' ends. A pCLNCX FLN#MEP construct was provided by Dr. Roger Tsien and is described in Martin et al. (2005). This construct originally contained a sequence for β-actin which was removed via PCR mutagenesis in addition to the insertion of the NsiI restriction site (a modified vector we

have named pCLC4) which allowed for the insertion of our DNA fragments containing the dynein intermediate chain.

All DNA constructs were transformed from frozen aliquots of competent bacteria suspended in CaCl2 solution. These aliquots were thawed and mixed with DNA constructs, then put through heat shock at 43°C. Depending on the concentrations needed, DNA constructs were isolated using the Mini Plasmid or Midi Fast Ion Plasmid Kits and plasmid sequences were verified by Sanger sequencing. DNA was introduced into Jurkat cells through electroporation. For the transformation, Jurkat cells were washed and resuspended in Opti-MEM reduced serum media at a cellular concentration of 2×10^7/mL and incubated with 10µg of plasmid DNA 15 minutes at 37°C. Cells were placed in 4mm gap transfection cuvettes and pulsed at 250 V (950 µF) using the Gene Pulser Electroporation System (Bio-Rad). After electroporation, cells were resuspended in fresh ACC growth media. Cells containing DISC1 or DIC constructs were grown under selection with 1 mg/mL G418, whereas cells containing Nde1 constructs were grown under selection with 2 µg/mL puromycin. Selection began 24 hours post-transfection and continued for two weeks. Afterwards, cells were sorted for the expression of fluorescent proteins using a FACSAria cell sorter.

DISC1 knockout with CRISPR/Cas9

The Cas9 and DISC1 sgRNA plasmids were transfected into the Gryphon viral packaging cell line using the Xfect transfection reagent. Fresh growth media was added 4 hours post-transfection. Forty-eight hours after transfection, the supernatants containing the viral particles were collected. For transduction, Jurkat cells or OT-1 CTLs were resuspending in media containing viral particles at a cellular concentration of 2×10^6/mL,

supplemented with 8 µg/mL polybrene, and placed in six well plates. These were spinfected through centrifugation at 500 × g and 30°C for 1 hour. Following this, cells were placed back in 37°C culture conditions to incubate. Centrifugation was repeated after every 12 hours of incubation, for 36 hours total. After the final centrifugation, the media was replaced with fresh growth media. Successful transduction was confirmed through observation of GFP and mCherry fluorescent proteins expressed by the Cas9 and sgRNA plasmids. Complete knockout of DISC1 in culture was achieved through FACSAria sorting of GFP and mCherry expressing cells, followed by verification through DISC1 Western blotting of the resultant cells. All cells were grown under selection with 1 mg/mL G418 Sulfate and 2 µg/mL puromycin. Selection began 36 hours post-transduction and continued for two weeks until sorting was conducted with a FACSAria cell sorter.

Preparation of cells for staining

To prepare coverslips for cell staining and fluorescent microscopy, coverslips were first cleaned with a 9:1 mixture of ethanol and 1M KOH for 1 hour. They were then washed in dH2O and coated with an aqueous solution of 0.1 µg/mL 30,000-70,000 kDa poly-l-lysine. These were rinsed again in dH2O and left to dry for 30 minutes at room temperature.

To prepare Jurkat-Raji cell conjugates, Raji cells were suspended at a concentration of 1×10^6/mL in serum-free RPMI 1640 and treated with SEE at 1 µg/mL for 1 hour at 37°C. They were subsequently stained with 10µM of CTB for 15 minutes at 37°C. Both Jurkat and Raji cells were washed with ACC media, paired at ratio of 3:2 Jurkat to Raji cells, and centrifuged at a light speed (500 g) for 5 minutes. Cells were then washed again with ACC and settled on poly-l-lysine coated coverslips at a total concentration of 1×10^6/mL for 15 minutes.

For immunostaining, cells settled on coverslips were fixed with a Phosphate Buffered Saline (PBS) solution of 1% paraformaldehyde for 30 minutes before being washed with PBS. Cells were then permeabilized with a 1:1 solution of ice-cold methanol and acetone for 15 minutes. Cells were washed again with PBS and blocked with a PBS solution of 5% goat serum and 0.5% Tween-20 for 30 minutes. Cells were then stained with a 1:50 solution of primary antibody in blocking solution for 1 hour. After primary antibody staining, the cells were then washed again with PBS and stained with a 1:100 solution of secondary antibody for another hour. After a final wash with PBS the coverslips were mounted onto slides with ProLong Gold antifade reagent overnight at room temperature before being stored long-term at -20°C.

Live mitochondria staining was achieved by staining Jurkat cells with 1μM MitoTracker Red for 15 minutes at 37°C before being conjugated with Raji cells. For staining mitochondria in fixed cell conjugates, Jurkat cells were treated with 2μM Rhodamine B Isothiocyanate for 15 minutes at 37°C before being conjugated with Raji cells and fixed as previously described in this section.

SDS-PAGE and Western blotting

For Western blots, cells were pelleted at 750 × g and the cell pellet was resuspended in lysis buffer containing 200 mM NaCl, 50 mM Tris at pH 8, 2 mM EDTA, 2 mM NaVO4, 20 mM NaF, 3 mM PMSF, 2 mM Imidazole, 1 mM Na-β-glycerophosphate, and 1% Triton X 100. The suspension was then passed through a 21-gage needle repeatedly to homogenize, and then clarified at 16,000 × g and 4°C for 10 minutes to remove cell debris. The lysate was then mixed with SDS-PAGE loading buffer to a final concentration containing 2% (w/v) SDS and 5% (v/v) β-mercaptoethanol.

Samples prepared in SDS-PAGE sample buffer were run through SDS-PAGE and transferred to nitrocellulose paper for Western blotting. Samples were blocked in a blocking solution of TBS with 0.1% Tween and 5% BSA. Primary antibody was then added, diluted to a concentration of 1 µg/mL in blocking solution. Primary antibodies were tagged with HRP using a goat anti-rabbit or goat anti-mouse HRP conjugated secondary antibody and treated with SuperSignal West Pico chemiluminescent substrate solution before being exposed to X-ray film.

Calcium measurement

To stain Jurkat cells with a calcium tracking dye, cells were washed and resuspended to a concentration of 1×10^6 cells per mL in pre-warmed PBS supplemented with 5 mM glucose, 1 mM CaCl2, and 1% FBS. Cells were incubated with 1 µM Indo1-AM for 30 minutes at 37°C, then washed and resuspended with pre-warmed PBS. After an additional 10 minutes incubating at 37°C, cells were transferred to 1 mL fluorometer cuvettes. Measurement of Indo-1 AM fluorescence was taken with a fluorometer set to 354nm excitation and 404nm/485nm dual emissions. Throughout measurement, cells were kept at 37°C and kept in suspension through agitation from the bottom of the cuvette with a metal stir bar.

To measure calcium signaling after TcR activation, 500 ng/mL Vβ8 anti-TcR antibody was added to Indo-1 treated Jurkat cells, then mixed with a bulb pipet. This was then followed by the addition of 500 ng/mL rabbit anti-mouse IgG to act as a crosslinker. After measurements were taken, 2 µM of ionomycin followed by 0.1 mg/mL digitonin and then 2 mM EGTA with 6 mM Tris base were added in order to act as a calibration control.

Preparation anti-TcR coated coverslips

To prepare coverslips, 10 μg/mL solution of mouse Vβ8 anti-TcR antibody was coated over dried poly-l-lysine treated coverslips for 3 hours. Coverslips were then washed in three 10 minute intervals with PBS and then either used directly or stored for up to 24 hours at 4°C. Jurkat cells in ACC growth media at a cellular concentration of 1×10^6/mL were settled onto antibody coated coverslips and used for imaging studies.

FLAsH-EDT2 synthesis and staining

FLAsH-EDT2 reagent was prepared as described by Adams & Tsien, 2008 and confirmed by HPLC/mass spectrometry. Jurkat cells containing the pCLC4-DIC construct were brought to a cellular concentration of 1×10^6/mL in ACC media and treated with titrated amounts of FLAsH-EDT2 until it was determined that 1μM FLAsH-EDT2 and 10μM 1,2-ethanedithiol for 1 hour at 37°C were the best conditions for minimizing background fluorescence. After treatment, cells were then washed with ACC containing 10μM 1,2-ethanedithiol and incubated for 30 minutes at 37°C. Cells were then washed again with ACC before use.

Preparation of bilayer experiments

Jurkat and primary CD4+ T-cells were added to planar bilayers which were prepared as described in Steblyanko et al., 2018. The procedure was adjusted by preparing bilayers with Cy5-ICAM1-His6 at 1 μg/mL in order to eliminate background fluorescence of Cy5 during imaging.

Cytotoxicity assay

A flow cytometry-based cytotoxicity assay was adapted from previous works (Mattis, Bernhardt, Lipp, & Förster, 1997; Nath et al., 2016). Mouse OT-1 CTLs were prepared by spinfection using viral particles containing DISC1 sgRNA and Cas9 constructs (DISC1 KO) or Cas9 alone (wildtype). CTLs were selected for with puromycin and/or G418 for 48 hours before being washed and mixed with EL-4 target cells in a round-bottom 96-well plate. To distinguish the target cells from the CTLs, EL-4 cells were labeled with 250nM CFSE for 30 minutes in PBS and then washed twice. Labeled EL-4 cells were then used directly for cytotoxicity assay or pulsed with 1μM SIINFEKL peptide for 1 hour. EL-4 cells were mixed with corresponding CTLs at a ratio of 1:1, 4:1, and 10:1 effectors to targets (E:T) to a final volume of 150μl in each well. The plate was incubated at 37°C for 6 hours. Propidium iodide (PI) was added to a concentration of 100μg/ml at the end of the assay and the cells were immediately analyzed for PI- and CFSE-stained cells using a BD Accuri C6 Plus flow cytometer. FACS data were analyzed using FlowJo software and presented after background normalization.

Imaging and data processing

Images were viewed using a Nikon inverted microscope and captured using a CMOS camera. The images were processed and analyzed using the ImageJ processing software. In order to determine protein accumulation at the synapse, a line of length 230 pixels and width 70 pixels was drawn on the Jurkat-Raji cell pairs such that the mid-point of the line (pixel 115) was on the synapse. Background intensity was obtained from a region outside the cell pairs and subtracted from the fluorescence intensity. The fluorescence was normalized by dividing all the pixel measurements by the average intensity of the row

furthest away from the synapse. Beginning at the synapse (row 115), intensity values for five-pixel groups were treated as one increment and used for statistical analysis (mean ± SE of the mean). The compound mean and standard error for the increments were plotted against mean intensity of fluorescence. A one-tailed T-test with independent variance was performed for the increments starting from the synapse and moving to the back of the Jurkat cell.

Cross-sectional imaging of the IS was taken with a Zeiss LSM 710 confocal microscope from the University of Texas ICMB core facilities. Image processing was done by reslicing z-stacks of images using ImageJ.

RESULTS

Immunofluorescence of DISC1 in T-cells

DISC1 was initially detected in Jurkat cells by its presence in immunoprecipitants of dynein complexes. Depending on which anti-DISC1 Ig was used, immunofluorescence showed that DISC1 was either at the immunological synapse (Boster Biological Ig) or in large puncta in the cytoplasm (Epitomics Ig) (Figure 2.1A &B). Although the Epitomics antibody is no longer available, using the Boster antibody we showed that DISC1 was also at the immunological synapse of Natural Killer cells (NK-92) bound to Daudi cells (Figure 2.1C) and in mouse OT-1 CTLs paired with peptide coated EL-4 cells (Figure 2.1D).

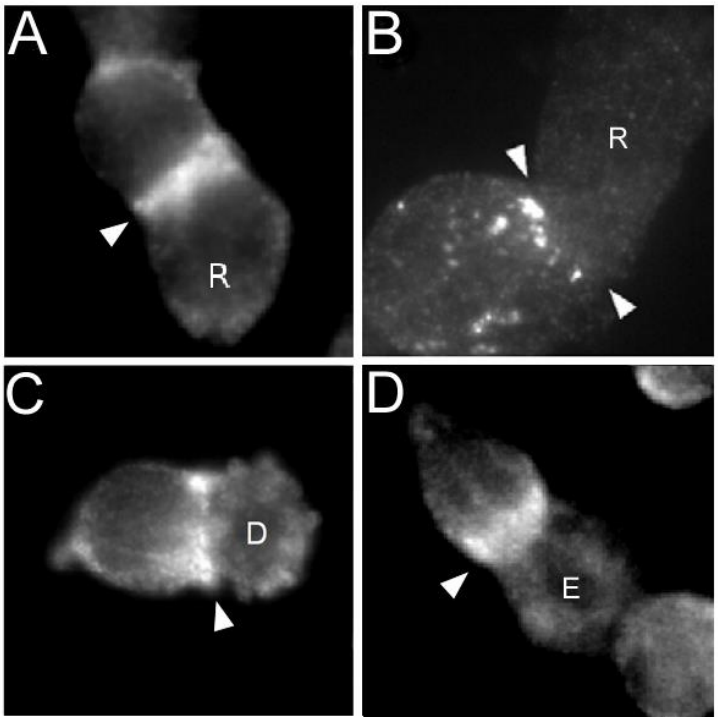

Figure 2.1: Immunofluorescence of DISC1 in T- and NK-cells

Jurkat cells were paired with SEE-coated Raji cells, fixed and immunostained for DISC1 using two different DISC1 antibodies. **(A)** The Boster antibody showed DISC1 at the synapse (white arrow). **(B)** The Epitomics antibody showed DISC1 in punctates that moved towards the synapse (white arrows). Raji cells are labeled 'R'. DISC1 can also be observed at the synapse immunostained with the Boster antibody in **(C)** NK cells paired with Daudi targets and fixed and **(D)** OT-1 CTLs paired with EL-4 targets and fixed (white arrows). Daudi cells are labeled 'D', and EL-4 cells are labeled 'E'.

DISC1 isoforms L and Lv are present in Jurkat T-cells

The observation of two different localization patterns of DISC1 suggested the possibility that there was more than one isoform of DISC1 in Jurkat cells. DNA sequence analysis of DISC1 clones revealed that there were two known isoforms present, L and Lv. To determine the localization pattern of these isoforms, pmeGFP was fused to either the N terminus (DISC1-L-C1-GFP; DISC1-Lv-C1-GFP) or C terminus of each DISC1 isoform (DISC1-L-N1-GFP; DISC1-Lv-N1-GFP) which were then expressed in Jurkat cells

(Figure 2.2). Neither of the C terminal constructs showed any obvious pattern of localization, and in particular they did not match the localization seen by immunofluorescence (Figure 2.3A-B). The N terminal-linked GFP constructs did correspond to the immunofluorescence data (Figure 2.3C-D). DISC1-L-C1-GFP (hereafter referred to as DISC1 L-GFP) localized around the MTOC of unstimulated Jurkat cells and accumulated at the IS when Jurkat cells were paired with SEE-coated Raji cells. DISC1-Lv-C1-GFP (hereafter referred to as DISC1 Lv-GFP) localized to large puncta in the cytoplasm of unstimulated Jurkat cells, and these puncta became concentrated near the IS of Jurkat-Raji pairs. Further analysis of these puncta using various fluorescent probes showed that MitoTracker staining matched the distribution of DISC1 Lv-GFP.

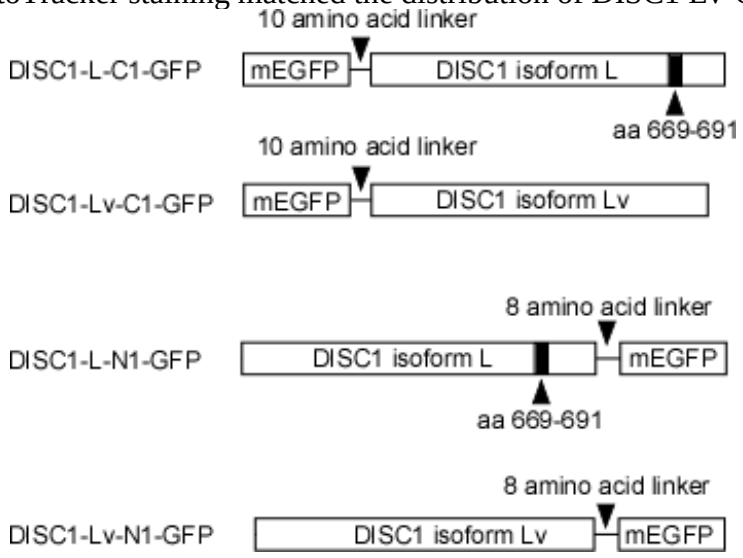

Figure 2.2: DISC1 GFP constructs

The schematic of different DISC1 GFP fusion proteins is shown, N to C terminus.

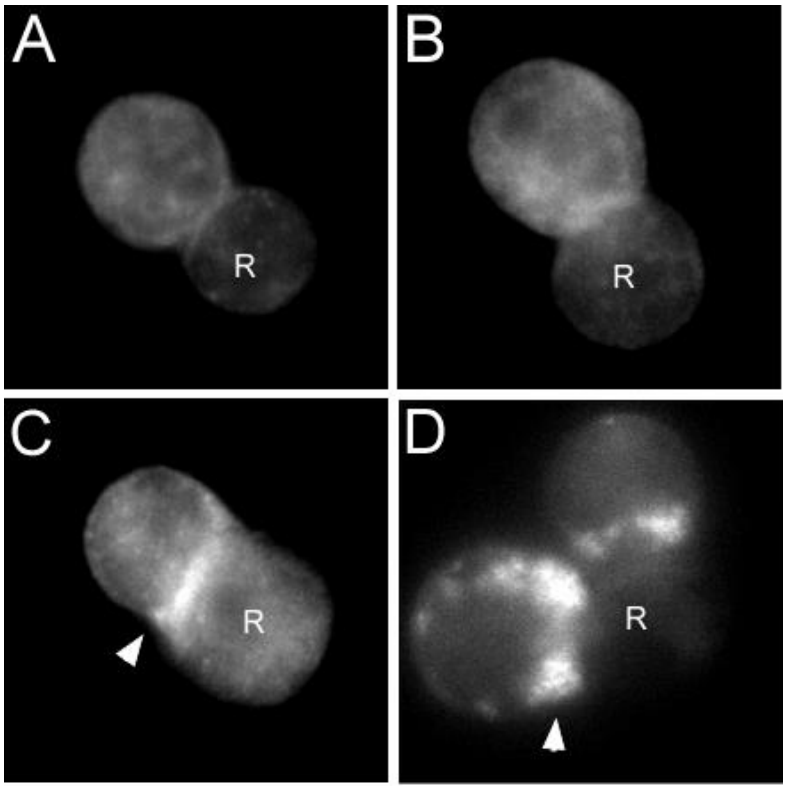

Figure 2.3: Localization of DISC1 GFP constructs

Jurkat cells expressing various DISC1 GFP constructs, paired with Raji cells, and imaged based on GFP fluorescence. **(A)** DISC1-L-N1-GFP and **(B)** DISC1-Lv-N1-GFP did not show any distinct subcellular localization. **(C)** DISC1-L-C1-GFP was found at the immunological synapse (white arrow), while **(D)** DISC1-Lv-C1-GFP localized to punctates which polarized towards the synapse. In all pictures Raji cells are labeled 'R'.

DISC1 siRNA knockdown

In order to determine the function of DISC1 in Jurkat cells we initially attempted to deplete DISC1 using DISC1-specific siRNA with a scrambled siRNA serving as a control. After 6 hours, DISC1 KD cells were stained with MitoTracker and paired with SEE-coated Raji cells. We found that KD inhibited the translocation of mitochondria to the IS (Figure 2.4A).

After 6 hours, DISC1 is nearly completely depleted from Jurkat cells, as assessed by Western Blots (Figure 2.4B). However, DISC1 quickly reaccumulates in Jurkat cells

only 12 hours after being transfected with siRNA. Apart from the disruption of mitochondria translocation, we saw minimal effects in the DISC1 KD, which made us question whether DISC1 was being completely depleted. This encouraged us to explore different methods for depleting DISC1 from Jurkat cells.

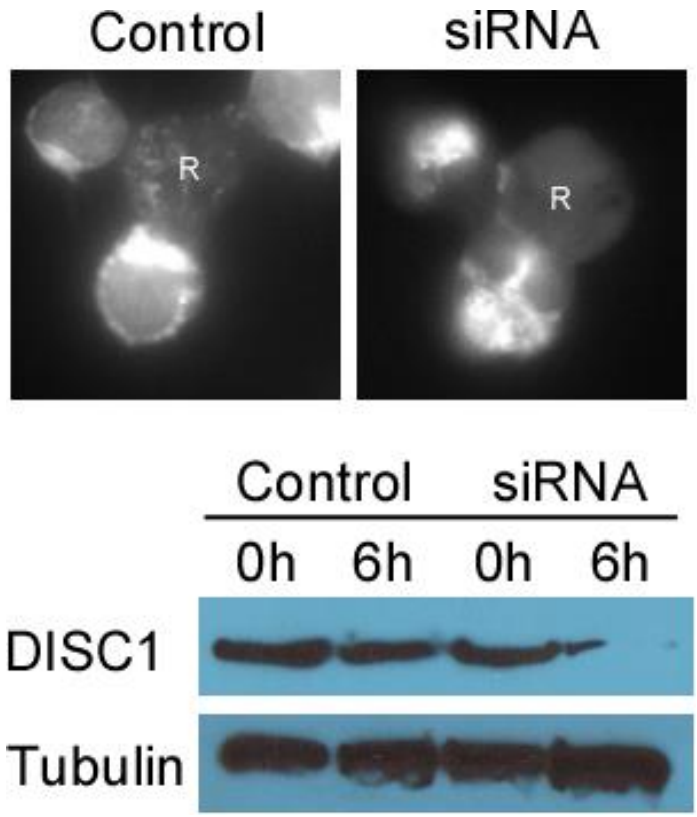

Figure 2.4: DISC1 RNAi

(A) Jurkat cells were transfected with control scramble RNA (Control), or siRNA targeting DISC1 (siRNA). After 6 hours cells were then stained for mitochondria, paired with SEE-coated Raji cells, and imaged. **(B)** Western blotting showed that 6 hours post transfection showed little DISC1 remaining in the cell. Tubulin was used as a loading control.

DISC1 knockout is achieved through CRISPR/Cas9

Due to uncertainties in the siRNA results, the CRISPR/Cas9 system was used to generate a stable DISC1 knockout (KO) line and complete loss of DISC1 expression was confirmed by Western blotting (Figure 2.5A). The original CRISPR and sgRNA plasmids expressed red or green fluorescent proteins, which interfered with efforts at immunostaining. However, by stopping selection, the original plasmids were rapidly lost leaving the cells non fluorescent. Immunostaining of these cells for DISC1 showed little or no fluorescence compared to wildtype (Figure 2.5B-C).

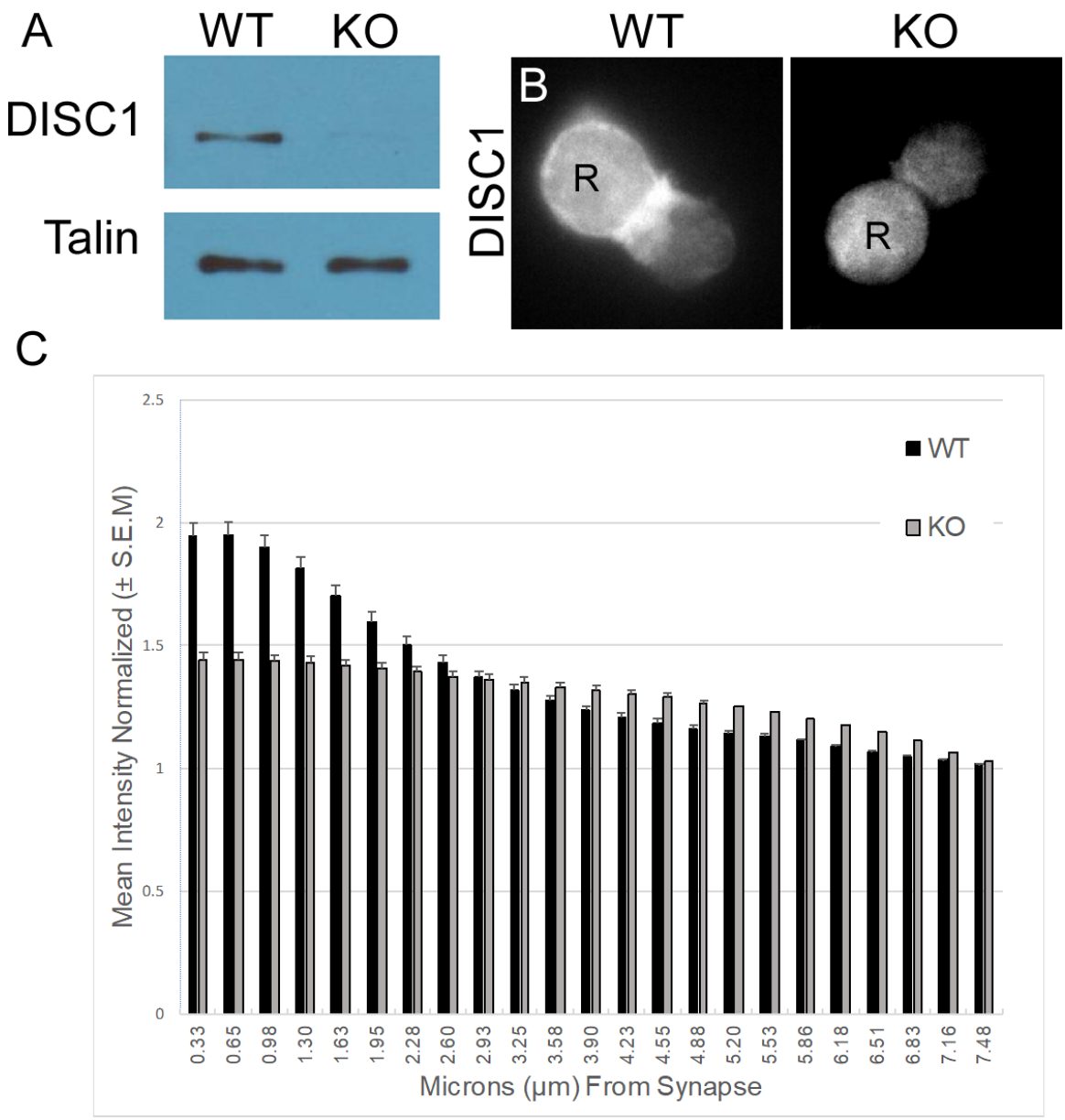

Figure 2.5: DISC1 CRISPR/Cas9 knockout

(A) DISC1 was assayed through Western blotting in wildtype (WT) and DISC1 knockout (KO) cells, using Talin as a loading control. **(B)** WT and KO Jurkat cells were paired with SEE-coated Raji cells, fixed and immunostained for DISC1. Raji cells are labeled 'R' in the pictures. **(C)** The distribution of DISC1 was analyzed from 30 immunostained images of WT and KO cell pairs, as described in the Materials and Methods. The boundary of the IS was defined as the maxima signal between the Jurkat and Raji pair. Mean intensity values ± SEM were plotted for 5 pixel-wide segments starting at the IS and moving to the back of the cell, then converted to distance in micrometers.

DISC1 Lv is needed for mitochondria accumulation at the IS

A second defect seen in the DISC1 KO cells is a failure of mitochondria to accumulate at the IS. To demonstrate this, the same four cell types used for analysis of MTOC translocation were used here to analyze mitochondrial movements. For this study mitochondria of Jurkat cells were selectively but permanently labeled with Rhodamine Isothiocyanate, paired with Raji cells, settled onto poly-l-lysine coverslips, and fixed (Figure 2.6). Compared to wildtype Jurkat cells, mitochondria were on average farther from the IS in DISC1 KO cells (Figure 2.6A-B), with a p-value of < 0.001 calculated when compared using a Student's T-test.

In order to determine if the defect in mitochondria translocation was dependent on a particular DISC1 isoform, DISC1 KO cells expressing either DISC1 L-GFP or DISC1 Lv-GFP were compared to the wildtype and DISC1 KO Jurkat cells. All four cell types were labeled with Rhodamine Isothiocyanate, paired with SEE-coated Raji cells and fixed as described above (Figure 2.6C-D). Comparisons showed that there was no significant difference between wildtype and DISC1-Lv expressing cells, whereas DISC1-L was not significantly different from the KO cells (Figure 2.6E). For a full comparison of results, see Table 2.2.

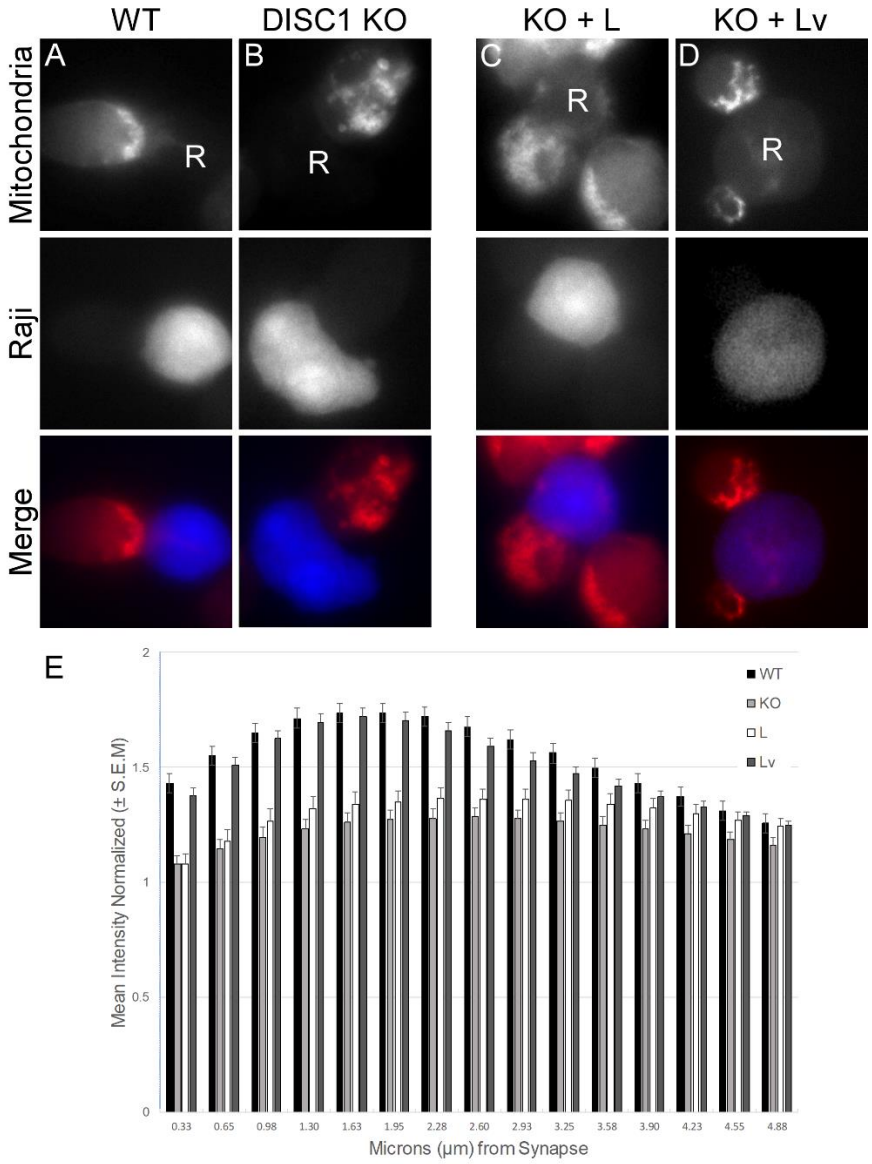

Figure 2.6: DISC1 Lv is needed for mitochondria accumulation at the IS

(A) Wildtype (WT) Jurkat cells, **(B)** DISC1 knockout (KO) Jurkat cells, **(C)** KO cells expressing a DISC1 L-GFP construct (KO+L), **(D)** and KO Jurkat cells expressing a DISC Lv-GFP construct (KO+Lv) were stained for mitochondria, paired with SEE-coated Raji cells, and fixed. The location of Raji cells was determined through staining with cell tracker blue and are labeled 'R' in other pictures. **(E)** The distribution of mitochondria was analyzed from 30 images of WT, KO, and KO+GFP cell pairs, as described in the Materials and Methods. The boundary of the IS was defined as the border of the Jurkat cell with the Raji cell, as determined with cell tracker blue staining. Mean intensity values ± SEM were plotted for 5 pixel-wide segments starting at the IS and moving to the back of the cell, then converted to distance in micrometers.

p-values	WT	KO	KO + L	KO + Lv
WT	-	0.000215	0.004286	0.440630
KO	-	-	0.298783	0.000396
KO + L	-	-	-	0.006438
KO + Lv	-	-	-	-

Table 2.2: Statistical analysis on the effects of DISC1 on mitochondria

Analysis of the results from Figure 2.6 using the Student's T-Test, one-tailed, unpaired. The average intensity of 5 pixel-wide segments across 30 samples for each variable cell type were calculated and compared. P values for these comparisons are shown above.

DISC1 L in needed for complete MTOC polarization

Having shown that DISC1 was not expressed in the DISC1-KO cell line, wildtype and DISC1 KO cells were used to analyze the role of DISC1 in synapse formation and organellar movements. To determine the role of DISC1 in MTOC translocation, Jurkat-Raji pairs were immunostained for tubulin and scored. The data, at first glance, showed that loss of DISC1 did not block MTOC polarization. However, there was a subtle difference detected when distances between the MTOC and the IS were quantified for DISC1-KO and untreated Jurkat cells. We found that the MTOC was on average farther from the IS in DISC1 KO cells than in wildtype cells (Figure 2.7A), with a p-value of < 0.001 calculated when compared using a Student's T-test.

In order to determine if the defect in MTOC translocation was dependent on a particular DISC1 isoform, DISC1 KO cells expressing either DISC1 L-GFP or DISC1 Lv-GFP were compared to the wildtype and DISC1 KO Jurkat cells. All four cell types were

paired with SEE-coated Raji cells, immunostained for tubulin and analyzed for MTOC translocation as described above (Figure 2.7B). Comparisons showed that there was no significant difference between wildtype and DISC1-L expressing cells, whereas DISC1-Lv was not significantly different from the KO cells (Figure 2.7C). For a full comparison of results, see Table 2.3.

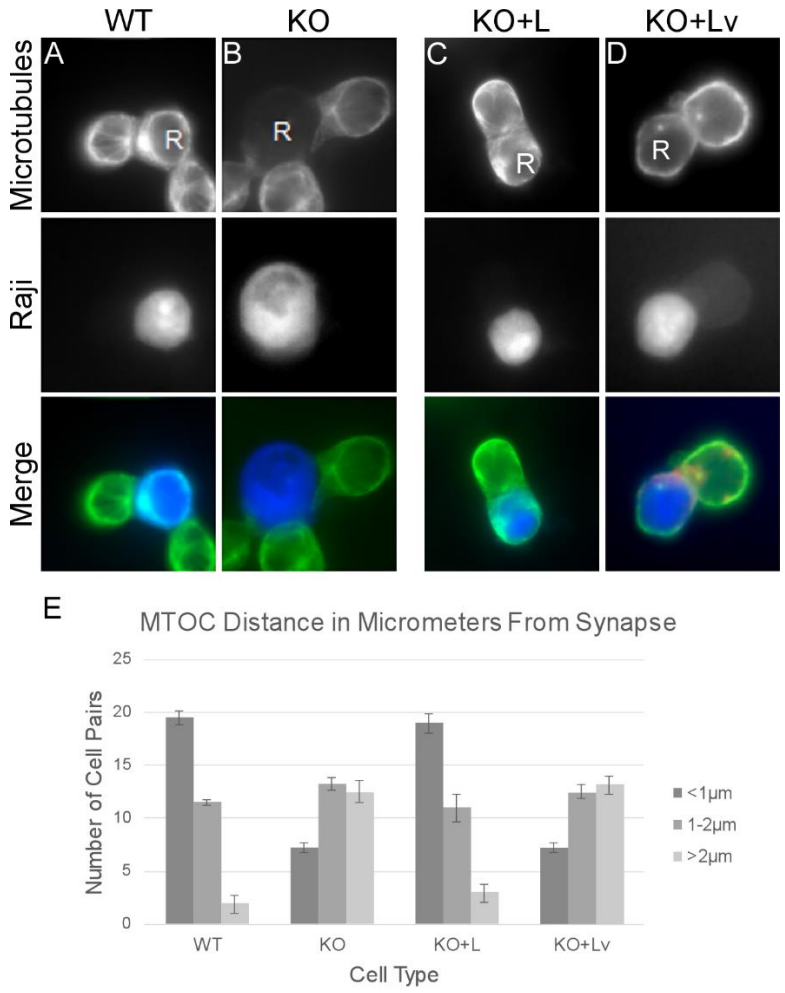

Figure 2.7: DISC1 L is needed for complete MTOC polarization

(A) Wildtype (WT) Jurkat cells, **(B)** DISC1 knockout (KO) Jurkat cells, KO Jurkat cells expressing a **(C)** DISC1 L-GFP construct (KO+L), and KO Jurkat cells expressing a **(D)** DISC1 Lv-GFP construct (KO+Lv) were paired with SEE-coated Raji cells, fixed and stained for beta-tubulin. The location of the MTOC in all samples was determined by taking the signal maxima of beta-tubulin stains. The location of Raji cells was determined through staining with cell tracker blue and are labeled 'R' in other pictures. Distance of the MTOC to the immunological synapse was taken by measuring the distance in pixels between the MTOC and the Raji cell. **(E)** The position of the MTOC relative to the immunological synapse was logged for each cell type (n=33) and arranged in groups by distance in micrometers (Jurkat size ~12 µm average). Results were compiled from the mean number of cells in groupings from four separate experiments with standard error calculated.

p-values	WT	KO	KO + L	KO + Lv
WT	-	0.000051	0.214343	0.000005
KO	-	-	0.002251	0.303279
KO + L	-	-	-	0.000409
KO + Lv	-	-	-	-

Table 2.3: Statistical analysis on the effects of DISC1 on MTOC polarization

MTOC positions from different cell types were compared with each other using a Student's T-Test (n=33). P values are shown above.

DISC1 knockout does not affect calcium signaling

One way that defects in intracellular organelle movements might arise is through a defect in cell signaling. One test for a defect in signaling was to determine if calcium transients were altered. To test for this possibility, Untreated and DISC1-KO Jurkat cells were loaded with Indo-1 AM, and calcium transients were recorded using a dual emission fluorometer (Photon Technology, NJ), (Figure 2.8). No observable difference in calcium signaling could be detected in cells with or without DISC1.

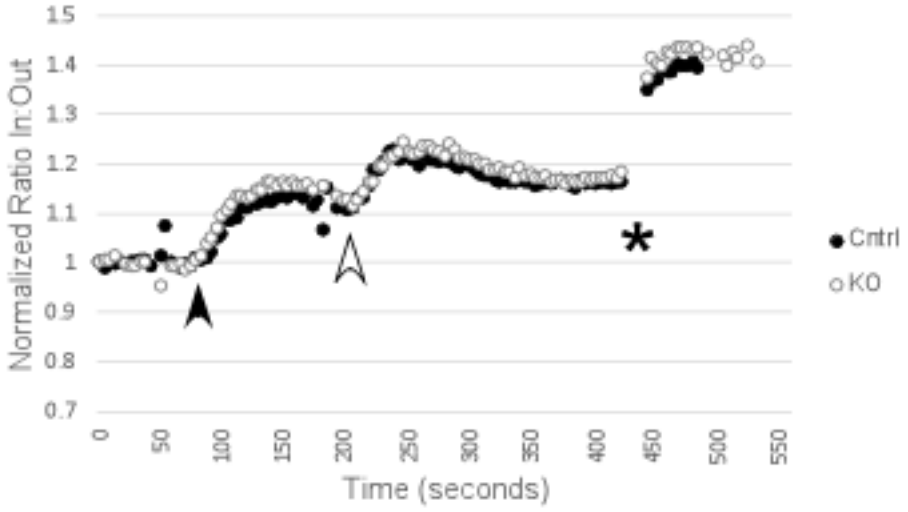

Figure 2.8: DISC1 KO has no effect on calcium signaling

Jurkat cells electroporated with control or NDE1 siRNA were loaded with indo-1-AM and stimulated with a mouse Vβ8 (anti-TcR) mAb (black arrow) followed by anti-mouse Ig (white arrow), and ionomycin (star). Ionomycin was used as control to raise intracellular Ca^{2+} levels. Data are plotted as Indo-1 emission ratios (404/485 nm), normalized to the base level, and are proportional to the free calcium ion concentration.

The interaction between Nde1/Lis1 and DISC1 at the IS

To determine if DISC1 is needed in order to recruit the Nde1/Lis1 complex to the IS we compared wildtype Jurkat cells to those where DISC1 was disrupted using the CRISPR/Cas9 system. Having shown that there was no DISC1 expression in the KO cells, normal and DISC1 KO Jurkat/Raji pairs were immunostained for Nde1 and Lis1. We found that Nde1/Lis1 was present at the IS in both cell lines (Figure 2.9A-B), although the amount of Nde1 at the synapse of the KO cells was slightly but measurably different than in wildtype cells ($p = 0.043$) (Figure 2.9C).

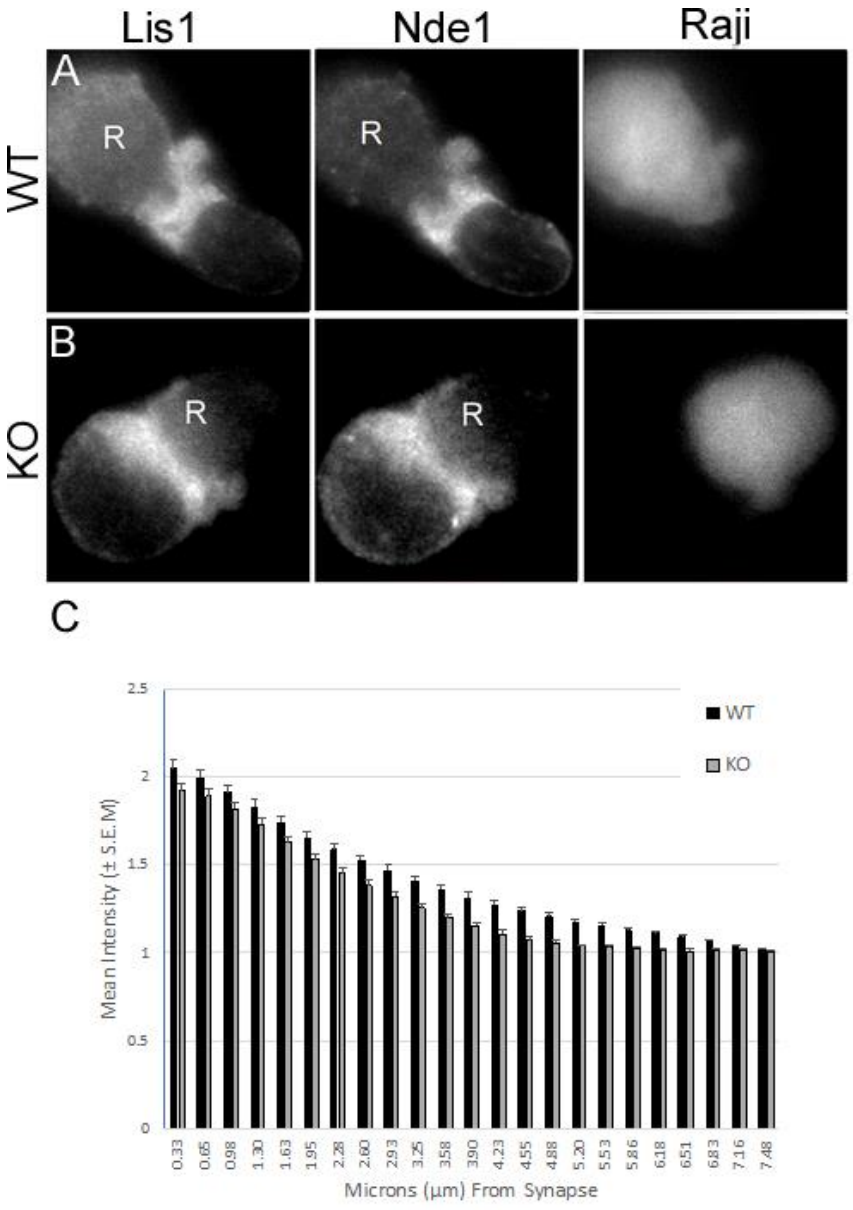

Figure 2.9: Nde1 localizes to the IS independently of Nde1

(A) Wildtype (WT) Jurkat cells or **(B)** DISC1 knockout (KO) Jurkat cells were paired with SEE-coated Raji cells, fixed, and immunostained for Nde1 or Lis1.The location of Raji cells was determined through staining with cell tracker blue and are labeled 'R' in other pictures. **(C)** The distribution of Nde1 was analyzed from 30 immunostained images of WT and KO cell pairs, as described in the Materials and Methods. The boundary of the IS was defined as the maxima signal between the Jurkat and Raji pair. Mean intensity values ± SEM were plotted for 5 pixel-wide segments starting at the IS and moving to the back of the cell, then converted to distance in micrometers.

Previous studies showed that Nde1 normally forms a ring at the IS corresponding to the pSMAC (Nath et al. 2016). Curiously, using confocal microscopy of Jurkat/Raji pairs we found that while Nde1 accumulates in a ring in wildtype Jurkat cells, it does not show any distinct localization in DISC1 KO cells (Figure 2.10A-B). Further, KO cells expressing DISC1 L or Lv GFP constructs showed a restored distribution of Nde1 into a ring (Figure 2.10C-D).

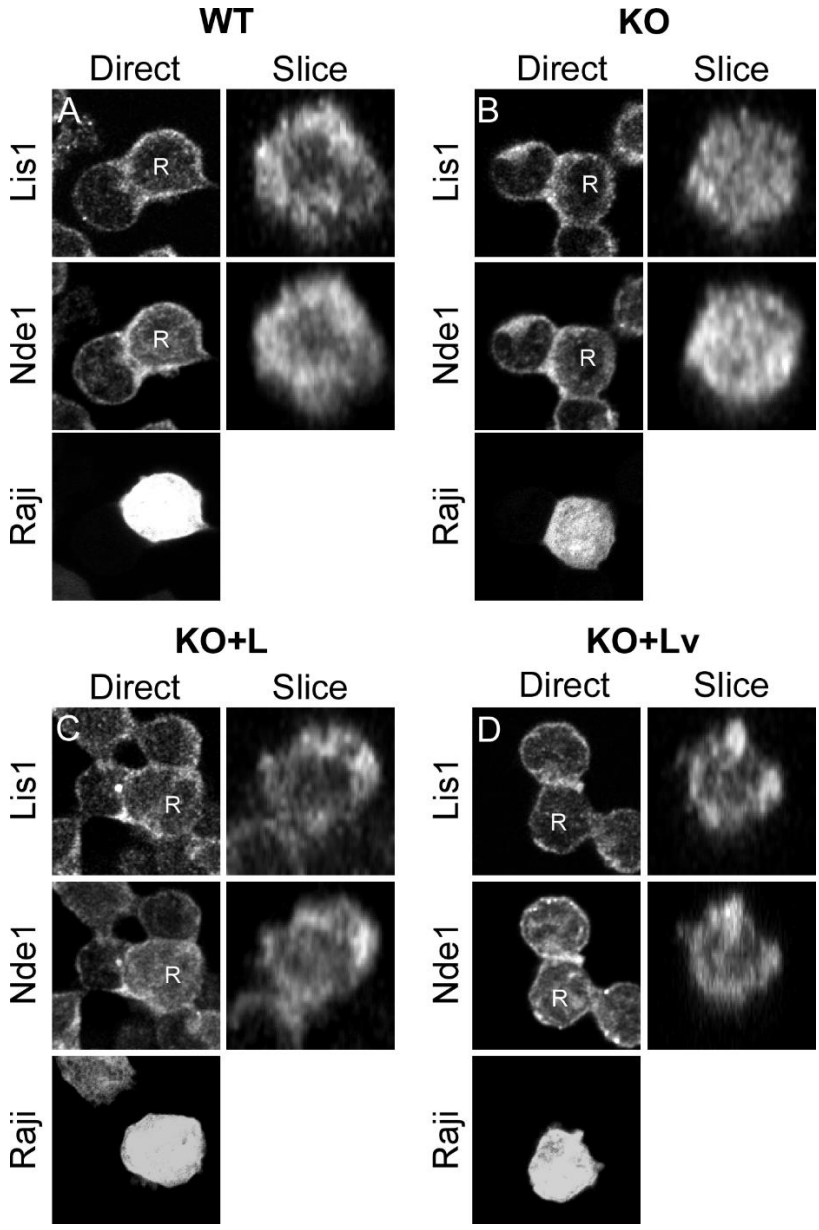

Figure 2.10: Nde1 does not localize into a ring in the absence of DISC1

(A) Wildtype (WT) Jurkat cells, **(B)** DISC1 knockout (KO) Jurkat cells, and DISC1 knockout Jurkat cells transfected with **(C)** DISC1 L-GFP (KO+L) or **(D)** DISC1 Lv-GFP (KO+Lv) were paired with SEE-coated Raji cells and fixed. These samples were immunostained for Nde1 and Lis1. Cell pairs were imaged using confocal microscopy, with Z slices generated at 0.5 micron steps. From direct perspective images of the cell pairs (Direct) and an orthogonal slice of the immunological synapse was generated using the Reslice function in ImageJ (Slice). Slices were cut along an axis through the Jurkat cell at the interface with the Raji cell. Raji cells are marked with 'R'.

Cross-sectional time-lapse of Nde1 at the synapse

In order to see how DISC1 and Nde1 organized at the synapse in real time, and how disruption of DISC1 might affect Nde1, we transfected an Nde1-mCherry construct into wildtype, KO, and KO cells already expressing DISC1 L-GFP or Lv-GFP. We settled these cells onto coverslips coated with Vβ8 TcR antibody and imaged GFP or mCherry fluorescence over the course of 180 seconds. In Jurkat cells expressing DISC1 L-GFP, we observed that DISC1 initially accumulates at a small patch at the IS and then spreads out to form a peripheral ring (Figure 2.11A).

In wildtype Jurkat cells expressing the Nde1 construct, Nde1-mCherry forms a similar pattern as DISC1 L-GFP, initially accumulating at the center before expanding out into a ring (Figure 2.11B). In DISC1 KO cells, Nde1-mCherry never forms a ring and instead stays within a central spot. The ring pattern of Nde1-mCherry was recovered in DISC1 KO cells expressing DISC1 L-GFP, but not in cells expressing DISC1 Lv-GFP. This result was replicated and verified through immunofluorescence of endogenous Nde1 and Lis1 (Figure 2.12A-D). Wildtype OT-1 CTLs and DISC1 knockout OT-1 cells were also compared (Figure 2.12E-F). Like our Jurkat DISC1 KO cell line, the absence of DISC1 in OT-1 DISC1 KO cells was confirmed through Western Blotting (2.12G).

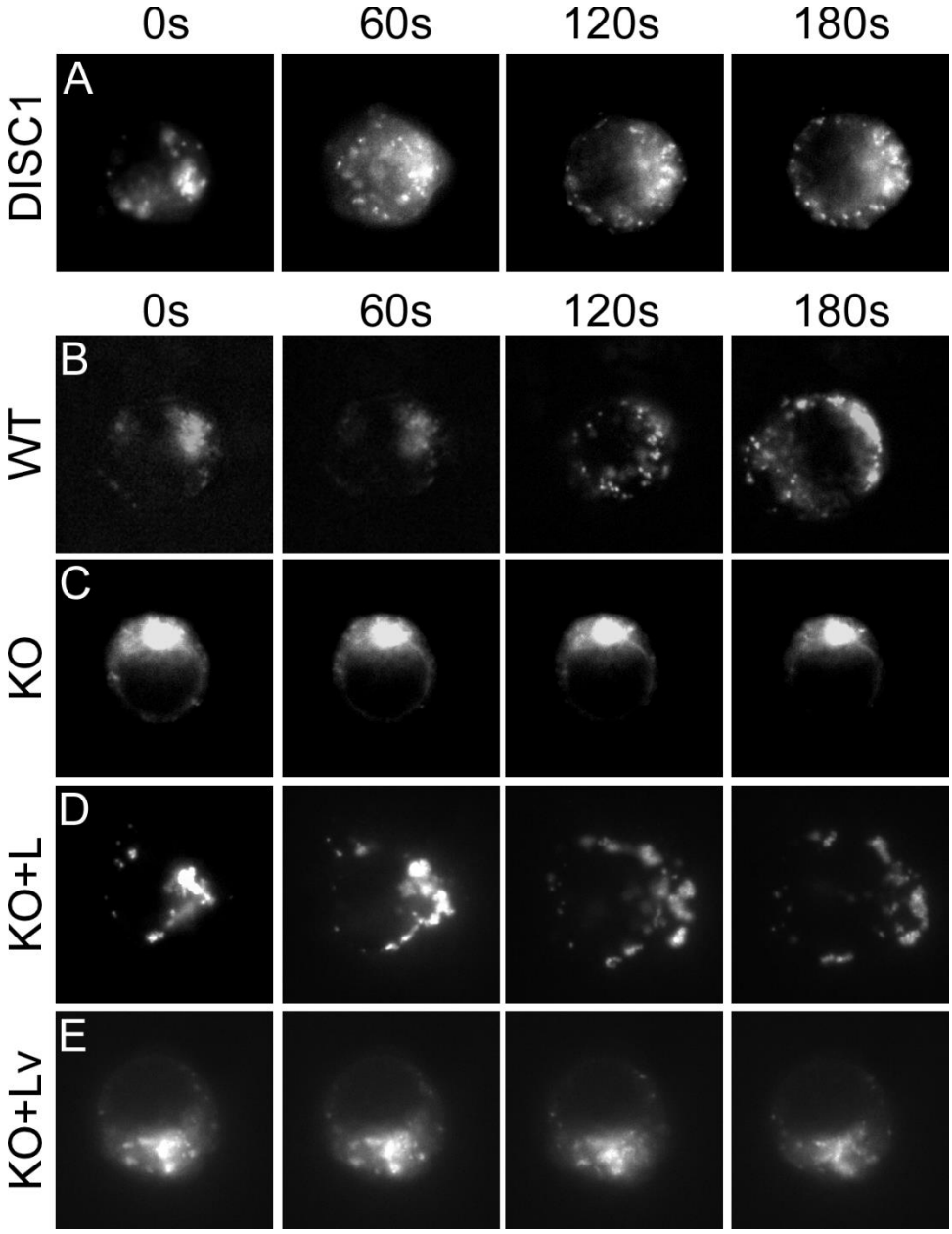

Figure 2.11: The DISC1-dependent movement of Nde1 at the IS

(A) Jurkat cells expressing DISC1 L-GFP were settled onto coverslips coated with Vβ8 anti-TcR antibody. Using standard epifluorescence, pictures were taken using of GFP every 60 seconds to generate a time-lapse. **(B)** Wildtype (WT) Jurkat cells, **(C)** DISC1 knockout (KO) Jurkat cells, **(D)** KO Jurkat cells transfected with DISC1 L-GFP, and **(E)** KO Jurkat cells transfected with DISC1 Lv-GFP were all transfected with an Nde1-mCherry construct. Cells were settled onto coverslips coated with Vβ8 anti-TcR antibody. Using standard epifluorescence, pictures were taken of mCherry every 60 seconds to generate a time-lapse.

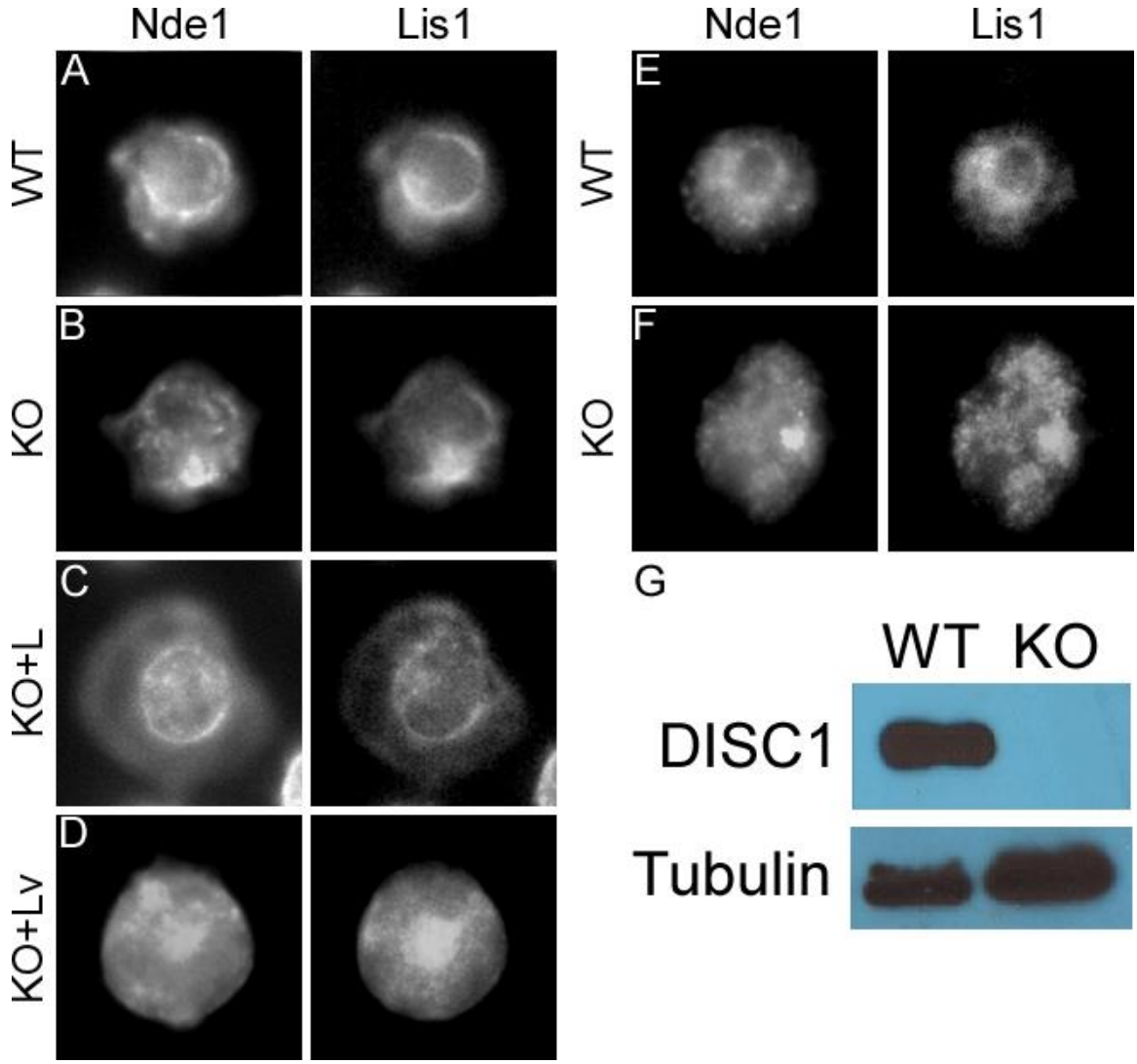

Figure 2.12: Immunofluorescence of Nde1/Lis1 interface in Jurkat and OT-1 cells

(A) Wildtype (WT) Jurkat cells, **(B)** DISC1 knockout (KO) Jurkat cells, **(C)** KO Jurkat cells transfected with DISC1 L-GFP, **(D)** and KO Jurkat cells transfected with DISC1 Lv-GFP were settled onto coverslips coated with Vβ8 anti-TcR antibody, fixed, immunostained for Nde1 or Lis1, and imaged using standard epifluorescence microscopy. The same was done for **(E)** wildtype (WT) OT-1 CTLs or **(F)** OT-1 DISC1 knockout (KO) CTLs. **(G)** DISC1 was assayed in WT and KO cells via Western Blot. No visible DISC1 was detected in the KO cells. Tubulin was used as a loading control.

Cross-sectional time-lapse of dynein at the synapse

Previous results showed that Nde1 was required for accumulation of dynein at the IS. Since loss of DISC1 affected the localization of Nde1 we sought to determine if the distribution of dynein at the IS was similarly affected. To answer this question, a tetracysteine tagged dynein intermediate chain (DIC-TC) was expressed in normal and DISC1 KO Jurkat cells. Proteins bearing the tetracysteine construct can be selectively labeled with the cell permeant fluorescein analog "fluorescein arsenical hairpin binder-ethanedithiol" (FLAsH-EDT2) (Adams et al., 2002). To minimize nonspecific binding, a series of concentrations were initially tested to find the minimum concentration of FLAsH-EDT2 to give adequate labeling. To monitor the cellular location of dynein during T-cell Jurkat cell activation, DIC-TC expressing cells were labeled with FLAsH-EDT2 and settled onto coverslips coated in anti-TcR antibody, then imaged for 180 seconds (Figure 2.12A). The results show that as with Nde1, DIC-TC initially accumulates at the center of the IS and then moves outward to form a peripheral ring corresponding to the pSMAC. However, in DISC1 KO cells, DIC-TC remains at the center of the synapse. Normal movement of the DIC-TC construct was restored when DISC1 isoform L (but not Lv) was re-expressed in the DISC1 KO cells (Figure 2.13B).

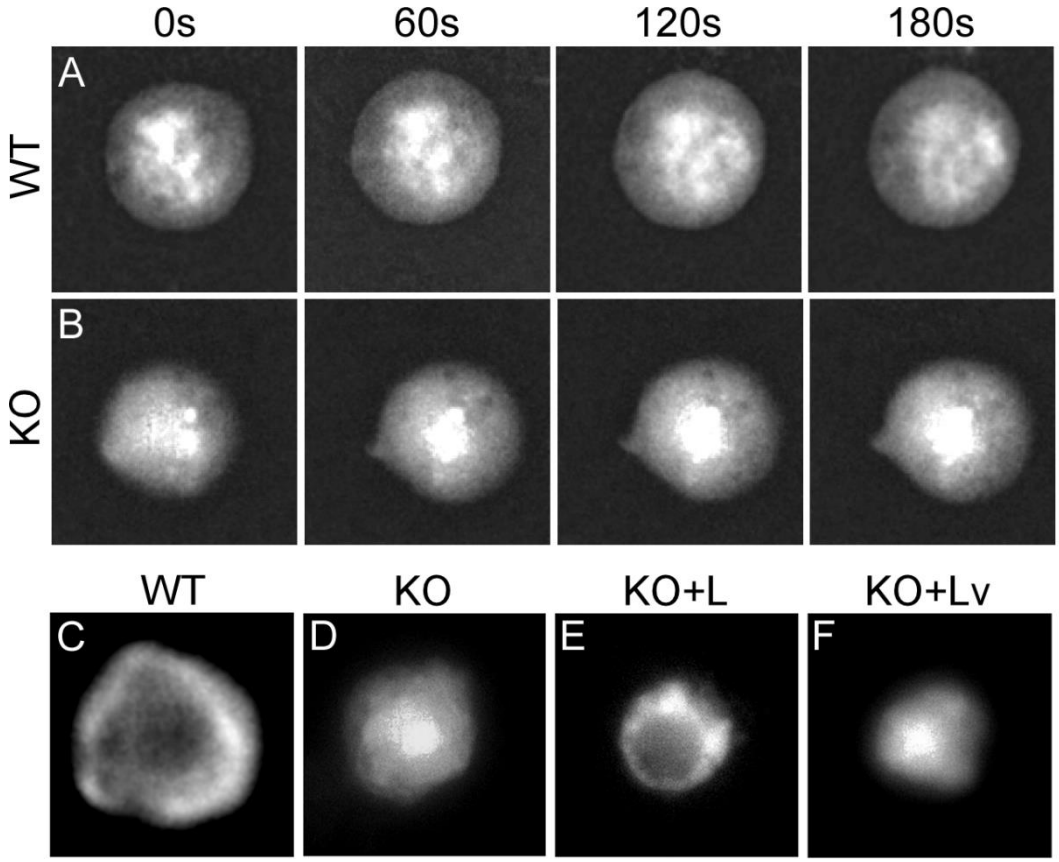

Figure 2.13: The DISC1 dependent movement of dynein at the IS

(A) Wildtype (WT) Jurkat cells and **(B)** DISC1 knockout (KO) Jurkat cells were transfected with a tetracysteine tagged dynein intermediate chain (DIC) construct. Cells were treated with FLAsH-EDT2, settled onto coverslips coated with Vβ8 anti-TcR antibody, and pictures were taken of FLAsH fluorescence every 60 seconds to generate a time-lapse. **(C)** WT Jurkat cells, **(D)** KO Jurkat cells, **(E)** KO Jurkat cells expressing DISC1 L-GFP, and **(F)** KO Jurkat cells expressing DISC1 Lv-GFP were settled onto coverslips coated with Vβ8 anti-TcR antibody, fixed, immunostained, and imaged for DIC.

DISC1 knockout does not reduce CTL cytotoxicity

Next, we investigated how these changes in organization of the dynein complex might affect the ability of mouse CTLs to lyse specific targets. Wildtype or DISC1 KO CTLs were paired and incubated for 6 hours with untreated or peptide-pulsed EL-4 cells at various ratios (E:T 1:1, 4:1, or 10:1). Afterwards, propidium iodide (PI) was added to label

dead cells. Flow cytometry was then used to quantify PI-stained dead cells and CFSE-stained target cells (Figure 2.14A). We found no significant difference in target killing between wildtype and DISC1 CTLs ($p < 0.001$).

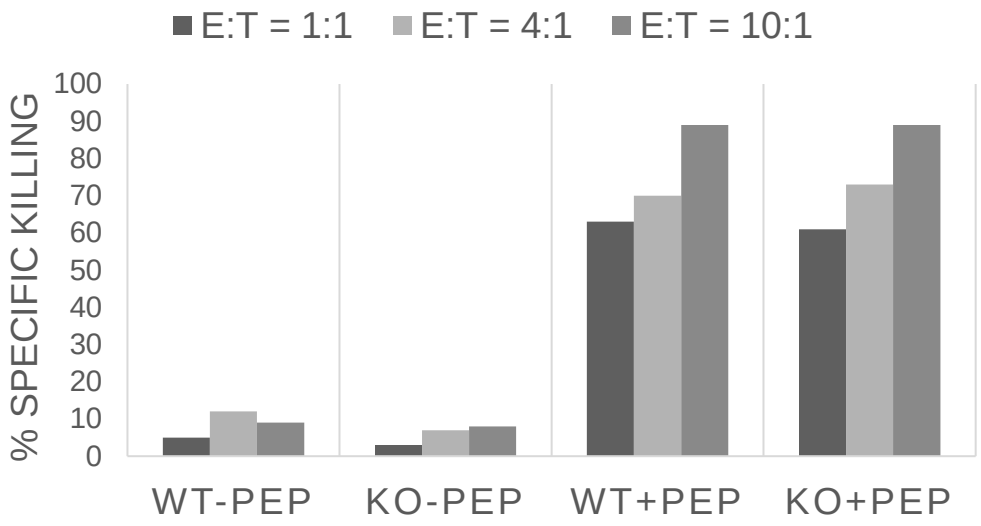

Figure 2.14: DISC1 is not needed in mouse CTL killing

Wildtype OT-1 CTLs (WT) and OT-1 DISC1 KO cells (KO) were mixed with EL-4 target cells at different effector to target ratios (E:T) for 6 h. EL-4 cells were either untreated (-pep) or pretreated with SIINFEKL peptide (+pep) as indicated. Target cell lysis was measured by flow cytometry and is presented as specific lysis percentage of the total target cells used for each assay condition.

DISC1 knockout does not inhibit the organization of LFA-1 or TcR

Finally, to determine if receptors at the IS still organize into the cSMAC and pSMAC we examined the distribution of CD3 and LFA-1 using Cy5-ICAM and FITC labeled anti-CD3 Ig anchored to supported lipid bilayers, as described in Stebvlanko et al., 2018. Cells from normal Jurkat, DISC1 KO, and DISC1 KO cells re-expressing DISC1 L-GFP or Lv-GFP were settled on the bilayers (Figure 2.15). No dramatic difference was observed in any of the cells tested.

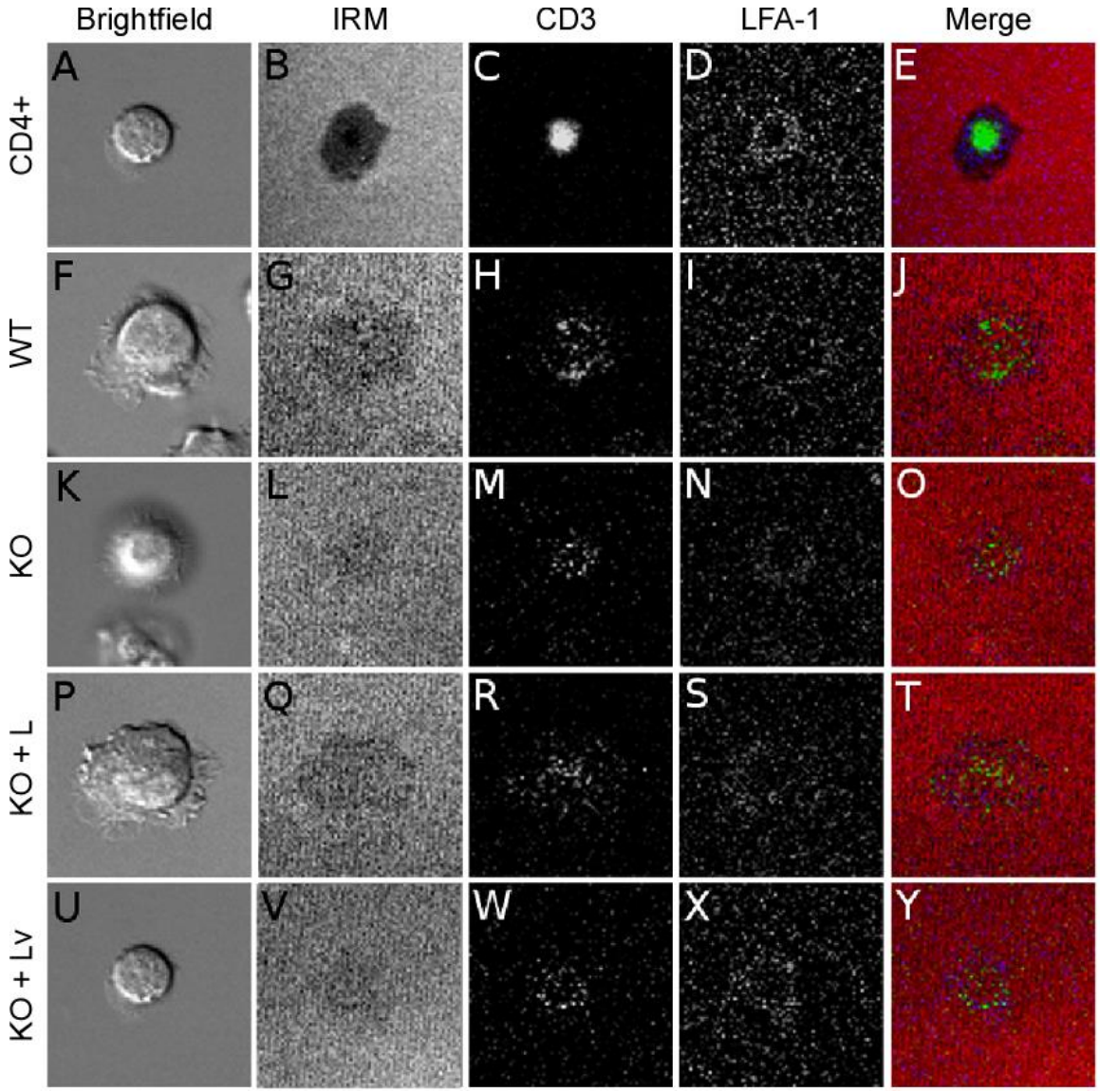

Figure 2.15: DISC1 depletion does not affect the organization of the cSMAC or pSMAC

Human CD4+ T-cells derived from PBMCs **(A-E)**, wildtype (WT) Jurkat T-cells **(F-J)**, DISC1 knockout (KO) Jurkat cells **(K-O)**, and DISC1 knockout Jurkat cells transfected with DISC1 L-GFP (KO+L) **(P-T),** or DISC1 Lv-GFP (KO+Lv) **(U-Y)** were settled onto planar bilayers containing fluorescently labeled ICAM1 and anti-CD3 antibody. Cells were then imaged at their interface through confocal microscopy. **(A, F, K, P, U)** Brightfield images of T-cells settled onto bilayer. (**B, G, L, Q, V)** Contact site between the cell and the bilayer taken with Interference Reflection Microscopy (IRM). **(C, H, M, R, W)** CD3 at the contact site visualized through fluorescent anti-CD3 antibody. **(D, I, N, S, X)** LFA-1 integrin at the contact site visualized through Cy5-ICAM1. **(E, J, O, T, Y)** Merged image of IRM, CD3, and LFA-1.

DISCUSSION

To our knowledge, this study is the first to directly document the effects of DISC1 in T-cells. In this study, we have observed DISC1 expressed in Jurkat cells and OT-1 cytotoxic T-lymphocytes (CTLs). Further, our work has shown two expressed isoforms, DISC1 L and Lv. This is unsurprising, as these two isoforms are the most widely expressed in humans (Taylor, Devon, Millar, & Porteous, 2003). The novel contribution of this work was the observation of that these isoforms have different localization in Jurkat cells, as seen with our N-terminal GFP constructs. We found Lv localized around mitochondria, whereas L accumulated at the IS. This result explained our earlier immunofluorescence findings whereby DISC1 was stained at both the IS and in puncta depending on the antibody used.

The finding that DISC1 Lv is associated with mitochondria and is needed for mitochondrial accumulation at the IS is similar to data obtained from neuronal cells (Norkett et al., 2016). Previous studies have shown that DISC1 is associated with the mitochondrial transport and fusion machinery through the interaction with the outer mitochondrial membrane GTPase proteins Miro1 and Miro2, the TRAK1 and TRAK2 mitochondrial trafficking adaptors, and the mitochondrial fusion proteins (mitofusins) (Norkett et al., 2016). Furthermore, the DISC1-TRAK-Miro complex is essential for mitochondria movements in neurons (Norkett et al., 2016). These movements are bi-directional, linking to dynein through the dynactin complex (Morlino et al., 2014) and to kinesin (Randall et al., 2013).

Mitochondria are known to take up calcium in a high capacity but low affinity manner. Through their accumulation at the IS, it is thought that mitochondria function as a calcium sink that prevents inactivation of calcium channels (Schwindling, 2010). It is also believed that mitochondria elevate ATP at the IS (Ledderose et al., 2014). This is supported

by studies showing that depolarization of mitochondria at the IS inhibits TcR accumulation at the IS (Baixauli et al., 2011).

Due to the link between mitochondria and sustained calcium signaling in T-cells (Gunter & Pfeiffer, 1990), we tested whether DISC1 KO cells affected calcium influx upon TcR stimulation. We did not observe a difference in the amplitude or timing of TcR-stimulated calcium influx between wildtype and DISC1 KO Jurkat cells. One potential explanation for this is that antibody stimulation of TcR is non-polarizing compared to stimulation through a synapse. Polarization of the mitochondria to the IS may be a necessary factor in the mitochondria-dependent effects on T-cell activation. In order to track polarized calcium influx during T-cell activation, imaging T-cell/target pairs with a calcium tracking dye like fura-2 may be necessary.

Our data show that DISC1 KO inhibits complete MTOC translocation to the synapse, which was only restored by expressing DISC1 L. DISC1 is a binding partner with Nde1/Lis1 and colocalizes with the complex at the IS. Previous studies showed that Nde1 is essential for MTOC translocation to the IS (Nath et al., 2016). While the MTOC does still approach the synapse in DISC1 KO, it gets much closer to the IS in wildtype Jurkat cells. We found that DISC1 L determines the location of Nde1, Lis1, and dynein at the synapse during T-cell activation, which might explain the subtle defects seen in MTOC translocation. The movement of these factors also explain some previous observations of MTOC translocation seen by Kuhn & Poenie (2002). In that study, modulated polarization microscopy was used to track MTOC movements in living T-cells. They showed that the MTOC initially moved in essentially a straight line towards the IS. Then, as it neared the IS, it began oscillating back and forth along the contact site. This suggests that initial movements of the MTOC to the synapse are mediated by the DISC1/Nde1/Lis1/dynein complex located at the center of the IS. Then, when the dynein complex expands to form a

ring corresponding to the pSMAC, the MTOC is pulled towards the edges of the ring where the dynein complexes are located. Competing dynein activity at different positions around the ring then give rise to the observed oscillatory MTOC movements.

It is interesting to consider why this complex moves from the center of the IS to the pSMAC. Similar observations have been reported where visible accumulation of actin begins at the center of the IS and then spreads peripherally to form a ring that first overlaps with, then extends past, the pSMAC giving rise to what is called the D ring. These observations suggest that the DISC1/Nde1/Lis1/dynein complex might be tied to the actin cytoskeleton and move with it. In support of this, the clearance of actin from the cSMAC happens concurrently with MTOC polarization (Ritter et al., 2015). However, based on the data collected it does not appear as though the movement of dynein from the cSMAC is needed for the secretion of cytolytic vesicles, as we found DISC1 seems to be entirely dispensable in CTL killing.

Focused secretion requires MTOC polarization, as well as Nde1 and dynein (Nath et al., 2016; Ogbomo et al., 2018). It is therefore plausible to imagine a model in which the movement of dynein from the cSMAC to the pSMAC facilitates a focused secretion zone at the cSMAC, which could be important for specific on-target killing. To account for this, future experiments examining the effects of DISC1 depletion on CTLs will measure for non-specific bystander killing.

In addition to specificity, focused secretion at the cSMAC could improve turnover and lead to more efficient, serial killing of targets. Beal et al. (2009) showed that aberrant signaling during T-cell activation could lead to secretion outside the bounds of the cSMAC. This led to less efficient killing, as vesicles took longer to reach peripheral secretion sites (Beal et al., 2009). To test whether DISC1 depletion might affect this, future experiments could expand the conditions of the killing assay to include a greater ratio of targets to

effector cells. Alternatively, live imaging could be used to measure the length of time involved in CTL to target engagement.

Beyond cytolytic granule secretion, the proper orientation of the MTOC is also important in the efficient deregulation of activation signaling at the IS (Griffiths, Tsun, & Stinchcombe, 2010). The positioning of the MTOC directly adjacent to the cSMAC promotes the accumulation of cSMAC-derived endosomes containing TcR, LAT, and Lck (Finetti et al., 2014; Finetti et al., 2017; Hu et al., 2016; Martínez-Martín et al., 2011; Wi et al., 2016). This trafficking process is remarkably similar to intraflagellar trafficking that occurs at the primary cilia of most cells, as several ciliary assembly proteins have been shown to localize to the MTOC and IS where they participate in this process (Finetti et al., 2014; Galgano et al., 2017; Vivar et al., 2016). Some of these proteins, like IFT20 and IFT54, are also DISC1 binding partners (Berbari et al., 2011; Camargo et al., 2007). In fact, in neurons DISC1 has been shown to be connected to receptor targeting at the primary cilia, and to ciliary growth in general (Marley & von Zastrow, 2010). Given this connection, DISC1 may regulate a similar process at the IS through the correct positioning of the MTOC. Future work should explore the interactions between DISC1 and IFT20 and IFT54 at the IS and determine whether DISC1 KO influences the accumulation of receptor-rich endosomes during IS formation.

In summary, the data presented shows that independent isoforms of DISC1 are needed in order to get complete mitochondria and MTOC translocation in T-cells. In the case of the latter effect, we found that Nde1/Lis1/dynein, the complex that drives MTOC translocation to the IS, requires DISC1 in order to properly organize at the pSMAC. Additional research is required to understand the full effects that DISC1 has on T-cell signaling and effector function. Given the link between mitochondria translocation to calcium and TcR signaling (Baixauli et al., 2011), Nde1/dynein to secretion (Nath et al.,

2016), and MTOC positioning to receptor endocytosis at the cSMAC (Griffiths, Tsun, & Stinchcombe; 2010), there are many pathways by which DISC1 could affect activation. Further experiments are necessary in order to place the observations made in this study within the larger scope of the immune response.

Chapter 3: DISC1, actin organization at the immunological synapse

INTRODUCTION

One of the prominent features of the immunological synapse is the accumulation of actin which begins at the center or cSMAC of the synapse and then spreads peripherally while clearing in the center. However, this rather straightforward pattern of actin dynamics does not fully account for the complexity of actin assembly nor its various functions in T cells. Defects in proper actin assembly are associated both with immunodeficiency and autoimmune dysfunctions (Wickramarachchi, Theofilopoulos, & Kono, 2010). Of the known functions associated with actin the regulation of stable adhesions, formation of TcR microclusters needed for sustaining antigenic signaling, calcium entry, and target-specific secretion (Hammer, Wang, Saeed, & Pedrosa, 2018).

Efforts at dissecting the regulation of actin at the IS have shown that there are multiple actin nucleators that can be broadly divided into Formin-mediated nucleators which generate straight actin filaments and nucleators that act through ARP 2/3 to generate branched actin filaments. These nucleators apparently compete for the same pool of actin since Formin inhibitors like SMIFH-2 enhance Arp2/3-dependant structures at the IS, while Arp2/3 inhibitors such as CK666 enhance Formin-dependent structures (Murugesan et al., 2016).

In T cells, the Formins mDia-1 and FMNL-1 form concentric arcs of straight actin filaments that prominent across the pSMAC (Murugesan et al., 2016). Myosin IIA organizes these filaments into bundles that move in a retrograde flow from the inner boundary of the dSMAC towards the cSMAC where the flow appears to end (Yi, Wu, Crites, & Hammer, 2012). This continuously cycling network connects to LFA-1 and TcR microclusters, which are located at the pSMAC and cSMAC, respectively (Comrie, Babich,

& Burkhardt, 2015). Adapter proteins Talin and Vinculin act as “clutch” molecules that connect LFA-1 to this flow and through tension converts LFA-1 into a high affinity state (Nolz et al., 2007).

At the dSMAC, Arp2/3-nucleated filaments form a lamellipodial actin network that extends radially to the synapse periphery. This is facilitated by the activation of the Rho family GTPases Cdc42 and Rac-1, which in turn activate the nucleation promoting factors Wiskott-Aldrich Syndrome Protein (WASp) and WASp-verprolin homologous protein 2 (WAVE2), respectively. WASp is recruited to the TcR at discrete microclusters within the dSMAC (about 33% of total TcR microclusters), where it acts as foci for de novo actin polymerization (Kumari et al., 2015). WASp mutant T-cells have minor defects in calcium signaling and IL-2 production, which is likely due to the blocked signaling between these foci and PLCγ (Cannon & Burkhardt, 2004; Kumari et al., 2015). WASp knockouts also have greater difficulty maintaining synapse symmetry and stability (Sims et al., 2007). These findings led Kumari, Curado, Mayya, and Dustin to hypothesize that WASp establishes nuclei of new actin to assist in “repairing” the dSMAC (Kumari, Curado, Mayya, & Dustin, 2014). Yet despite all these proposed effects, loss of WASp leads to relatively few gross changes in actin structure (Kumari et al., 2015).

WAVE2 accumulates at the dSMAC, although it is most prominent at the leading edge of lamellipodial protrusions which are constantly extending and retracting over the target cell (Nolz et al., 2006). Compared to WASp knockdown, T-cells depleted of WAVE2 do not properly form lamellar actin at the dSMAC and have difficulty spreading across target surfaces (Nolz et al., 2006). WAVE2 is also needed to recruit Talin to the IS and promote the high affinity form of LFA-1, while WAVE2 depleted T-cells have difficulty maintaining adhesions with targets (Jankowska et al., 2018; Nolz et al., 2006; Nolz et al., 2007). While depletion of WASp and WAVE2 affect calcium signaling at the

IS, WAVE2's effects are independent of PLCγ (Nolz et al., 2006). The current evidence is that they are somehow regulating activation of the calcium release activated channels (CRAC channels). From all of this it is evident then that WASp and WAVE2 have distinct effects and their functions extend beyond simply nucleating actin.

Signaling of WASp, WAVE2, and other elements affecting Arp2/3

The actin nucleators WASP and WAVE2 are activated by RAC and possible Cdc42 which in turn depend on the guanine nucleotide exchange factors (GEFs) that include the DOCK180 superfamily and Vav. Vav is activated through the TcR /LAT/SLP-76 or ADAP/SLP-76 (Baker et al., 2009; M. Ku, Yablonski, Manser, Lim, & Weiss, 2001; Tybulewicz, 2005). Interestingly, there is some evidence that indicates that Vav promotes Rac-1 and Cdc42 activation outside its normal GEF function (Miletic et al., 2009). This would suggest that GTP exchange at Rac-1 and Cdc42 is instead facilitated by other GEFs, such as the Dock180 superfamily (Laurin & Côté, 2014). Supporting this idea, Dock2 and Dock8 have been shown to be necessary for the respective accumulation of Rac-GTP and Cdc42-GTP during T-cell cell activation, and knockout of Dock2 causes a similar depletion of lamellar actin at the IS as WAVE2 knockdown (Janssen et al., 2016; Sanui et al., 2003).

Dock180-family proteins are recruited to areas dense in the lipid phosphatidylinositol (3,4,5) trisphosphate (PIP3) (Laurin & Côté, 2014). Phospho-inositol dynamics at the membrane appear to heavily affect the activation and clearance of actin at the IS (Huse, 2014). PIP3 also promotes the activation of Akt, which itself is known to regulate Cdc42 and Rac-1 during IS formation (Carlin et al., 2011; Sánchez-Martín et al., 2004). Both TcR and LFA-1 are known to activate PI3-Kinase, which subsequently enriches the membrane in PIP3 (Sánchez-Martín et al., 2004; Shim, Jung, & Lee, 2011). As clustered TcR and LFA-1 are both sites of actin signaling at the IS, all this suggests that

they maintain PIP3-rich zones for recruiting actin-regulating factors like Dock2, Dock8, and Akt. Thus, while there is progress unraveling pathways signaling to the actin cytoskeleton, much remains uncertain as to how these various signaling pathways are regulated, how they direct specific actin functions and how these orchestrate various T cell functions.

LFA-1, DISC1, and Girdin

Studies detailed in this chapter extend the complexity of actin regulation by introducing the new players, Disrupted in Schizophrenia (DISC1) and Girdin. While the function of these proteins has not been previously described in T cells, they have been studies in some detail in neurons. For example, in neurogenesis DISC1 has been linked to formation of actin-based dendritic spines, and to the motility of cortical interneurons which depend on Girders of Actin Filaments (Girdin) (Hayashi-Takagi et al., 2010; Steinecke, Gampe, Nitzsche, & Bolz, 2014). In addition to being an actin crosslinker, Girdin has also been shown to have GEF activity, which leads to the activation of RhoA and Cdc42 in human epithelial cells (Leyme, Marivin, Perez-Gutierrez, Nguyen, & Garcia-Marcos, 2015). Girdin regulates integrin signaling in Glioblastoma and this depends on both DISC1 and AKT (Gu et al., 2014) (Leyme et al., 2015; Steinecke et al., 2014). Here, the Girdin/DISC1 complex recruits PI3K and facilitates Akt phosphorylation in a positive feedback loop (Leyme, Marivin, & Garcia-Marcos, 2016; Steinecke et al., 2014)

Actin and LFA1 are prominent components of the pSMAC where DISC1 and Girdin accumulate. However, as we show, DISC1-Girdin, NDE1, and dynein all initially accumulate at the center of the IS and them move to the periphery, reminiscent of the movements of actin. We show that DISC1 links to Talin and thus likely also to LFA-1 at the pSMAC. Knockout of either DISC1 or Girdin greatly diminishes the formation of actin

at the IS in both Jurkat T-cells and mouse OT-1 CD8+ cells. Finally, we show that actin inhibitors prevent dynein and other DISC1 binding partners from accumulating at the IS. In summary, our findings indicate that the DISC1/Girdin complex becomes associated with the IS through LFA-1 and actin and promotes a novel signaling pathway for actin formation at the IS.

MATERIALS AND METHODS

Cell lines, reagents, and antibodies

The Jurkat (E6.1) T lymphocytes and Raji B lymphocytes were obtained from the American Type Central Collection. Opti-MEM cell media (Cat # 31985062) was obtained from Gibco Thermo-Fisher. Heat-inactivated fetal bovine serum (FBS) was obtained from Atlas Biologicals (Cat # F-0500-D). The 4 mm gap transfection cuvettes were obtained from Fisher Scientific (Cat # FB104). Goat serum (Cat # G2093), poly-l-lysine (Cat # P2636), and Cytochalasin B (Cat # C6762) were obtained from Sigma-Aldrich. SuperSignal West Pico chemiluminescent substrate solution (Cat # 34580) and X-ray film (Cat # 34090) were obtained from Thermo Scientific. G418 Sulfate was purchased from Gold Biotechnology (Cat # G-418-5). All restriction enzymes were obtained from New England Biolabs. Mini Plasmid and Midi Fast Ion Plasmid Kits were obtained from IBI Scientific (Cat # IB47111, IB47111). Xfect transfection reagent was obtained from Clonetech (Cat # 631318). ProLong Gold Anti-Fade Mounting Reagent was obtained from Life Technologies (Cat # P36930). The Cas9, DISC1, and Girdin sgRNA plasmids were obtained from Genecopoeia (Cat # CP-LvC9NU-02-B, HCP268459-LvSG03-1-B, HCP259879-LvSG03-1-B). Partially purified Staphylococcus Enterotoxin E (SEE) was obtained from Toxin Technologies (Cat # ET404).

DISC1 rabbit polyclonal antibody (Cat # PA2023) and Talin mouse monoclonal antibody (Cat # MA1092) were obtained from Boster Biological. CCDC88A (Girdin) rabbit polyclonal antibody (Cat # A16132) was obtained from Abclonal. Lis1 mouse monoclonal antibody (Cat # L7391), GFP polyclonal rabbit antibody (Cat # G1544), and beta-tubulin mouse monoclonal antibody (Cat # T8328) were obtained from Sigma-Aldrich. The TcR Vβ8 mouse monoclonal antibody was obtained from BD Biosciences (Cat # 555604). Goat anti-rabbit AlexaFluor 594 conjugated antibody (Cat # A11037) and goat anti-mouse FITC conjugated antibody (Cat # F2012) were obtained from Invitrogen. Goat anti-mouse horse radish peroxidase (HRP) conjugated antibody (Cat # A9917) and goat anti-rabbit HRP conjugated antibody (Cat # A0545) were obtained from Sigma-Aldrich. Cell Tracker Blue (CTB; Cat # C2110) was obtained from Invitrogen. TRITC conjugated Phalloidin (Cat # P-1951) was obtained from Sigma-Aldrich.

Jurkat and Raji cells were grown RPMI 1640 supplemented with 24 mM sodium bicarbonate, 1 mM sodium pyruvate, 2 mM l-glutamine, 50 µM beta-mercaptoethanol, 10,000 U/mL penicillin, 10 mg/mL streptomycin, and 10% (v/v) FBS (ACC growth media).

DNA constructs

We began identifying possible DISC1 isoforms expressed in Jurkat cells by adapting an RT-PCR method used by Nakata et al (2009). First, total Jurkat mRNA was isolated using the RNeasy Midi Kit. This mRNA was converted into a cDNA library using a MMLV reverse transcriptase kit. Using eight different sets of primers, DISC1 exon fragments were identified from this cDNA library through PCR (Table 1). Through this

method, DISC1 L and Lv isoforms were identified and verified through Sanger sequencing on an Applied Biosystems 3730 DNA Analyzer (UT ICMB Core Facilities).

Full sized DNA fragments for DISC1 isoform L and Lv were synthesized through PCR of Jurkat cDNA. A tagless DISC1 construct was made by making DNA fragments of DISC1 isoform L and Lv containing the XhoI and XmaI restriction sites. These fragments were inserted into a peGFP-N1 vector which contained a premature stop codon at the start of the GFP sequence, created through site directed mutagenesis.

Full-sized Girdin DNA fragments were derived from our Jurkat cDNA library using PCR. A C-terminal GFP-tagged Girdin construct was made by first adding XhoI and XmaI restriction sites to the ends of Girdin DNA fragments. These fragments were then inserted into a peGFP-N1 plasmid. We used a peGFP-C1 plasmid which contained a monomeric GFP sequence, using PCR point editing to change the 206th amino acid from an alanine to a lysine.

All DNA constructs were transformed from frozen aliquots of competent bacteria suspended in CaCl2 solution. These aliquots were thawed and mixed with DNA constructs, then put through heat shock at 43°C. Depending on the concentrations needed, DNA constructs were isolated using the Mini Plasmid or Midi Fast Ion Plasmid Kits and plasmid sequences were verified by Sanger sequencing. DNA was introduced into Jurkat cells through electroporation. For the transformation, Jurkat cells were washed and resuspended in Opti-MEM reduced serum media at a cellular concentration of 2×10^7/mL and incubated with 10µg of plasmid DNA 15 minutes at 37°C. Cells were placed in 4mm gap transfection cuvettes and pulsed at 250V (950µF) using the Gene Pulser Electroporation System (Bio-Rad). After electroporation, cells were resuspended in fresh ACC growth media. Cells containing constructs were grown under selection with 1 mg/mL G418. Selection began 24

hours post-transfection and continued for two weeks. Afterwards sorted for the expression of fluorescent proteins using FACSAria cell sorter.

CRISPR/Cas9 gene knockouts

A DISC1 or Girdin sgRNA plasmid and a Cas9 plasmid were transfected into the Gryphon viral packaging cell line using the Xfect transfection reagent. Fresh growth media was added 4 hours post-transfection. Forty-eight hours after transfection, the supernatants containing the viral particles were collected. For transduction, 2×10^6 Jurkat cells in six well plates were spinfected at 500 × g and 30°C for 1 hour with media containing viral particles and 8 µg/mL polybrene. Spinfection through centrifugation was repeated every 12 hours for 36 hours. After the final centrifugation, the media was replaced with fresh growth media. Successful transduction was confirmed through observation of GFP and mCherry fluorescent proteins expressed by the Cas9 and sgRNA plasmids. Complete knockout of DISC1 in culture was achieved through FACSAria sorting of GFP and mCherry expressing cells, followed by verification through DISC1 Western blotting of the resultant cells. Cells were grown under selection with 1 mg/mL G418 Sulfate and 2 µg/mL puromycin. Selection began 36 hours post-transduction and continued for two weeks until sorting was conducted with a FACSAria cell sorter.

Preparation of cell conjugates for staining

To prepare coverslips for cell staining and fluorescent microscopy, coverslips were first cleaned with a 9:1 mixture of ethanol and 1M KOH for 1 hour. They were then washed

in dH2O and coated with an aqueous solution of 0.1 µg/mL 30,000-70,000 kDa poly-l-lysine. These were rinsed again in dH2O and left to dry for 30 minutes at room temperature.

To prepare Jurkat-Raji cell conjugates, Raji cells were suspended at a cellular concentration of 1×10^6/mL in serum-free1 RPMI 1640 and treated with SEE at 1 µg/mL for 1 hour at 37°C. They were subsequently stained with 10µM of CTB for 15 minutes at 37°C. In experiments using Cytochalasin B (Cyt-B), Jurkat cells were treated with 20 µg/mL Cyt-B for 1 hour. Both Jurkat and Raji cells were washed with ACC media, paired at ratio of 3:2 Jurkat to Raji cells, and centrifuged at a light speed (500 g) for 5 minutes. Cells were then washed again with ACC and settled on poly-l-lysine coated coverslips at a total concentration of 1×10^6/mL for 15 minutes.

For immunostaining, cells settled on coverslips were fixed with a Phosphate Buffered Saline (PBS) solution of 1% paraformaldehyde for 30 minutes before being washed with PBS. Cells were then permeabilized with a 1:1 solution of ice-cold methanol and acetone for 15 minutes. Cells were washed again with PBS and blocked with a PBS solution of 5% goat serum and 0.5% Tween-20 for 30 minutes. Cells were then stained with a 1:50 solution of primary antibody in blocking solution for 1 hour. After primary antibody staining, the cells were then washed again with PBS and stained with a 1:100 solution of secondary antibody or TRITC-Phalloidin in blocking solution for another hour. After a final wash with PBS the coverslips were mounted onto slides with ProLong Gold antifade reagent overnight at room temperature before being stored long-term at -20°C.

Immunoprecipitation and Western blotting

Jurkat cells meant to be stimulated prior to lysis and immunoprecipitation were pelleted at 750 × g and resuspended in RPMI at a cellular concentration of 1×10^6/mL.

Cells were treated with 500 ng/mL Vβ8 anti-TcR antibody and incubated at 37°C for 30 minutes. After that, cells were pelleted at 750 × g and resuspended in lysis buffer containing 200 mM NaCl, 50 mM Tris at pH 8, 2 mM EDTA, 2 mM NaVO4, 20 mM NaF, 3 mM PMSF, 2 mM Imidazole, 1 mM Na-β-glycerophosphate, and 1% Triton X 100. The suspension was then passed through a 21-gage needle repeatedly to homogenize and clarified at 16,000 × g and 4°C for 10 minutes to remove cell debris.

To prepare beads for immunoprecipitation, 5 µg antibody was added to 300µL PBS and 80µL of a 50% slurry of Protein A Agarose beads. This solution was mixed gently on a rotator overnight at 4°C. The next day, beads were washed with cell lysis buffer for 15 minutes and added to cell lysate made from 1×10^7 Jurkat cells as previously described. Cells were then incubated on a rotator at 4°C for 2 hours. Afterwards, cells were washed with PBS 4 times before being mixed with SDS-PAGE loading buffer and boiled for 5 minutes to unbind collected protein from the agarose beads. The lysate was then mixed with SDS-PAGE loading buffer to a final concentration containing 2% (w/v) SDS and 5% (v/v) β-mercaptoethanol.

Samples prepared in SDS-PAGE sample buffer were run through SDS-PAGE and transferred to nitrocellulose paper for Western blotting. Samples were blocked in a blocking solution of TBS with 0.1% Tween and 5% BSA. Primary antibody was then added, diluted to a concentration of 1 µg/mL in blocking solution. Primary antibodies were tagged with HRP using a goat anti-rabbit or goat anti-mouse HRP conjugated secondary antibody and treated with SuperSignal West Pico chemiluminescent substrate solution before being exposed to X-ray film.

Imaging and data processing

Images were viewed using a Nikon inverted microscope and captured using a CMOS camera. The images were processed and analyzed using the ImageJ processing software. In order to determine protein accumulation at the synapse, a line of length 230 pixels and width 70 pixels was drawn on the Jurkat-Raji cell pairs such that the mid-point of the line (pixel 115) was on the synapse. Background intensity was obtained from a region outside the cell pairs and subtracted from the fluorescence intensity. The fluorescence was normalized by dividing all the pixel measurements by the average intensity of the row furthest away from the synapse. Beginning at the synapse (row 115), intensity values for five-pixel groups were treated as one increment and used for statistical analysis (mean ± SE of the mean). The compound mean and standard error for the increments were plotted against mean intensity of fluorescence. A one-tailed T-test with independent variance was performed for the increments starting from the synapse and moving to the back of the Jurkat cell.

Cross-sectional imaging of the IS was taken with a Zeiss LSM 710 confocal microscope from the University of Texas ICMB core facilities. Image processing was done by reslicing z-stacks of images using ImageJ.

RESULTS

DISC1 isoform L promotes actin polymerization at the immunological synapse

Rhodamine-phalloidin staining of fixed Jurkat/Raji pairs reveals strong actin accumulation in normal Jurkat cells stimulated with SEE-coated Raji cells. The presence of detectable actin at the IS significantly diminished in DISC1 KO Jurkat cells compared to wildtype controls (Figure 3.1A-C, $p < 0.001$). The transfection of a tagless DISC1

isoform L construct into DISC1 KO cells was observed to recover the presence of an actin band, although a similar DISC1 isoform Lv construct did not (Figure 3.1D-E). Using DISC1 KO cells expressing GFP tagged DISC1 constructs (prepared as described in Chapter 2), we found that cells expressing a tagged DISC1 isoform L or Lv did not form an observable band of actin at the IS (Figure 3.1F-G). Imaging a cross-section of the immunological synapse through confocal microscopy showed that actin is still present at the IS in DISC1 KO cells, though greatly diminished compared to wildtype (Figure 3.2A-B). All traces of actin at the IS can be eliminated in DISC1 KO cells further treated with Latrunculin B (Figure 3.2C).

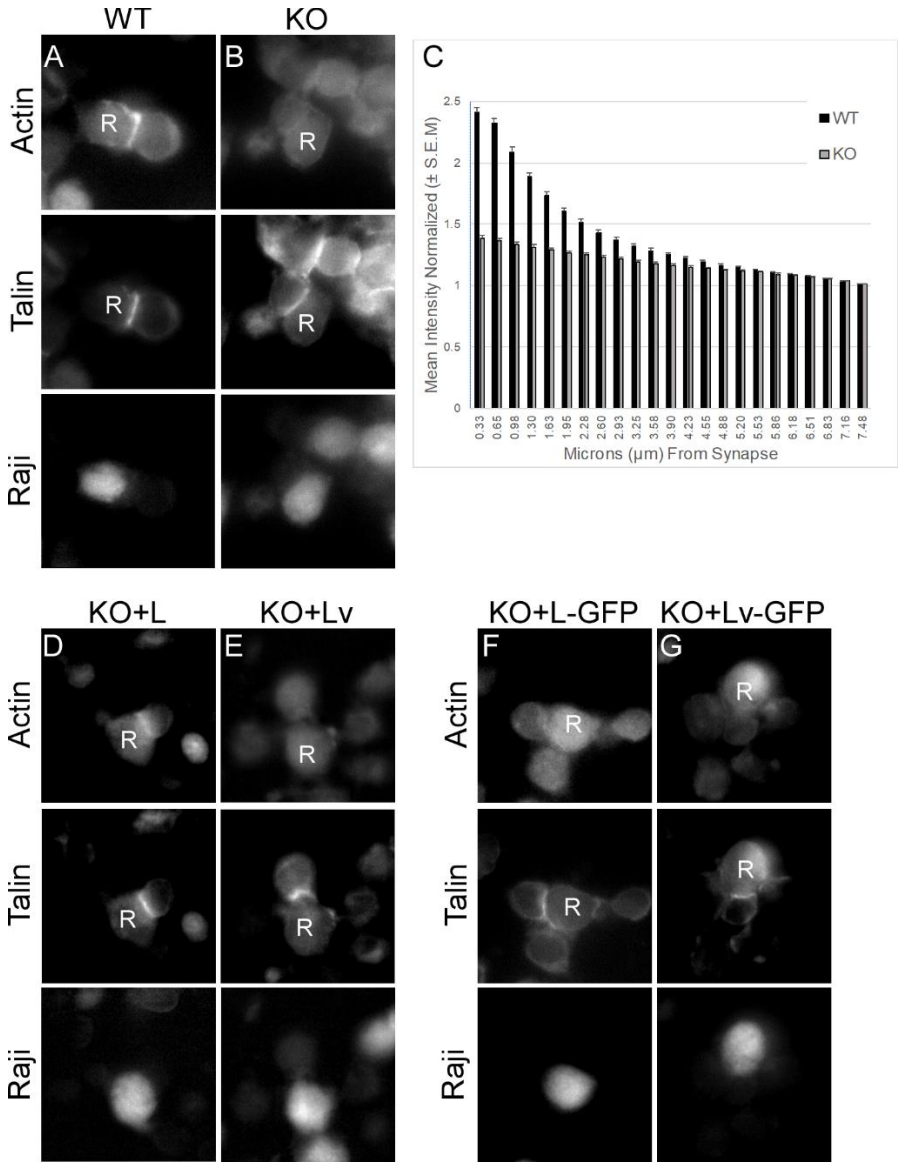

Figure 3.1: Actin is depleted from the synapse in the absence of DISC1 L

(A) Wildtype (WT) Jurkat cells and **(B)** DISC1 knockout (KO) Jurkat cells were paired with SEE-coated Raji cells and fixed. These samples were stained with TRITC-phalloidin and immunostained for Talin. The location of Raji cells was determined through staining with cell tracker blue and are labeled 'R' in other pictures. **(C)** The distribution of actin was analyzed from 30 stained images of WT and KO cell pairs, as described in the Materials and Methods. The boundary of the IS was defined as the maxima signal between the Jurkat and Raji pair. Mean intensity values ± SEM were plotted for 5 pixel-wide segments starting at the IS and moving to the back of the cell, then converted to distance in micrometers. KO cells expressing **(D)** DISC1 L (KO+L), **(E)** DISC1 Lv (KO+Lv), **(F)** DISC1 L-GFP (KO+L-GFP), and **(G)** DISC1 Lv-GFP (KO+Lv-GFP) were also stained through the method described above.

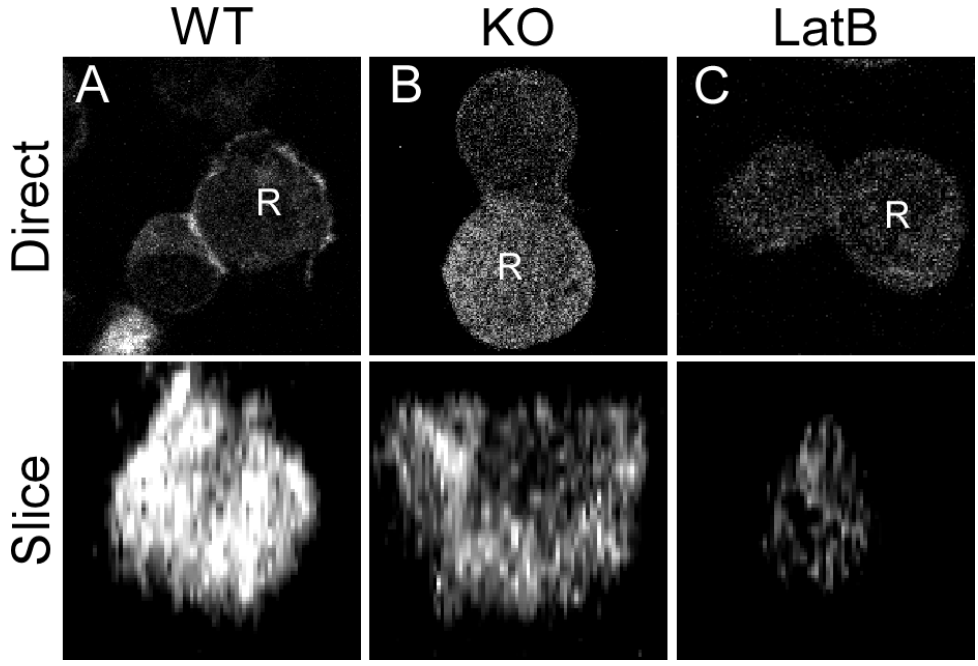

Figure 3.2: Confocal imaging of IS actin in DISC1 knockout

(A) Wildtype (WT) Jurkat cells, **(B)** DISC1 knockout (KO) Jurkat cells, and **(C)** KO cells treated with Latrunculin B (LatB) were paired with SEE-coated Raji cells, fixed, and stained with TRITC-phalloidin. Cell pairs (Direct) and cross sections of the IS (Slice) under TRITC fluorescence is depicted. Cell pairs were imaged using confocal microscopy, with Z slices generated at 0.5 micron steps.

DISC1 forms a complex with Talin upon T-Cell stimulation

We had previously shown that DISC1 localizes in a ring at the pSMAC, so to bridge the connection between DISC1 and the pSMAC and to actin we began to look to probe for DISC1 binding partners that are part of focal adhesion complexes. Through immunoprecipitation followed by SDS-PAGE and Western Blotting, we found that Talin becomes complexed with DISC1 in Jurkat cells stimulated through TcR with Vβ8 antibody followed by crosslinking by a secondary antibody (Figure 3.3A). Using DISC1 KO cells expressing DISC1 L or Lv GFP constructs, through GFP immunoprecipitation we found that DISC1 isoform L is a more prevalent binding partner to Talin compared to DISC1 isoform Lv (Figure 3.3B).

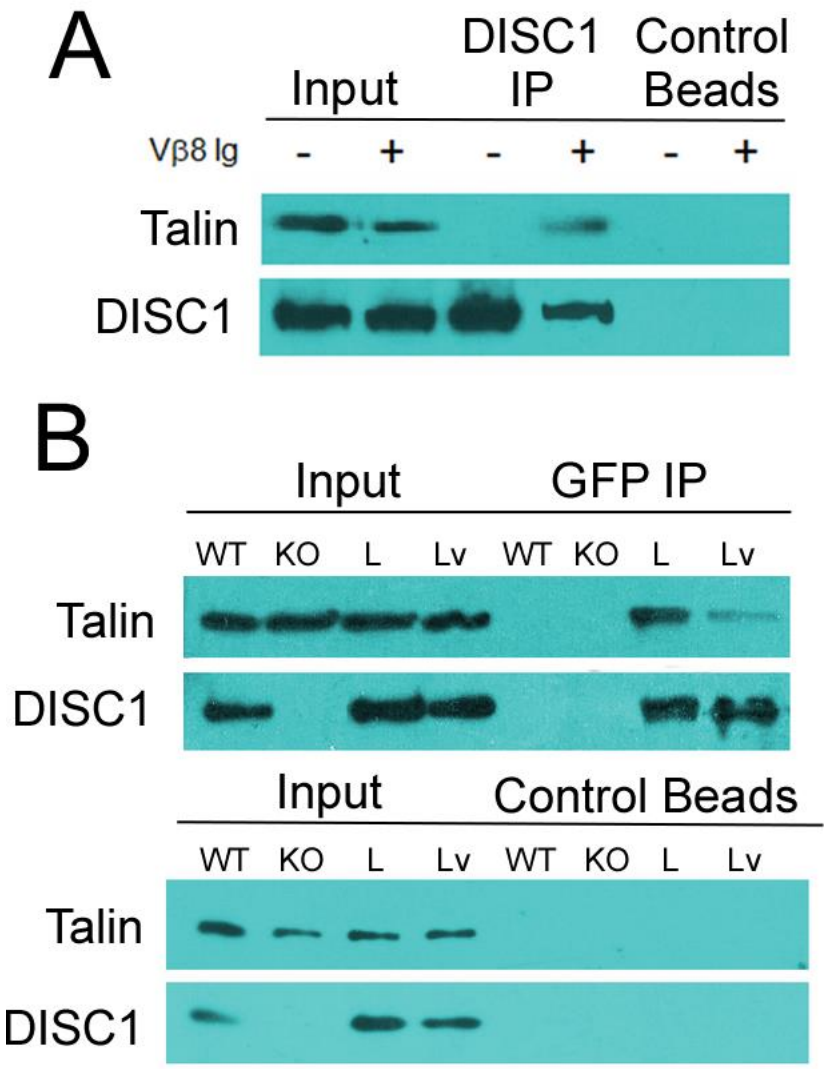

Figure 3.3: DISC1 immunoprecipitation of Talin

DISC1 was immunoprecipitated from Jurkat cells that were treated and untreated with anti-TcR Ig. Samples probed for DISC1 and Talin on blots transferred from SDS-PAGE gels. **(A)** Talin coimmunoprecipitates with DISC1 when Jurka cells are stimulated with anti-TcR. **(B)** DISC1-GFP was immunoprecipitated from lysates of either normal Jurkat cells or DISC1 KO cells, or KO cells re-expressing either DISC1 L-GFP or LV-GFP. Control blots for A and B show no obvious nonspecific binding to the beads.

Girdin is a DISC1 binding partner

We discovered that the actin associated protein Girdin is expressed in Jurkat cells and localizes to the immunological synapse in Jurkat/Raji pairs (Figure 3.4A-B). Through immunoprecipitation followed by SDS-PAGE and Western blotting, Girdin was shown to form a complex with DISC1 in Jurkat cells (Figure 3.4C).

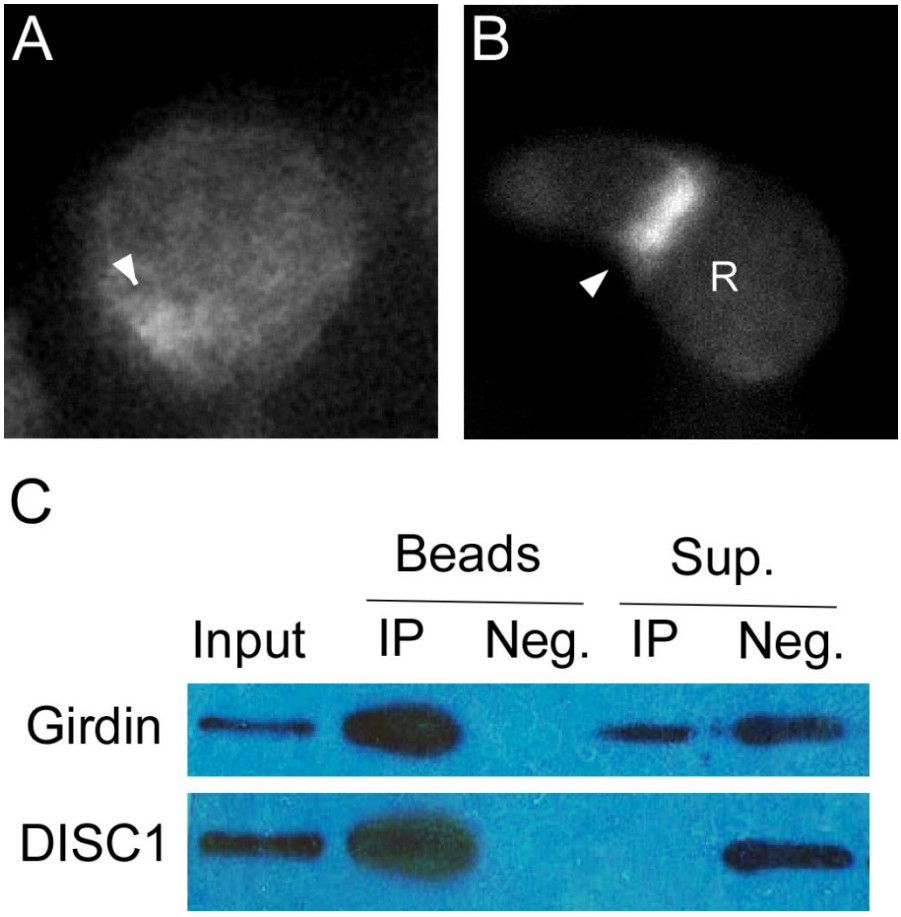

Figure 3.4: Girdin binds to DISC1 and is needed for abundant actin filaments at the IS

(A) Jurkat cells were fixed and immunostained for Girdin or **(B)** paired with SEE-coated Raji cells, fixed and immunostained for Girdin (Girdin marked by a white arrow). **(C)** DISC1 was immunoprecipitated from Jurkat cells. Samples were then probed for Girdin and DISC1 through Western blotting. Control beads (Neg.) showed no obvious nonspecific binding and Girdin and DISC1 were detectable in the supernatant (Sup.) of control beads.

Girdin promotes actin polymerization at the immunological synapse

To explore the effect that Girdin disruption has on T-cell activation, we created a Girdin CRISPR/Cas9 Knockout Jurkat cell line (Girdin KO). To show that Girdin was absent in this cell line, we immunostained Jurkat/Raji pairs for Girdin and found that fluorescence was significantly lower in Girdin KO cells compared to wildtype Jurkat cells (Figure 3.5A-C, $p < 0.001$). Through SDS-PAGE and Western blotting we also showed that there was no detectable Girdin in our Girdin KO cell line (Figure 3.5D). Additionally, we re-expressed a GFP tagged Girdin construct and confirmed that it had the same localization as endogenous Girdin (Figure 3.5E-F).

Similar to what was found in the DISC1 KO cell line, the presence of actin at the IS detected through Phalloidin staining was shown to be significantly diminished in Girdin KO Jurkat cells compared to wildtype (Figure 3.6A-B, $p < 0.001$). Using Girdin KO cells expressing a GFP tagged Girdin, detectable actin at the IS was recovered and fluorescence was shown to not be significantly different than actin from the IS formed in wildtype Jurkat cells (Figure 3.6C-D, $p = 0.186$).

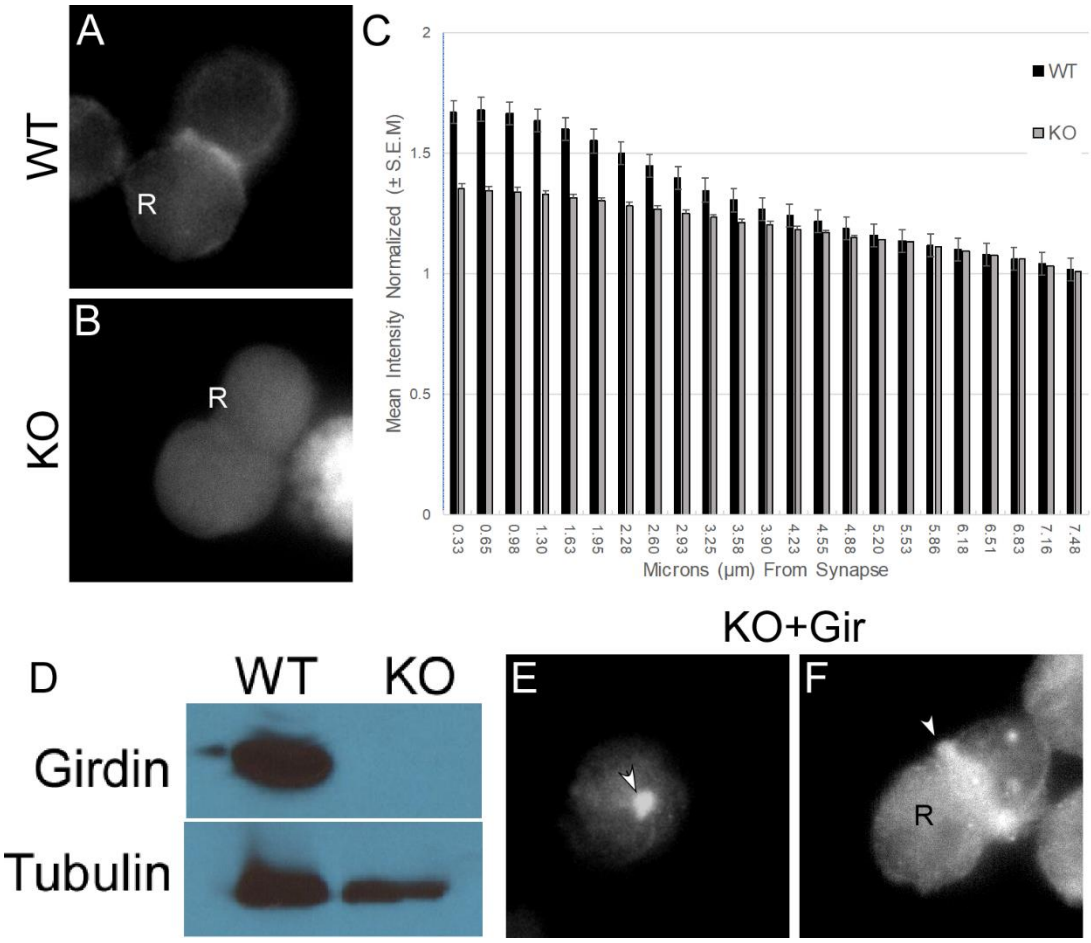

Figure 3.5: Girdin CRISPR/Cas9 and Girdin-GFP Construct

(A) Wildtype Jurkat cells (WT) or **(B)** Girdin knockout (KO) cells were paired with SEE-coated Raji cells and immunostained for Girdin. **(C)** The distribution of Girdin was analyzed from 30 immunostained images of WT and KO cell pairs, as described in the Materials and Methods. The boundary of the IS was defined as the maxima signal between the Jurkat and Raji pair. Mean intensity values ± SEM were plotted for 5 pixel-wide segments starting at the IS and moving to the back of the cell, then converted to distance in micrometers. **(D)** Girdin was assayed through Western blotting in WT and KO cells, using beta-Tubulin as a loading control. **(E)** KO Jurkat cells expressing a Girdin GFP construct (KO+Gir) were observed for GFP fluorescence, or **(F)** paired with SEE-coated Raji cells and observed for GFP fluorescence. Fluorescence from Girdin staining or GFP fluorescence marked with a white arrow in pictures. In all cell pairs Raji cells are marked with an 'R'

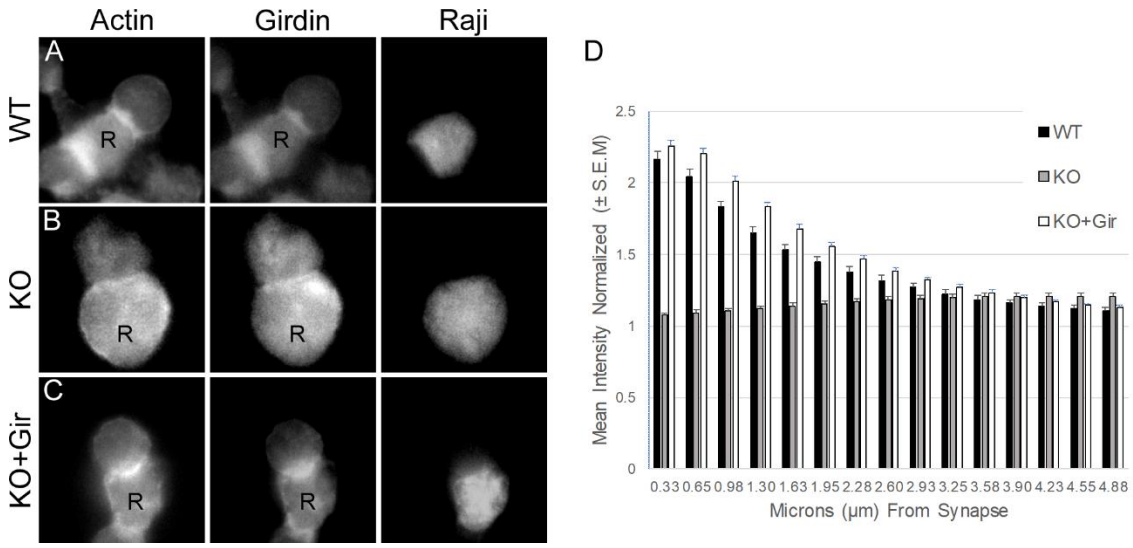

Figure 3.6: The effects of Girdin knockout on IS actin

(A) Wildtype (WT) Jurkat cells, **(B)** Girdin knockout (KO) Jurkat cells, and **(C)** KO Jurkat cells transfected with a GFP-Girdin construct (KO+Gir) were paired with SEE-coated Raji cells and fixed. These samples were stained with TRITC-phalloidin and immunostained for Girdin. The location of Raji cells were distinguished through staining with cell tracker blue and are labeled 'R' in other pictures. **(D)** The distribution of Actin was analyzed from 30 stained images of WT, KO, and KO+Gir cell pairs, as described in the Materials and Methods. Mean intensity values ± SEM were plotted for 5 pixel-wide segments starting at the IS and moving to the back of the cell, then converted to distance in micrometers.

Cytochalasin B and Latrunculin B inhibit MTOC translocation to the synapse

We found that the actin inhibitors Cytochalasin B (CytB) and Latrunculin B (LatB) diminishes detectable actin at the IS similarly to or greater than DISC1 and Girdin knockout. We found that they also disrupt MTOC translocation to the IS (Figure 3.7). This disruption was significant ($p < 0.0001$), but surprisingly also more severe than the disruption of MTOC polarization in DISC1 KO cells ($p = 0.0002$). Through immunofluorescence, we also found that these same actin inhibitors also disrupt the accumulation of the Nde1/Lis1/dynein complex to the IS (Figure 3.8).

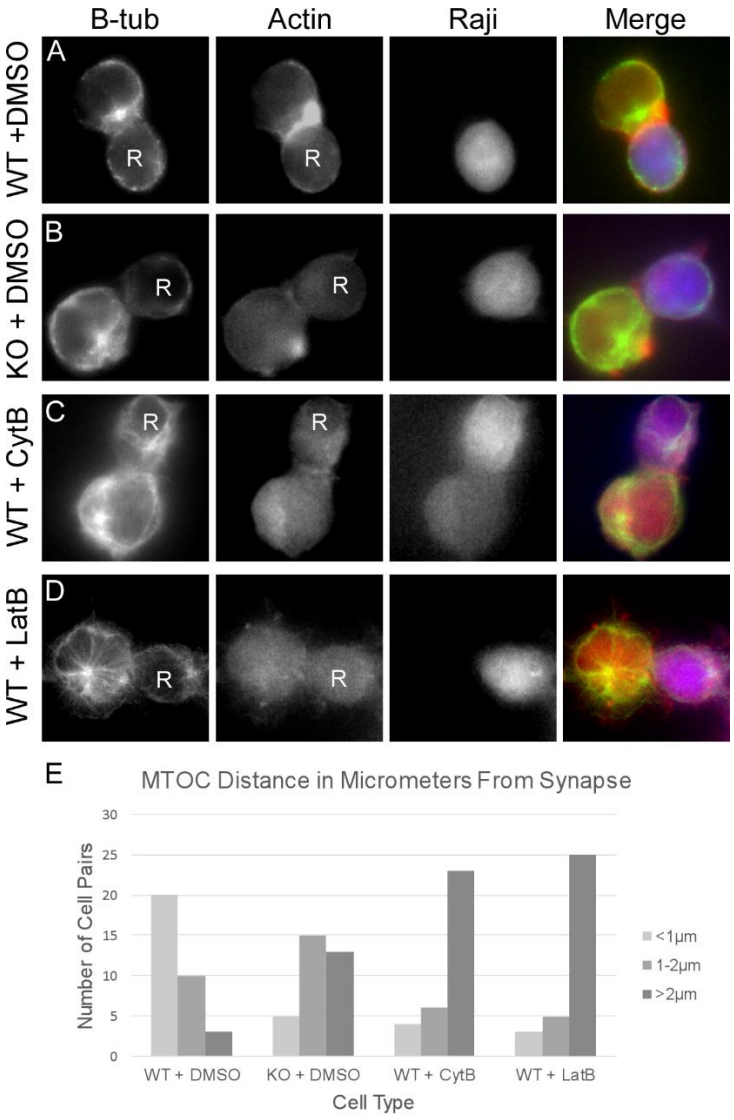

Figure 3.7: MTOC polarization is blocked by actin inhibitors cytochalasin B and latrunculin B

(A) Wildtype (WT) Jurkat cells treated with DMSO, **(B)** DISC1 knockout (KO) cells treated with DMSO, **(C)** WT Jurkat cells treated with Cytochalasin B (CytB), and **(D)** WT Jurkat cells treated with Latrunculin B (LatB) were paired with SEE-coated Raji cells and fixed. Cells were stained for Actin with Phalloidin-TRITC and immunostained with beta-tubulin. The location of Raji cells was determined through staining with cell tracker blue and are labeled 'R' in other pictures. The location of the MTOC in all samples was determined by taking the signal maxima of beta-tubulin stains. Distance of the MTOC to the immunological synapse was taken by measuring the distance in pixels between the MTOC and the Raji cell. **(E)** The position of the MTOC relative to the immunological synapse was logged for each cell type (n=33) and arranged in groups by distance in micrometers.

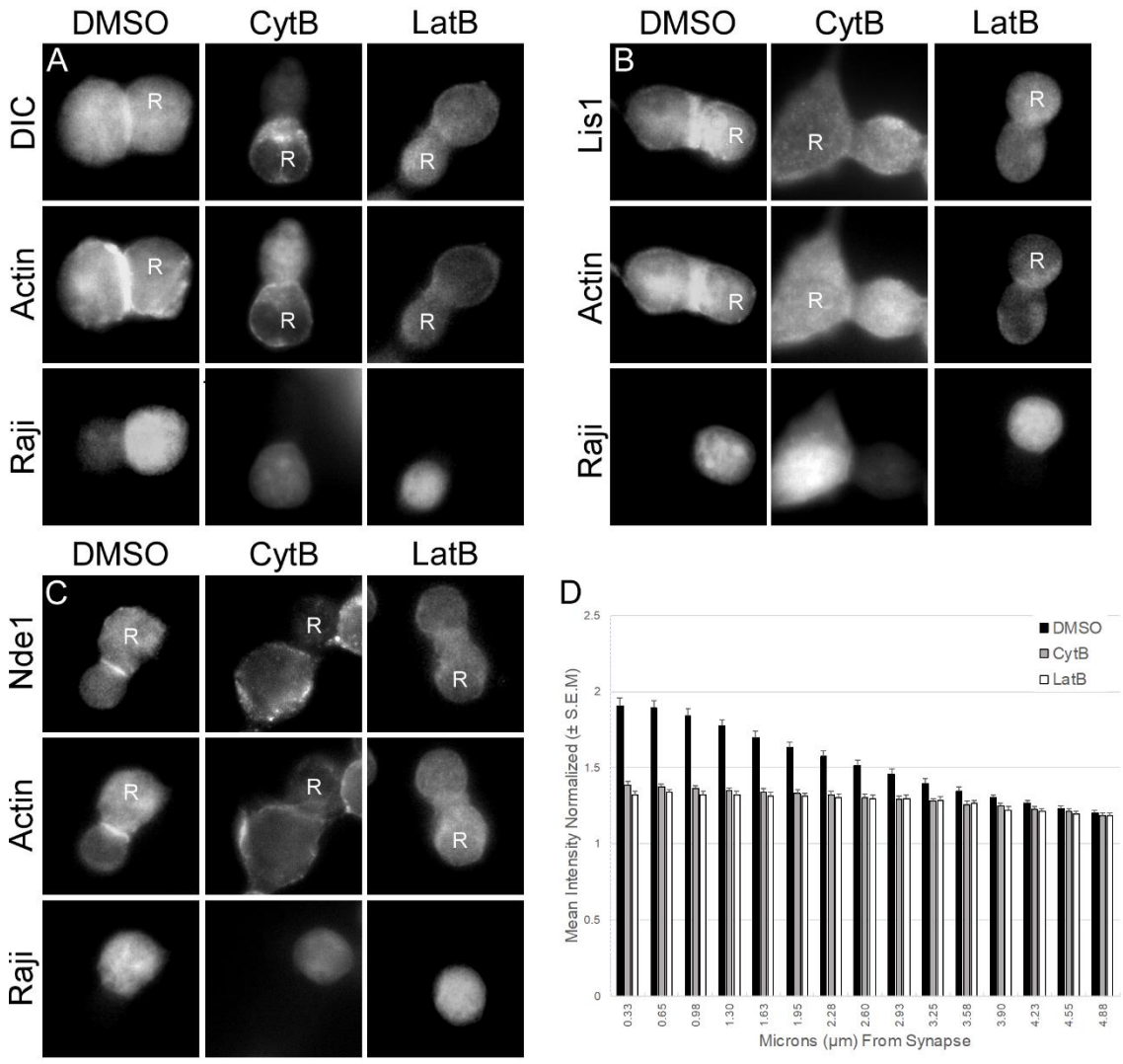

Figure 3.8: Actin inhibitors block dynein, Lis1, and Nde1 accumulation at the synapse

Jurkat cells were treated with DMSO, Cytochalasin B (CytB), or Latrunculin B (LatB), paired with SEE-coated Raji cells, and fixed. Cells were stained for Actin with Phalloidin-TRITC and immunostained for either. **(A)** Dynein Intermediate Chain (DIC), **(B)** Lis1, or **(C)** Nde1. The location of Raji cells was determined through staining with cell tracker blue and are labeled 'R' in other pictures. **(D)** The distribution of Nde1 was analyzed from 30 immunostained images of CytB treated and untreated cell pairs, as described in the Materials and Methods. The boundary of the IS was defined as the maxima signal between the Jurkat and Raji pair. Mean intensity values ± SEM were plotted for 5 pixel-wide segments starting at the IS and moving to the back of the cell, then converted to distance in micrometers.

DISCUSSION

In this study, we found that DISC1 coimmunoprecipitated with Talin when Jurkat cells are activated either with anti-TcR antibody or with the PKC activator phorbol myristate acetate (not shown). TcR engagement alone can induce integrin clustering and talin accumulation at the pSMAC (Simonson, Franco, & Huttenlocher, 2006). The fact that DISC1 also accumulates at the pSMAC and becomes linked to Talin suggests that it is ultimately connected to LFA-1 as well. One aspect of these studies is puzzling. Previous data showed that DISC1 L is the only isoform that accumulates at the IS, while Lv accumulates at mitochondria. Yet both isoforms coimmunoprecipitate with Talin. However, yeast two hybrid studies have shown that DISC1 interacts with a number of actin binding proteins (Ishizuka et al., 2006). In neurons, actin is needed for short distance movements down the axon and for anchoring mitochondria to the cell cortex (Boldogh & Pon, 2006). DISC1 also localizes to these actin-rich spines (Hayashi-Takagi et al.,2010). In T cells, localization of mitochondria at the pSMAC requires the actomyosin-associated Dynamin-like Protein 1 (Drp1) (Baixauli et al., 2011; Ji, Hatch, Merrill, Strack, & Higgs, 2015; Martín-Cófreces, Vicente-Manzanares, & Sánchez-Madrid, 2018). Thus, it seems plausible that DISC1 L and Lv could become intertwined through their connections to the actin cytoskeleton.

The linkage of DISC1 to integrins has some precedent in neurons. For example, overexpression of DISC1 leads to higher expression of β1-integrin on the cell surface where they accumulated in neurites like dendritic spines (Hattori et al., 2010). Again, this connection links DISC1 to actin as well, as one study looking at the regulation of dendritic spines showed that DISC1 regulates the activity of Rac to extend spines during the formation of neurological synapses (Hayashi-Takagi et al., 2010). DISC1 isoform L has been shown to colocalize to actin stress fibers in some cell types (Taylor, Devon, Millar,

& Porteous, 2003). In another study, DISC1 was shown to be needed for the migration of cortical neurons and had a direct impact on the regulation of F-actin in the cell (Steinecke et al., 2014). RNASeq analysis of neurons that carry a DISC1 frameshift mutation show that DISC1 affects the expression of genes related to synapse formation, neurite outgrowth, and actin remodeling (Malavasi et al., 2018).

Our results show that actin at the IS is dramatically reduced in the absence of DISC1. This effect was specific to DISC1 since introduction of isoform L in the DISC1 KO cells restored actin at the IS. This was not seen when DISC1 isoform Lv, was expressed in the DISC1 KO cells. It should be noted however that only expression of the native DISC1 L isoform, as opposed to the N-terminal GFP-DISC1 L, was able to restore actin accumulation at the IS. We suspect this is due to the fact that Girdin, which is also required for actin accumulation at the IS, binds to the N-terminus of DISC1. It appears then that the GFP tag interferes with Girdin binding (Soares et al., 2011).

To show that Girdin was required for actin accumulation at the IS, the Girdin gene was disrupted using the CRISPR/Cas9 system. The results from the Girdin KO were essentially identical to the DISC1 KO in that little actin accumulated at the IS. When the Girdin-GFP construct was introduced into the Girdin KO line, actin at the IS was restored. Girdin is known to be involved in actin remodeling, stress fiber formation and lamellipodia formation (Hayashi-Takagi et al., 2010; Leyme, Marivin, Perez-Gutierrez, Nguyen, & Garcia-Marcos, 2015; Steinecke, Gampe, Nitzsche, & Bolz, 2014). Our results are thus consistent with data from other systems. Given the activity of Girdin in other cell systems we would propose that Girdin is directly involved in stimulating actin accumulation whereas DISC1 is responsible for bringing it to the IS.

Girdin displays a number of different activities in the cell. It crosslinks actin filaments but it also stimulates their formation through PI3K/Akt pathway (Leyme et al.,

2016). Its ability to promote actin assembly appears to depend on one of the Dock GEFs (Janssen et al., 2016; Laurin & Côté, 2014; Sanui et al., 2003). Indeed, the degree of actin loss at the synapse is similar to the results reported WAVE2 knockdown although the WAVE2 knockdown has additional effects on Talin and calcium signaling (Jankowska et al., 2018; Nolz et al., 2006).

We have seen that DISC1, dynein, and Nde1 all seem to show a remarkably similar pattern of movement to the peripheral spread of actin (Chapter 2). However, the peripheral movement of the DISC1 complex seems to stop at the pSMAC which could be due to the linkage with Talin and LFA-1. The parallels to actin movement further extend to the clearing of actin at the IS. It has been previously reported that PKCθ inhibits at least some of the activities of Girdin (Lopez-Sanchez et al., 2013). Since PKCθ accumulates at the center of the synapse, inhibiting Girdin could be responsible for the clearing of actin.

Our studies have focused on the role of dynein and dynein binding proteins in MTOC translocation and organization of the IS. One alternative model for MTOC translocation has been the proposal that microtubules become linked to actin such that as actin spreads to the periphery, microtubules are drawn with it causing the MTOC to move forward (Banerjee et al., 2007; Stinchcombe, Majorovits, Bossi, Fuller, & Griffiths, 2006; Gomez et al., 2007). Experimental support for this model shows that treatment of T-cells with actin disrupting drugs completely blocked MTOC translocation (Filbert et al., 2012; Orange et al., 2003). This effect was distinct from the minor inhibition of the MTOC observed in our DISC1 KO cell line we have previously observed (Chapter 2). Thus, there is a marked difference between the diminished actin due to DISC1 knockdown compared to the effects of Cytochalasin B or Latrunculin. We also found that treatment of T-cells with Latrunculin or Cytochalasin B resulted in a complete loss of the Nde1-dynein complex from the IS, whereas the DISC1 KO does not prevent the accumulation of the rest of the

dynein complex. Previous studies showed that Nde1 was required for recruitment of dynein to the IS and for MTOC translocation (Nath et al, 2016). On the other hand, the absence of DISC1 and to a large degree, actin, did not block the MTOC from moving most of the way to the IS. Therefore, rather than supporting an actin-based model for MTOC translocation, the data from these drug treatments support the idea of a linkage between the DISC1 dynein complex and actin. They also support the idea that there are multiple pools of actin and that loss of actin seen in the DISC1 / Girdin KO cells is different than the loss of actin due to treatment with cytochalasin B or latrunculin.

A final point to make is how nicely the current results dovetail with the live cell modulated polarization microscopy of Kuhn and Poenie (2002). In tracking MTOC translocation to the IS they found that initially, the MTOC moved linearly to the IS. Then, as the MTOC came near the IS, it began to oscillate laterally. In Chapter 2 we showed that the Nde1–dynein complex first accumulates at the center of the IS. Dynein at the center of the IS would tend to pull the MTOC straight towards the IS. Then, the dynein complex moves peripherally to form a ring through the remodeling of actin and DISC1/Girdin. At this point the MTOC would be at the center of the ring and opposing dynein forces would act to pull the MTOC laterally in an oscillating manner.

Chapter 4: Conclusions and Future Work

The formation of the immunological synapse (IS) is accompanied by a large-scale reorganization of the actin and microtubule cytoskeletons. Some have proposed that translocation of the Microtubule Organizing Center (MTOC) is due a linkage between actin and microtubules. This idea states that as actin moves to the periphery of the IS microtubules are pulled laterally, which in turn pulls the MTOC forward (Banerjee et al., 2007; Stinchcombe, Majorovits, Bossi, Fuller, & Griffiths, 2006). This model seemingly derives support from the observation that certain drugs that block actin assembly also block MTOC translocation (Filbert et al., 2012; Orange et al., 2003). Our previous studies, on the other hand, show that MTOC translocation depends on dynein (Combs et al; Nath et al., 2016). In this study we have resolved these apparent discrepancies.

We have characterized the functions of DISC1 in T-cells, including its connection to both actin and the dynein complex. Our initial studies of DISC1 showed that it localized to the pSMAC where it associated with dynein and the adapter Nde1/Lis1, a complex that is needed for MTOC translocation to the IS. Closer examination showed that there were two isoforms of DISC1 expressed in Jurkat T-cells, L that accumulated at the IS and Lv which localized around mitochondria. By utilizing CRISPR/Cas9 knockout of the DISC1 gene, as well as GFP constructs for the DISC1 isoforms expressed exogenously in DISC1 knockout cells, we found that DISC1 depletion blocked the translocation mitochondria to the IS (which was recovered by Lv) and prevented the complete translocation of the MTOC (which was recovered by L). The latter effect was subtle but significant.

Having shown that DISC1 forms a complex with Nde1, Lis1 and dynein, we examined the dynamics of these proteins at the IS. We found that DISC1 L, Nde1, and dynein initially accumulated at the center of the IS before spreading out peripherally to the pSMAC. These movements were reminiscent of the distribution and dynamics of actin at

the synapse. When DISC1 was disrupted, the normal accumulation of actin at the IS was lost while dynein and Nde1 remained at the center of the IS. These results are consistent with the idea that movement of the dynein/Nde1/Lis1/DISC1 complex to the pSMAC is dependent on forming a connection with the actin cytoskeleton.

Our data do not support a role for actin as generating the force for MTOC translocation. Firstly, dynein is absolutely required for MTOC translocation. This has been shown by studies where either inhibition of dynein with molecular traps or loss of dynein from the synapse leads to failure of MTOC translocation (Combs et al., 2006; Christian & Poenie, unpublished; Nath et al., 2016). Furthermore, in this current study loss of actin from DISC1 disruption did not affect the movement of the MTOC to the center of the IS. Finally, a fixed connection to an actin ring does not explain the oscillatory movements whereas dynein is known to generate similar oscillation (Vogel et al., 2009; Yamamoto, West, McIntosh, & Hiraoka, 1999; Yamamoto et al., 2001; Yeh et al., 1995).

Several observations may give clues as to how DISC1 L might be linked to the movements of dynein and NDE1 from the center to the periphery. Firstly, we found that DISC1 forms a complex with Talin, thus linking the DISC1/Nde1/dynein complex to LFA-1 and actin. Secondly, we found that through its association with DISC1, the actin binding protein Girdin induces F-actin accumulation at the IS. Lastly, treatment of cells with Cytochalasin B or Latrunculin led to a complete loss of the dynein complex from the IS. These results suggest a model wherein the dynein complex becomes linked to actin at the center of the IS which then moves laterally where the complex becomes linked to LFA-1 and Talin at the pSMAC (Figure 4.1). This model would explain why treatment of cells with Cytochalasin B or Latrunculin results in a failure of MTOC translocation. It is not that actin spreading is generating force for MTOC translocation, but rather it is due to the loss of dynein from the IS.

Our data shows that the dynamics of dynein localization at the IS nicely explains the live cell MTOC dynamics at the IS reported by Kuhn and Poenie (2001). They reported that the MTOC initially moved linearly towards the IS and then started oscillating laterally as it came near to the cSMAC. Their observations are consistent with data shown here that dynein is initially located at the center of the IS which would pull in the MTOC directly to the cSMAC. However, as dynein moves to form a peripheral ring corresponding to the pSMAC, there would be opposing forces pulling on the MTOC laterally. This would be expected to result in the observed lateral oscillations of the MTOC.

These studies of DISC1 help clarify some issues, but they also raise numerous questions. The dramatic loss of actin at the IS due to disruption of DISC1 or Girdin are similar in extent to data shown for depletion of WAVE2 (Jankowska et al., 2018; Nolz et al., 2006). However, loss of WAVE2 affects calcium signaling whereas loss of DISC1 does not. Furthermore, loss of actin due to DISC1 disruption did not have the same effect as treatment with Cytochalasin or Latrunculin, indicating that some actin structures remain after the loss of DISC1. This was also evident in confocal micrographs that showed a greater depletion of actin due to Latrunculin than due to disruption of DISC1.

How DISC1 might affect signaling during T-cell activation deserves more study. In Chapter 2 we suggested that DISC1 may be a down regulator of T-cell activation based on its effects on MTOC translocation. This explanation is supported by the fact that DISC1 disruption often leads to the development of schizophrenia, a mental disorder that is linked to hyperactive and autoimmune immune responses resulting in inflammation of the brain (Müller, Weidinger, Leitner, & Schwarz, 2015).

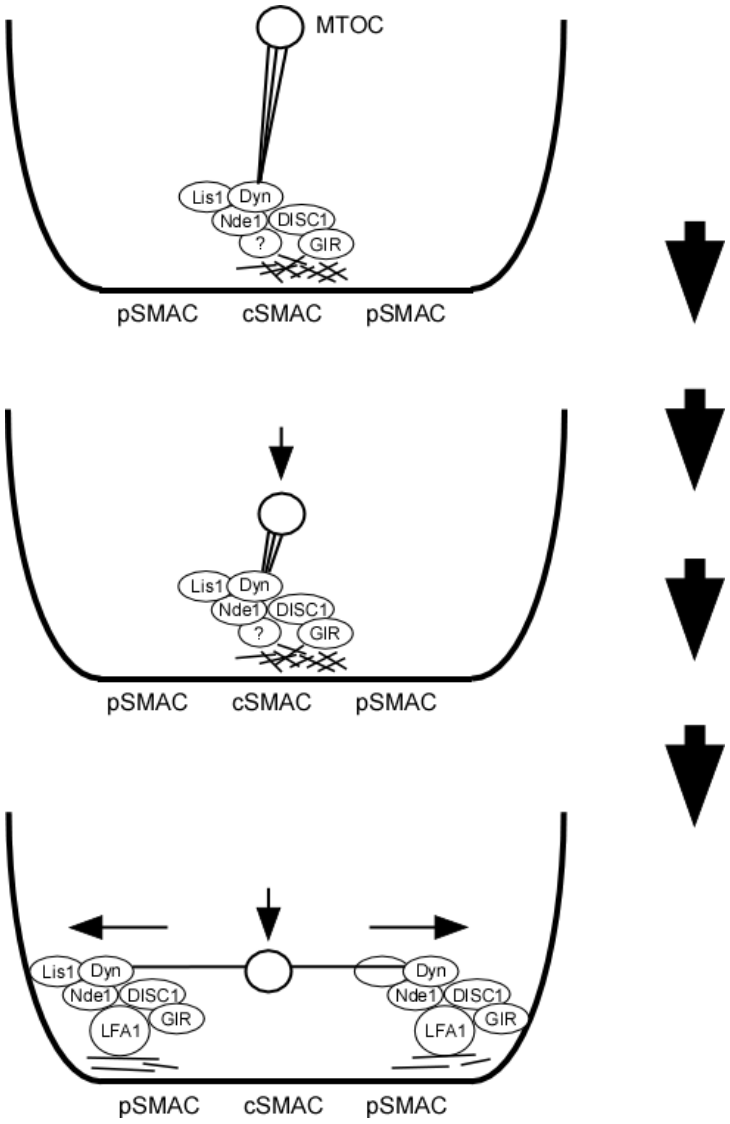

Figure 4.1: Model for DISC1 complex at the immunological synapse

A model for how the movement of the MTOC might be explained based on our observations of DISC1. In this schema, DISC1 and Nde1 initially accumulate at the synapse, although Nde1 can be recruited independently from DISC1. They become associated to the synapse at actin filaments, although given our data it is clear that there is an unknown element bringing Nde1/Lis1 to the synapse independent of DISC1. After this complex is recruited, dynein motor function can reel the MTOC in from the cSMAC. As actin reorganizes, the complex becomes associated with LFA-1 at the pSMAC through DISC1. This lateral movement of the complex pulls the MTOC closer to the cSMAC.

Furthering this association, there are several immune abnormalities that have been observed in mice carrying a mutant DISC1 gene. A summary of these observations is presented in Table 4.1. Many of the characterized defects on the immune system come from inbred Swiss mice (SJL/J, FVB/NJ, and SWR/J) that have been genotyped for a 25bp deletion at Exon 6 of the DISC1 gene (Δ25 DISC1^{del}). This mutation results in a premature stop codon that produces a non-functional C-terminal truncation of the protein (Ritchie & Clapcote, 2013). These mouse lines often develop or are easily susceptible to autoimmune dysfunctions (Haran-Ghera, Ben-Yaakov, Peled, & Bentwich, 1973; Hutchings, Varey, & Cooke, 1986; Jane-wit et al., 2002; Owens & Bonavida, 1976), including Experimental Autoimmune Encephalomyelitis (EAE) (Rajan, Asensio, Campbell, & Brosnan, 2000). They also are prone to a CD4+ bias and have hyperactive inflammatory responses driven by these cells (E.-M. Kim, Bae, Choi, & Hong, 2012; Turner, Keefe, Sugawara, Yamada, & Orme, 2003; Wong et al., 2007). In FVB/NJ and SWR/J mice, cytokines IFNγ, IL-4, IL-5, and IL-10 have also been shown to be dysregulated under certain conditions. In DISC1 mutants outside the Swiss mouse model, altered cytokine profiles have also been observed in mice expressing a DISC1 C-terminal truncation analogous to the Δ25 mutant or in mice expressing a DISC1 point mutant (L100P) that has been shown to inhibit the formation and plasticity of neurological synapses in the hippocampus (Cui et al., 2016). These studies primarily focused on the development of schizophrenia-like phenotypes in newborn mice, using fetal mice presented with a neonatal immune challenge (Maternal Immune Activation, MIA). IL-1β, IL-2, IL-5, and IL-6 were among the cytokines observed to be affected, either directly through expression of the mutant or in combination with MIA.

DISC1 Expressed	Observations	References
Δ25 DISC1^{del} SJL/J mice	Reticular cell sarcomas resembling Hodgkin's disease. Complications related to hypersensitivity and autoimmunity. High numbers of $CD4^+$ cells. No effects on $CD8^+$ cytotoxic killing. Defects in proliferation of $CD8^+$ suppressor cells.	[1], [2], [3], [4], [5]
FVB/NJ mice	High susceptibility to *Clonorchis sinensis* parasite marked by higher IL-4, IL-5, IL-10, IL-13 and TGF-β. Bias to $CD4^+$ over $CD8^+$.	[6], [7]
SWR/J mice	Complications related to autoimmunity. High susceptibility to infection by M*ycobacterium tuberculosis* marked by lower amount of intracellular IFNγ, delayed recruitment of effector T-cells. Early expulsion of nematode parasites marked by higher $CD4^+$ immune response.	[4], [8], [9]
Inducible ΔC 1001, 1302B mice	Higher base levels of IL-1β and IL-5. Maternal Immune Activation with poly I:C leads to augmented increase in IL-2.	[10]
L100P 100P mice	Maternal Immune Activation with poly I:C leads to Higher levels of IL-1β, IL-6, and TNF-alpha and lower IL-12 in the fetus.	[11], [12]

Table 4.1: Summary of immune dysfunction seen in DISC1 mutant mice

References: [1] Haran-Ghera, et al., 1973. [2] Owens & Bonavida, 1976. [3] Hutchings, Varey, & Cooke, 1986. [4] Jane-wit et al., 2002. [5] Rajan, Campbell, & Brosnan, 2000. [6] Kim, Bae, Choi, & Hong, 2012. [7] Chaudhuri et al., 2013. [8] Turner et al., 2003. [9] Wong et al., 2007. [10] Abazyan et al., 2010. [11] Lipina et al., 2013. [12] Desbonnet et al., 2017.

IL-2 has pleiotropic effects on T-cell fate but is commonly known to be produced by activated CD4+ cells (Ross & Cantrell, 2018). From the other cytokines, some connections can be made to the immune dysfunction observed in DISC1 mutant mice. Dysregulated IL-1β and IL-6 are prominently involved in autoimmunity and chronic inflammation, especially related to CD4+ TH1 cells (Dinarello, 2009; Tanaka, Narazaki, & Kishimoto, 2014). Both are upregulated in EAE, to which SJL/J mice are especially susceptible (Lin & Edelson, 2017; Quintana et al., 2009; Rajan et al., 2000). This is an interesting connection to DISC1 because encephalitis in humans is often misdiagnosed as schizophrenia, and shares many of the same hallmarks (Najjar, Steiner, Najjar, & Bechter,

2018). Other experiments show that FVB/NJ and SWR/J mice overproduce IL-4, -5, and -10 in response to infection with a helminth parasite. While these cytokines are normally produced by CD4+ cells in such infections, FVB/NJ and SWR/J mice appear to be unable to properly regulate this response. The shared characteristics among the Swiss mice appear to be a bias towards activating CD4+ immune responses and hyperactivity of those cells resulting in overproduction of cytokines (Silva-Filho, Caruso-Neves, & Pinheiro, 2014; Zhu, Yamane, & Paul, 2010). An imbalance of IL-1β, IL-2, IL-4, and IL-6 is also commonly seen in schizophrenia (Guo, Liu, Wang, Feng, & Zhang, 2015; Y.-K. Kim et al., 2004; Schwarz, Müller, Riedel, & Ackenheil, 2001). Given the common connection of DISC1 dysfunction between these mice and schizophrenia, it is possible that DISC1 is needed to properly regulate the activation of T-cells.

Connecting all of this to signaling at the IS, future work might look at Cyclin-dependent kinase 5 (Cdk5). Much like DISC1, Cdk5 regulates actin remodeling in neurodevelopment (Shah & Rossie, 2018). Cdk5 is expressed during T-cell activation and phosphorylates proteins at the IS like the actin effector Coronin 1a (Askew et al., 2011). Although T-cells lacking Cdk5 are still capable of carrying out effector functions, depleting the protein from hematopoietic tissue in mice results in resistance to induction of EAE (Pareek et al., 2010). Cdk5 has also been shown to promote allogeneic T-cell responses related to graft versus host disease (Askew et al., 2017). It is clear then that depleting Cdk5 has the possibility of attenuating some hyperactive and autoimmune responses. To connect this to DISC1, it has been shown that Cdk5 directly interacts with DISC1 binding partners Girdin and Nde1. Girdin is phosphorylated by Cdk5 which modulates its interactions with Akt (Bhandari et al., 2015). Nde1 is phosphorylated and deregulated by Cdk5 (Pandey & Smith, 2011). Through these connections it is therefore possible that Cdk5 and DISC1 share a similar pool of targets at the IS and may be involved in opposing functions.

Exploring this may allow for further characterization on the effects of DISC1 and provide a connection to the hyperactive and autoimmune dysfunctions seen in DISC1 mutant mice.

This initial description of the role DISC1 in T-cells has unveiled a number of roles it plays at the synapse and in signaling. It is interesting to think about how these findings add further parallels between immunological and neuronal synapses. Furthermore, it raises the question of whether DISC1 might be linked to schizophrenia through its effects on the immune system. In the past, some models for schizophrenia pointed to immune system dysregulation during development as the cause of schizophrenia. For example, the possibility of cytokine storms due to immune reactions were thought to disrupt normal brain development. Even so, most studies of DISC1 have focused on neuronal activities. However, the connection between schizophrenia has recently come to the fore. As one review stated, "immunopathogenesis has emerged as one of the most compelling etiological models of schizophrenia" (Debnath, 2015). While models relating immune effects to schizophrenia are largely correlative, this study provides a concrete link between a known factor for schizophrenia and T cells.

References

Abazyan, B., Nomura, J., Kannan, G., Ishizuka, K., Tamashiro, K. L., Nucifora, F., . . . Pletnikov, M. V. (2010). Prenatal Interaction of Mutant DISC1 and Immune Activation Produces Adult Psychopathology. Biological Psychiatry, 68(12), 1172-1181.

Abrahamsen, H., Baillie, G., Ngai, J., Vang, T., Nika, K., Ruppelt, A., . . . Taskén, K. (2004). TCR- and CD28-Mediated Recruitment of Phosphodiesterase 4 to Lipid Rafts Potentiates TCR Signaling. The Journal of Immunology, 173(8), 4847-4858.

Alonso, R., Mazzeo, C., Rodriguez, M. C., Marsh, M., Fraile-Ramos, A., Calvo, V., . . . Izquierdo, M. (2011). Diacylglycerol kinase α regulates the formation and polarisation of mature multivesicular bodies involved in the secretion of Fas ligand-containing exosomes in T lymphocytes. Cell Death And Differentiation, 18, 1161.

Alkuraya, Fowzan S., Cai, X., Emery, C., Mochida, Ganeshwaran H., Al-Dosari, Mohammed S., Felie, Jillian M., . . . Walsh, Christopher A. (2011). Human Mutations in NDE1 Cause Extreme Microcephaly with Lissencephaly. The American Journal of Human Genetics, 88(5), 536-547.

Andrés-Delgado, L., Antón, O. M., & Alonso, M. A. (2013). Centrosome polarization in T cells: a task for formins. Frontiers in immunology, 4, 191. doi:10.3389/fimmu.2013.00191

Angus, K. L., & Griffiths, G. M. (2013). Cell polarisation and the immunological synapse. Current Opinion in Cell Biology, 25(1), 85-91.

Arthur, A. L., Yang, S. Z., Abellaneda, A. M., & Wildonger, J. (2015). Dendrite arborization requires the dynein cofactor NudE. Journal of Cell Science, 128(11), 2191-2201.

Askew, D., Pareek, T., Eid, S., Keller, M., Guardia-Wolff, R., Pierce, E., . . . Cooke, K. R. (2011). A Novel Role for Lymphocyte Expression of the Cyclin-Dependent Kinase 5 (CDK5) in the Generation of Allogeneic T Cell Responses After BMT. Biology of Blood and Marrow Transplantation, 17(2), S160.

Askew, D., Pareek, T. K., Eid, S., Ganguly, S., Tyler, M., Huang, A. Y., . . . Cooke, K. R. (2017). Cyclin-dependent kinase 5 activity is required for allogeneic T-cell responses after hematopoietic cell transplantation in mice. Blood, 129(2), 246-256.

Austin, C. P., Kandpal, G., Morris, J. A., & Ma, L. (2003). DISC1 (Disrupted-In-Schizophrenia 1) is a centrosome-associated protein that interacts with MAP1A, MIPT3, ATF4/5 and NUDEL: regulation and loss of interaction with mutation. Human Molecular Genetics, 12(13), 1591-1608.

Bader, J. R., & Vaughan, K. T. (2010). Dynein at the kinetochore: Timing, Interactions and Functions. Seminars in cell & developmental biology, 21(3), 269–275. doi:10.1016/j.semcdb.2009.12.015

Baixauli, F., Martín-Cófreces, N. B., Morlino, G., Carrasco, Y. R., Calabia-Linares, C., Veiga, E., . . . Sánchez-Madrid, F. (2011). The mitochondrial fission factor dynamin-related protein 1 modulates T-cell receptor signalling at the immune synapse. The EMBO Journal, 30(7), 1238-1250.

Baker, R. G., Hsu, C. J., Lee, D., Jordan, M. S., Maltzman, J. S., Hammer, D. A., . . . Koretzky, G. A. (2009). The Adapter Protein SLP-76 Mediates "Outside-In" Integrin Signaling and Function in T Cells. Molecular and Cellular Biology, 29(20), 5578-5589.

Banerjee, P.P., Pandey, R., Zheng, R., Suhoski, M.M., Monaco-Shaver, L. & Orange, J.S. (2007). Cdc42-interacting protein-4 functionally links actin and microtubule networks at the cytolytic NK cell immunolical synapse. The Jornal of experimental medicine. 204(10), 2305-2320.

Bakircioglu, M., Carvalho, Ofélia P., Khurshid, M., Cox, James J., Tuysuz, B., Barak, T., . . . Woods, C. G. (2011). The Essential Role of Centrosomal NDE1 in Human Cerebral Cortex Neurogenesis. The American Journal of Human Genetics, 88(5), 523-535.

Becart, S., Altman, A. (2009). SWAP-70-like adapter of T cells: a novel Lck-regulated guanine nucleotide exchange factor coordinating actin cytoskeleton reorganization and Ca2+ signaling in T cells. Immunological reviews, 232: 319–333.

Bertrand, F., Müller, S., Roh, K.-H., Laurent, C., Dupré, L., & Valitutti, S. (2013). An initial and rapid step of lytic granule secretion precedes microtubule organizing center polarization at the cytotoxic T lymphocyte/target cell synapse. Proceedings of the National Academy of Sciences, 110(15), 6073.

Bettelli, E., Prabhu Das, M., Howard, E. D., Weiner, H. L., Sobel, R. A., & Kuchroo, V. K. (1998). IL-10 Is Critical in the Regulation of Autoimmune Encephalomyelitis as Demonstrated by Studies of IL-10- and IL-4-Deficient and Transgenic Mice. The Journal of Immunology, 161(7), 3299-3306.

Bezakova, G., & Ruegg, M. A. (2003). New insights into the roles of agrin. Nature Reviews.Molecular Cell Biology, 4(4), 295-308.

Bhandari, D., Lopez-Sanchez, I., To, A., Lo, I.-C., Aznar, N., Leyme, A., . . . Ghosh, P. (2015). Cyclin-dependent kinase 5 activates guanine nucleotide exchange factor GIV/Girdin to orchestrate migration–proliferation dichotomy. Proceedings of the National Academy of Sciences, 112(35), E4874-E4883.

Borgne, M., & Shaw, A. S. (2013). Do T Cells Have a Cilium? Science, 342(6163), 1177-1178.

Bour-Jordan, H., Esensten, J. H., Martinez-Llordella, M., Penaranda, C., Stumpf, M., & Bluestone, J. A. (2011). Intrinsic and extrinsic control of peripheral T-cell tolerance by costimulatory molecules of the CD28/B7 family. Immunological Reviews, 241(1), 180-205.

Bradshaw, N. J., Ogawa, F., Antolin-Fontes, B., Chubb, J. E., Carlyle, B. C., Christie, S., . . . Millar, J. K. (2008). DISC1, PDE4B, and NDE1 at the centrosome and synapse. Biochemical and Biophysical Research Communications, 377(4), 1091-1096.

Bradshaw, N. J., Soares, D. C., Carlyle, B. C., Ogawa, F., Davidson-Smith, H., Christie, S., . . . Millar, J. K. (2011). PKA Phosphorylation of NDE1 Is DISC1/PDE4 Dependent and Modulates Its Interaction with LIS1 and NDEL1. The Journal of Neuroscience, 31(24), 9043-9054.

Bradshaw, N. J., Hennah, W., & Soares, D. C. (2013). NDE1 and NDEL1: twin neurodevelopmental proteins with similar 'nature' but different 'nurture'. Biomolecular concepts, 4(5), 447–464. doi:10.1515/bmc-2013-0023

Braiman A., Barda-Saad M., Sommers C.L., & Samelson L.E. (2006). Recruitment and activation of PLCgamma1 in T cells: a new insight into old domains. EMBO J., 25(4), 774-784.

Bray, C., Wright, D., Haupt, S., Thomas, S., Stauss, H., & Zamoyska, R. (2018). Crispr/Cas Mediated Deletion of PTPN22 in Jurkat T Cells Enhances TCR Signaling and Production of IL-2. Frontiers in Immunology, 9(2595).

Britt, D. J., Farías, G. G., Guardia, C. M., & Bonifacino, J. S. (2016). Mechanisms of Polarized Organelle Distribution in Neurons. Frontiers in cellular neuroscience, 10, 88. doi:10.3389/fncel.2016.00088

Busson, S., Dujardin, D., Moreau, A., Dompierre, J., & Mey, J. R. D. (1998). Dynein and dynactin are localized to astral microtubules and at cortical sites in mitotic epithelial cells. Current Biology, 8(9), 541-544.

Carisey, A. F., Mace, E. M., Saeed, M. B., Davis, D. M., & Orange, J. S. (2018). Nanoscale Dynamism of Actin Enables Secretory Function in Cytolytic Cells. Current Biology, 28(4), 489-502.e489.

Carlyle, B. C., Mackie, S., Christie, S., Millar, J. K., & Porteous, D. J. (2011). Co-ordinated action of DISC1, PDE4B and GSK3β in modulation of cAMP signalling. Molecular Psychiatry, 16, 693.

Chaudhuri, A., Wilson, N. S., Yang, B., Paler Martinez, A., Liu, J., Zhu, C., . . . Ashkenazi, A. (2013). Host genetic background impacts modulation of the TLR4 pathway by RON in tissue-associated macrophages. Immunology & Cell Biology, 91(7), 451-460.

Chen, D., & Rothenberg, E. V. (1994). Interleukin 2 transcription factors as molecular targets of cAMP inhibition: delayed inhibition kinetics and combinatorial transcription roles. The Journal of experimental medicine, 179(3), 931-42.

Cherezova, A. L., Negulyaev, J. A., Zenin, V. V., & Semenova, S. B. (2018). Extracellular pH Regulates the Entry of Calcium into Jurkat T-cells. Cell and Tissue Biology, 12(1), 41-47.

Chiang, S. S., Riedel, M. , Schwarz, M. and Mueller, N. (2013), Schizophrenia-specific Th2-shift. Psychiatry Clin Neurosci, 67: 228-236.

Combs, J., Kim, S.J., Tan, S., Ligon, L.A., Holzbaur, E.L., Kuhn, J., & Poenie, M. (2006). Recruitment of dynein to the Jurkat immunological synapse. Proceedings of the National Academy of Sciences of the United States of America, 103(40), 14883-14888.

Comrie, W. A., Babich, A., & Burkhardt, J. K. (2015). F-actin flow drives affinity maturation and spatial organization of LFA-1 at the immunological synapse. The Journal of Cell Biology, 208(4), 475-491.

Comrie, W. A., Li, S., Boyle, S., & Burkhardt, J. K. (2015). The dendritic cell cytoskeleton promotes T cell adhesion and activation by constraining ICAM-1 mobility. The Journal of Cell Biology, 208(4), 457-473.

Courtney, A. H., Lo, W.-L., & Weiss, A. (2018). TCR Signaling: Mechanisms of Initiation and Propagation. Trends in Biochemical Sciences, 43(2), 108-123.

Crispens, C.G. (1973). Some characteristics of strain SJL-JDg mice. Lab Anim Sci, 23(3), 408-413.

Cui, L., Sun, W., Yu, M., Li, N., Guo, L., Gu, H., & Zhou, Y. (2016). Disrupted-in-schizophrenia1 (DISC1) L100P mutation alters synaptic transmission and plasticity in the hippocampus and causes recognition memory deficits. Molecular brain, 9(1), 89. doi:10.1186/s13041-016-0270-yDeringer, M.K. (1970). Mammary tumors in strains BL-LyDe and SWR-LyDe mice. J Natl Cancer Inst, 45(2), 215-218.

Debnath, M., Adaptive Immunity in Schizophrenia: Functional Implications of T Cells in the Etiology, Course and Treatment. J Neuroimmune Pharmacol, 2015. 10(4): p. 610-9.

Desbonnet, L., Cox, R., Tighe, O., Lai, D., Harvey, R. P., Waddington, J. L., & O'Tuathaigh, C. M. P. (2017). Altered cytokine profile, pain sensitivity, and stress responsivity in mice with co-disruption of the developmental genes Neuregulin-1×DISC1. Behavioural Brain Research, 320, 113-118.

Di Donato, N., Chiari, S., Mirzaa, G. M., Aldinger, K., Parrini, E., Olds, C., … Dobyns, W. B. (2017). Lissencephaly: Expanded imaging and clinical classification. American journal of medical genetics. Part A, 173(6), 1473–1488. doi:10.1002/ajmg.a.38245

Dilek, N., Poirier, N., Hulin, P., Coulon, F., Mary, C., Ville, S., . . . Vanhove, B. (2013). Targeting CD28, CTLA-4 and PD-L1 Costimulation Differentially Controls Immune Synapses and Function of Human Regulatory and Conventional T-Cells. PLoS ONE, 8(12), e83139.

Dinarello, C. A. (2009). Interleukin-1β and the Autoinflammatory Diseases. New England Journal of Medicine, 360(23), 2467-2470.

Dinic, J., Riehl, A., Adler, J., & Parmryd, I. (2015). The T cell receptor resides in ordered plasma membrane nanodomains that aggregate upon patching up the receptor. Sci Rep. 5, 10082.

Drexhage, R.C., Hoogenboezem, T.A., Cohen, D., Versnel, M A., Nolen, W.A., van Beveren, N. J.M., & Drexhage, H.A. (2011). An activated set point of T-cell and monocyte inflammatory networks in recent-onset schizophrenia patients involves both pro- and anti-inflammatory forces. International Journal of Neuropsychopharmacology, 14(6), 746-755. doi:10.1017/s1461145710001653

Dustin, M. L. (2008). T-cell activation through immunological synapses and kinapses. Immunological Reviews, 221(1), 77-89.

Dustin, M. L. (2014). The Immunological Synapse. Cancer Immunology Research, 2(11), 1023-1033.

Dustin, M. L., Chakraborty, A. K., and Shaw, A. S. (2010). Understanding the structure and function of the immunological synapse. Cold Spring Harb. Perspect. Biol. 2:a002311.

Dustin, M. L., & Choudhuri, K. (2016). Signaling and Polarized Communication Across the T Cell Immunological Synapse. Annual Review of Cell and Developmental Biology, 32(1), 303-325.

Dustin, M. L., & Colman, D. R. (2002). Neural and Immunological Synaptic Relations. Science, 298(5594), 785-789. doi:10.1126/science.1076386

Feau, S., Schoenberger, S. P., Altman, A., & Becart, S. (2013). SLAT Regulates CD8+ T Cell Clonal Expansion in a Cdc42-and NFAT1-Dependent Manner. J Immunol. 190: 174–183.

Feng, Y., & Walsh, C. A. (2004). Mitotic Spindle Regulation by Nde1 Controls Cerebral Cortical Size. Neuron, 44(2), 279-293.

Filbert, E. L., Le Borgne, M., Lin, J., Heuser, J. E., & Shaw, A. S. (2012). Stathmin regulates microtubule dynamics and microtubule organizing center polarization in activated T cells. Journal of immunology (Baltimore, Md. : 1950), 188(11), 5421–5427. doi:10.4049/jimmunol.1200242

Finetti F, Cassioli C, Baldari CT. Transcellular communication at the immunological synapse: a vesicular traffic-mediated mutual exchange. F1000Res. 2017;6:1880. Published 2017 Oct 24. doi:10.12688/f1000research.11944.1

Finetti, F., Patrussi, L., Masi, G., Onnis, A., Galgano, D., Lucherini, O. M., . . . Baldari, C. T. (2014). Specific recycling receptors are targeted to the immune synapse by the intraflagellar transport system. Journal of Cell Science, 127(9), 1924.

Galgano, D., Onnis, A., Pappalardo, E., Galvagni, F., Acuto, O., & Baldari, C. T. (2017). The T cell IFT20 interactome reveals new players in immune synapse assembly. Journal of cell science, 130(6), 1110–1121. doi:10.1242/jcs.200006

Germain, R.N. (2002). T-cell development and the CD4-CD8 lineage decision. Nat Rev Immunol, 2(5), 309-322.

Gil-Krzewska, A., Saeed, M. B., Oszmiana, A., Fischer, E. R., Lagrue, K., Gahl, W. A., . . . Krzewski, K. (2018). An actin cytoskeletal barrier inhibits lytic granule release from natural killer cells in patients with Chediak-Higashi syndrome. Journal of Allergy and Clinical Immunology, 142(3), 914-927.e916. doi:10.1016/j.jaci.2017.10.040

Gioia, L., Siddique, A., Head, S. R., Salomon, D. R., & Su, A. I. (2018). A genome-wide survey of mutations in the Jurkat cell line. BMC Genomics, 19(1).

Gohla, A., and Bokoch, G.M. (2002) 14-3-3 regulates actin dynamics by stabilizing phosphorylated cofilin. Current Biology, 12(19), 1704-1710.

Golubovskaya, V., & Wu, L. (2016). Different Subsets of T Cells, Memory, Effector Functions, and CAR-T Immunotherapy. Cancers, 8(3), 36.

Gomez, T.S., Kumar, K., Medeiros, R.B., Shimizu, Y., Leibson, P.J., & Billadeau, D.D. (2007). Formins regulate the actin-related protein 2/3 complex-independent polarization of the centrosome to the immunological synapse. Immunity, 26(2), 177-190.

Goodridge, H. S., Reyes, C. N., Becker, C. A., Katsumoto, T. R., Ma, J., Wolf, A. J., . . . Underhill, D. M. (2011). Activation of the innate immune receptor Dectin-1 upon formation of a ‘phagocytic synapse’. Nature, 472, 471.

Grakoui, A., Bromley, S. K., Sumen, C., Davis, M. M., Shaw, A. S., Allen, P. M., & Dustin, M. L. (2015). Pillars Article: The Immunological Synapse: A Molecular Machine Controlling T Cell Activation. Science. 1999. 285: 221–227. The Journal of Immunology, 194(9), 4066-4072.

Gu, F., Wang, L., He, J., Liu, X., Zhang, H., Li, W., . . . Ma, Y. (2014). Girdin, an actin-binding protein, is critical for migration, adhesion, and invasion of human glioblastoma cells. Journal of Neurochemistry, 131(4), 457-469.

Gunter, T. E., & Pfeiffer, D. R. (1990). Mechanisms by which mitochondria transport calcium. American Journal of Physiology-Cell Physiology, 258(5), C755-C786.

Guo, J., Liu, C., Wang, Y., Feng, B., & Zhang, X. (2015). Role of T helper lymphokines in the immune-inflammatory pathophysiology of schizophrenia: Systematic review and meta-analysis. Nordic Journal of Psychiatry, 69(5), 364-372.

Gwack, Y., Feske, S., Srikanth, S., Hogan, P. G., & Rao, A. (2007). Signalling to transcription: Store-operated Ca2+ entry and NFAT activation in lymphocytes. Cell Calcium, 42(2), 145-156.

Harada, Y., Tanaka, Y., Terasawa, M., Pieczyk, M., Habiro, K., Katakai, T., Hanawa-Suetsugu, K., Kukimoto-Niino, M., Nishizaki, T., Shirouzu, M., Duan, X., Uruno, T., Nishikimi, A., Sanematsu, F., Yokoyama, S., Stein, J.V., Kinashi, T., Fukui, Y.

(2012). DOCK8 is a Cdc42 activator critical for interstitial dendritic cell migration during immune responses. Blood. 119: 4451–4461.

Haran-Ghera, N., Ben-Yaakov, M., Peled, A., & Bentwich, Z. (1973). Immune Status of SJL/J Mice in Relation to Age and Spontaneous Tumor Development2. JNCI: Journal of the National Cancer Institute, 50(5), 1227-1235.

Hashimoto-Tane, A., Sakuma, M., Ike, H., Yokosuka, T., Kimura, Y., Ohara, O., & Saito, T. (2016). Micro-adhesion rings surrounding TCR microclusters are essential for T cell activation. The Journal of experimental medicine, 213(8), 1609–1625. doi:10.1084/jem.20151088

Hattori, T., Shimizu, S., Koyama, Y., Yamada, K., Kuwahara, R., Kumamoto, N., . . . Tohyama, M. (2010). DISC1 regulates cell–cell adhesion, cell–matrix adhesion and neurite outgrowth. Molecular Psychiatry, 15, 798. doi:10.1038/mp.2010.60

Hayashi-Takagi, A., Takaki, M., Graziane, N., Seshadri, S., Murdoch, H., Dunlop, A. J., ...Sawa, A. (2010). Disrupted-in-schizophrenia 1 (DISC1) regulates spines of the glutamate synapse via Rac1. Nature Neuroscience, 13(3), 327+.

Hirokawa, N., Niwa, S., and Tinaka, Y. (2010). Molecular motors in neurons: transport mechanisms and roles in brain function, development, and disease. Neuron, 68, 610-638.

Hivroz, C., & Saitakis, M. (2016). Biophysical Aspects of T Lymphocyte Activation at the Immune Synapse. Frontiers in Immunology, 7(46).

Hogg, N., Patzak, I., & Willenbrock, F. (2011). The insider's guide to leukocyte integrin signalling and function. Nat Rev Immunol, 11(6), 416-426.

Hui, K. L., Balagopalan, L., Samelson, L. E., & Upadhyaya, A. (2015). Cytoskeletal forces during signaling activation in Jurkat T-cells. Molecular Biology of the Cell, 26(4), 685-695.

Huse, M., Quann, E. J., & Davis, M. M. (2008). Shouts, whispers and the kiss of death: directional secretion in T cells. Nature Immunology, 9, 1105.

Hutchings, P. R., Varey, A. M., & Cooke, A. (1986). Immunological defects in SJL mice. Immunology, 59(3), 445–450.

Irvine D.J., Purbhoo M.A., Krogsgaard M., Davis M.M. (2002) Direct observation of ligand recognition by T cells. Nature. 419: 845–849.

James, R., Adams, R. R., Christie, S., Buchanan, S. R., Porteous, D. J., & Millar, J. K. (2004). Disrupted in Schizophrenia 1 (DISC1) is a multicompartmentalized protein that predominantly localizes to mitochondria. Molecular and Cellular Neuroscience, 26(1), 112-122.

Janssen, E., Tohme, M., Hedayat, M., Leick, M., Kumari, S., Ramesh, N., . . . Geha, R. S. (2016). A DOCK8-WIP-WASp complex links T cell receptor to the actin

cytoskeleton. Journal of Clinical Investigation, 126(10), 3837-3851. doi:http://dx.doi.org.ezproxy.lib.utexas.edu/10.1172/JCI85774

Jane-wit, D., Yu, M., Edling, A. E., Kataoka, S., Johnson, J. M., Stull, L. B., . . . Tuohy, V. K. (2002). A Novel Class II-Binding Motif Selects Peptides That Mediate Organ-Specific Autoimmune Disease in SWXJ, SJL/J, and SWR/J Mice. The Journal of Immunology, 169(11), 6507-6514.

Jankowska, K. I., & Burkhardt, J. K. (2017). Analyzing Actin Dynamics at the Immunological Synapse. Methods in molecular biology (Clifton, N.J.), 1584, 7-29

Jankowska, K. I., Williamson, E. K., Roy, N. H., Blumenthal, D., Chandra, V., Baumgart, T., & Burkhardt, J. K. (2018). Integrins Modulate T Cell Receptor Signaling by Constraining Actin Flow at the Immunological Synapse. Frontiers in Immunology, 9(25).

Jiang, P., Enomoto, A., Jijiwa, M., Kato, T., Hasegawa, T., Ishida, M., . . . Takahashi, M. (2008). An Actin-Binding Protein Girdin Regulates the Motility of Breast Cancer Cells. Cancer Research, 68(5), 1310-1318.

Jo, E.-K., Wang, H., & Rudd, C. E. (2005). An essential role for SKAP-55 in LFA-1 clustering on T cells that cannot be substituted by SKAP-55R. The Journal of Experimental Medicine, 201(11), 1733-1739.

Joseph, N., Reicher, B., & Barda-Saad, M. (2014). The calcium feedback loop and T cell activation: How cytoskeleton networks control intracellular calcium flux. Biochimica et Biophysica Acta (BBA) - Biomembranes, 1838(2), 557-568.

Junker, C., & Hoth, M. (2011). Immune synapses: mitochondrial morphology matters. Embo j, 30(7), 1187-1189. doi:10.1038/emboj.2011.72

Kamiya, A., Kubo, K., Tomoda, T., Takaki, M., Youn, R., Ozeki, Y., . . . Sawa, A. (2005). A schizophrenia-associated mutation of DISC1 perturbs cerebral cortex development. Nature Cell Biology, 7(12), 1167-78.

Khan, A., Bose, C., Yam, L., Soloski, M., & Rupp, F. (2001). Physiological Regulation of the Immunological Synapse by Agrin. Science, 292(5522), 1681-1686

Kim, E.-M., Bae, Y. M., Choi, M.-H., & Hong, S.-T. (2012). Cyst formation, increased anti-inflammatory cytokines and expression of chemokines support for Clonorchis sinensis infection in FVB mice. Parasitology International, 61(1), 124-129.

Kim S, Dynlacht BD. (2013) Assembling a primary cilium. Curr Opin Cell Biol. 25(4):506-11.

Kim, S., Zaghloul, N. A., Bubenshchikova, E., Oh, E. C., Rankin, S., Katsanis, N., Obara, T. and Tsiokas, L. (2011). Nde1-mediated inhibition of ciliogenesis affects cell cycle re-entry. Nat. Cell Biol. 13, 351-360.

Kim, Y.K., Myint, A.M., Lee, B.H., Han, C.S., Lee, H.J., Kim, D.J., & Leonard, B.E. (2004). Th1, Th2 and Th3 cytokine alteration in schizophrenia. Progress in Neuro-Psychopharmacology and Biological Psychiatry, 28(7), 1129-1134. doi:http://dx.doi.org/10.1016/j.pnpbp.2004.05.047

Kuhn, J. R., & Poenie, M. (2002). Dynamic Polarization of the Microtubule Cytoskeleton during CTL-Mediated Killing. Immunity, 16(1), 111-121

Kumari, S., Depoil, D., Martinelli, R., Judokusumo, E., Carmona, G., Gertler, F. B., . . . Dustin, M. L. (2015). Actin foci facilitate activation of the phospholipase C-γ in primary T lymphocytes via the WASP pathway. eLife, 4, e04953.

Kumari, S., Mak, M., Poh, Y., Tohme, M., Watson, N., Melo, M., . . . Irvine, D. (2018). Cytoskeletal tension actively sustains the T cell immunological synapse. bioRxiv, 437236

Kuokkanen, E., Sustar, V., & Matilla, P.K. (2015). Molecular control of B cell activation and immunological synapse formation. Traffic. 16(4), 311-326.

Lam, C., Vergnolle, M. A. S., Thorpe, L., Woodman, P. G., & Allan, V. J. (2010). Functional interplay between LIS1, NDE1 and NDEL1 in dynein-dependent organelle positioning. Journal of Cell Science, 123(2), 202-212.

Ledderose, C., Bao, Y., Lidicky, M., Zipperle, J., Li, L., Strasser, K., Shapiro, N. I., … Junger, W. G. (2014). Mitochondria are gate-keepers of T cell function by producing the ATP that drives purinergic signaling. The Journal of biological chemistry, 289(37), 25936-45.

Li, C., Inglis, P. N., Leitch, C. C., Efimenko, E., Zaghloul, N. A., Mok, C. A., . . . Leroux, M. R. (2008). An Essential Role for DYF-11/MIP-T3 in Assembling Functional Intraflagellar Transport Complexes. PLOS Genetics, 4(3), e1000044.

Lilja, J., & Ivaska, J. (2018). Integrin activity in neuronal connectivity. Journal of Cell Science, 131(12), jcs212803. doi:10.1242/jcs.212803

Lin, C.-C., & Edelson, B. T. (2017). New Insights into the Role of IL-1β in Experimental Autoimmune Encephalomyelitis and Multiple Sclerosis. The Journal of Immunology, 198(12), 4553-4560.

Lindsten, T., Lee, K. P., Harris, E. S., Petryniak, B., Craighead, N., Reynolds, P. J., . . . Gray, G. S. (1993). Characterization of CTLA-4 structure and expression on human T cells. The Journal of Immunology, 151(7), 3489-3499.

Lipina, T. V., Zai, C., Hlousek, D., Roder, J. C., & Wong, A. H. C. (2013). Maternal Immune Activation during Gestation Interacts with Disc1 Point Mutation to Exacerbate Schizophrenia-Related Behaviors in Mice. The Journal of Neuroscience, 33(18), 7654-7666.

Lipina, T. V., & Roder, J. C. (2014). Disrupted-In-Schizophrenia-1 (DISC1) interactome and mental disorders: Impact of mouse models. Neuroscience & Biobehavioral Reviews, 45, 271-294.

Litman GW, Cooper MD: Why study the evolution of immunity? Nat Immunol 8: 547–548, 2007

Liu, J., Liu, R., Gray, P., Liu, Z., Cui, X., Li, G., & Liu, Z. (2017). Development of a luciferase reporter Jurkat cell line under the control of endogenous interleukin-2 promoter. Journal of Immunological Methods, 451, 48-53.

Liu, L., Lu, J., Li, X., Wu, A., Wu, Q., Zhao, M., . . . Song, H. (2018). The LIS1/NDE1 Complex Is Essential for FGF Signaling by Regulating FGF Receptor Intracellular Trafficking. Cell Reports, 22(12), 3277-3291.

Liu, X., & Hajnoczky, G. (2009). Ca2+-dependent regulation of mitochondrial dynamics by the Miro-Milton complex. Int J Biochem Cell Biol, 41(10), 1972-1976. doi:10.1016/j.biocel.2009.05.013

López-Sánchez, I., Garcia-Marcos, M., Mittal, Y., Aznar, N., G Farquhar, M., & Ghosh, P. (2013). Protein kinase C-theta (PKC) phosphorylates and inhibits the guanine exchange factor, GIV/Girdin. Proceedings of the National Academy of Sciences of the United States of America, 110. doi:10.1073/pnas.1303392110

Mace, E. M., Zhang, J., Siminovitch, K. A., & Takei, F. (2010). Elucidation of the integrin LFA-1–mediated signaling pathway of actin polarization in natural killer cells. Blood, 116(8), 1272-1279.

Mace, E. M., & Orange, J. S. (2014). Lytic immune synapse function requires filamentous actin deconstruction by Coronin 1A. Proceedings of the National Academy of Sciences, 111(18), 6708-6713.

Mahler, J.F., Stokes, W., Mann, P.C., Takaoka, M., & Maronpot, R.R. (1996). Spontaneous lesions in aging FVB/N mice. Toxicol Pathol, 24(6), 710-716.

Mao, Y., Ge, X., Frank, C. L., Madison, J. M., Koehler, A. N., Doud, M. K., . . . Tsai, L. H. (2009). Disrupted in schizophrenia 1 regulates neuronal progenitor proliferation via modulation of GSK3beta/beta-catenin signaling. Cell, 136(6), 1017-1031. doi:10.1016/j.cell.2008.12.044

Marley, A.; von Zastrow, M. DISC1 regulates primary cilia that display specific dopamine receptors. PLoS ONE 2010, 5, e10902.

Marraffini, L. A. (2015). CRISPR-Cas immunity in prokaryotes. Nature, 526, 55.

Martín-Cófreces, N. B., Alarcón, B., & Sánchez-Madrid, F. (2011). Tubulin and actin interplay at the T cell and antigen-presenting cell interface. Frontiers in Immunology, 2, 24-24. doi:10.3389/fimmu.2011.00024

Martín-Cófreces, N. B., Baixauli, F., & Sánchez-Madrid, F. (2014). Immune synapse: conductor of orchestrated organelle movement. Trends Cell Biol, 24(1), 61-72.

Martín-Cófreces, N. B., Robles-Valero, J., Cabrero, J. R., Mittelbrunn, M., Gordón-Alonso, M., Sung, C.-H., . . . Sánchez-Madrid, F. (2008). MTOC translocation modulates IS formation and controls sustained T cell signaling. The Journal of Cell Biology, 182(5), 951-962.

Martín-Cófreces, N. B., & Sánchez-Madrid, F. (2018). Sailing to and Docking at the Immune Synapse: Role of Tubulin Dynamics and Molecular Motors. Frontiers in Immunology, 9(1174).

Martínez-Martín N, Fernández-Arenas E, Cemerski S, et al. T cell receptor internalization from the immunological synapse is mediated by TC21 and RhoG GTPase-dependent phagocytosis. Immunity. 2011;35(2):208-22.

Matanis, T., Akhmanova, A., Wulf, P., Del Nery, E., Weide, T., Stepanova, T., . . . Hoogenraad, C. C. (2002). Bicaudal-D regulates COPI-independent Golgi–ER transport by recruiting the dynein–dynactin motor complex. Nature Cell Biology, 4, 986.

Mattis, A. E., G. Bernhardt, M. Lipp, and R. Fo¨rster. (1997). Analyzing cytotoxic T lymphocyte activity: a simple and reliable flow cytometry-based assay. J. Immunol. Methods 204: 135–142.

McKenney, R. J., Vershinin, M., Kunwar, A., Vallee, R. B., & Gross, S. P. (2010). LIS1 and NudE Induce a Persistent Dynein Force-Producing State. Cell, 141(2), 304-314.

Ménasché, G., Kliche, S., Chen, E. J., Stradal, T. E., Schraven, B., & Koretzky, G. (2007). RIAM links the ADAP/SKAP-55 signaling module to Rap1, facilitating T-cell-receptor-mediated integrin activation. Molecular and cellular biology, 27(11), 4070–4081. doi:10.1128/MCB.02011-06

Mentlik, A. N., Sanborn, K. B., Holzbaur, E. L., & Orange, J. S. (2010). Rapid Lytic Granule Convergence to the MTOC in Natural Killer Cells Is Dependent on Dynein But Not Cytolytic Commitment. Molecular Biology of the Cell, 21(13), 2241-2256.

Mittelbrunn, M., Gutiérrez-Vázquez, C., Villarroya-Beltri, C., González, S., Sánchez-Cabo, F., González, M. Á., . . . Sánchez-Madrid, F. (2011). Unidirectional transfer of microRNA-loaded exosomes from T cells to antigen-presenting cells. Nature Communications, 2, 282.

Miyoshi, K., Asanuma, M., Miyazaki, I., Diaz-Corrales, F. J., Katayama, T., Tohyama, M., & Ogawa, N. (2004). DISC1 localizes to the centrosome by binding to kendrin. Biochemical and Biophysical Research Communications, 317(4), 1195-1199.

Monda, J. K., & Cheeseman, I. M. (2018). Nde1 promotes diverse dynein functions through differential interactions and exhibits an isoform-specific proteasome association. Molecular biology of the cell, 29(19), 2336–2345. doi:10.1091/mbc.E18-07-0418

Monks, C. R. F., Freiberg, B. A., Kupfer, H., Sciaky, N., & Kupfer, A. (2015). Pillars Article: Three-Dimensional Segregation of Supramolecular Activation Clusters in T cells. Nature. 1998. 395: 82–86. The Journal of Immunology, 194(9), 4061-4065.

Morlino G., Barreiro O., Baixauli F., Robles-Valero J., González-Granado J.M., Villa-Bellosta R., Cuenca J., Sánchez-Sorzano C.O., Veiga E., Martín-Cófreces N.B., et al. (2014) Miro-1 links mitochondria and microtubule Dynein motors to control lymphocyte migration and polarity. Mol. Cell. Biol. 2014;34:1412–1426.

Nakata, K., Lipska, B. K., Hyde, T. M., Ye, T., Newburn, E. N., Morita, Y., . . . Kleinman, J. E. (2009). DISC1 splice variants are upregulated in schizophrenia and associated with risk polymorphisms. Proceedings of the National Academy of Sciences, 106(37), 15873-15878.

Nath, S., Christian, L., Tan, S.Y., Ki, S., Ehrlich, L.I.R., & Poenie, M. (2016). Dynein Separately Partners with NDE1 and Dynactin To Orchestrate T Cell Focused Secretion. The Journal of Immunology. doi:10.4049/jimmunol.1600180

Nikkilä, H. V., Müller, K., Ahokas, A., Rimón, R., & Andersson, L. C. (2001). Increased frequency of activated lymphocytes in the cerebrospinal fluid of patients with acute schizophrenia. Schizophrenia Research, 49(1–2), 99-105. doi:http://dx.doi.org/10.1016/S0920-9964(99)00218-2

Norcross, M. A. (1984). A synaptic basis for T-lymphocyte activation. Annales d'immunologie, 135D(2), 113-134.

Norkett, R., Modi, S., Birsa, N., Atkin, T. A., Ivankovic, D., Pathania, M., . . . Kittler, J. T. (2016). DISC1-dependent Regulation of Mitochondrial Dynamics Controls the Morphogenesis of Complex Neuronal Dendrites. J Biol Chem, 291(2), 613-629. doi:10.1074/jbc.M115.699447

Nurmi, S. M., Gahmberg, C. G., & Fagerholm, S. C. (2006). 14-3-3 proteins bind both filamin and alphaLbeta2 integrin in activated T cells. Ann N Y Acad Sci, 1090, 318-325. doi:10.1196/annals.1378.035

Obsil, T., & Obsilova, V. (2011). Structural basis of 14-3-3 protein functions. Semin Cell Dev Biol, 22(7), 663-672. doi:10.1016/j.semcdb.2011.09.001

Orange, J. S., Harris, K. E., Andzelm, M. M., Valter, M. M., Geha, R. S., & Strominger, J. L. (2003). The mature activating natural killer cell immunologic synapse is formed in distinct stages. Proceedings of the National Academy of Sciences of the United States of America, 100(24), 14151–14156. doi:10.1073/pnas.1835830100

Orange J. S. (2008). Formation and function of the lytic NK-cell immunological synapse. Nature reviews. Immunology, 8(9), 713–725. doi:10.1038/nri2381

Owens, M.H., & Bonavida, B. (1976). Immune Functions Characteristic of SJL/J Mice and Their Association with Age and Spontaneous Reticulum Cell Sarcoma. Cancer Research, 36(3), 1077-1083.

Ozeki, Y., Tomoda, T., Kleiderlein, J., Kamiya, A., Bord, L., Fujii, K., . . . Sawa, A. (2003). Disrupted-in-Schizophrenia-1 (DISC-1): Mutant truncation prevents binding to NudE-like (NUDEL) and inhibits neurite outgrowth. Proceedings of the National Academy of Sciences, 100(1), 289-294.

Pandarakalam, J.P. (2013). Is autoimmunity involved in the aetiology of schizophrenia? Progress in Neurology and Psychiatry, 17(1), 24-28. doi:10.1002/pnp.267

Papa, I., & Vinuesa, C. G. (2018). Synaptic Interactions in Germinal Centers. Frontiers in immunology, 9, 1858. doi:10.3389/fimmu.2018.01858

Pauker, M. H., Reicher, B., Fried, S., Perl, O., & Barda-Saad, M. (2011). Functional Cooperation between the Proteins Nck and ADAP Is Fundamental for Actin Reorganization. Molecular and Cellular Biology, 31(13), 2653-2666.

Pistillo, M. P., Tazzari, P. L., Palmisano, G. L., Pierri, I., Bolognesi, A., Ferlito, F., . . . Ferrara, G. B. (2003). CTLA-4 is not restricted to the lymphoid cell lineage and can function as a target molecule for apoptosis induction of leukemic cells. Blood, 101(1), 202-209.

Quintana, A., Müller, M., Frausto, R. F., Ramos, R., Getts, D. R., Sanz, E., . . . Campbell, I. L. (2009). Site-Specific Production of IL-6 in the Central Nervous System Retargets and Enhances the Inflammatory Response in Experimental Autoimmune Encephalomyelitis. The Journal of Immunology, 183(3), 2079-2088.

Rajan, A. J., Asensio, V. C., Campbell, I. L., & Brosnan, C. F. (2000). Experimental Autoimmune Encephalomyelitis on the SJL Mouse: Effect of γδ T Cell Depletion on Chemokine and Chemokine Receptor Expression in the Central Nervous System. The Journal of Immunology, 164(4), 2120-2130.

Randall, K.L., Chan, S.S., Ma, C.S., Fung, I., Mei, Y., Yabas, M., Tan, A., Arkwright, P.D., Al Suwairi, W., Lugo Reyes, S.O., Yamazaki-Nakashimada, M.A., Garcia-Cruz Mde, L., Smart, J.M., Picard, C., Okada, S., Jouanguy, E., Casanova, J.L., Lambe, T., Cornall, R.J., Russell, S., Oliaro, J., Tangye, S.G., Bertram, E.M., Goodnow, C.C. (2011) DOCK8 deficiency impairs CD8 T cell survival and function in humans and mice. J Exp Med. 208: 2305–2320.

Reck-Peterson, S. L., Redwine, W. B., Vale, R. D., & Carter, A. P. (2018). The cytoplasmic dynein transport machinery and its many cargoes. Nature Reviews Molecular Cell Biology, 19(6), 382-398.

Ritchie, D., & Clapcote, S. (2013). Disc1 deletion is present in Swiss-derived inbred mouse strains: implications for transgenic studies of learning and memory. Laboratory Animals, 47(3), 162–167.

Ritter, A. T., Angus, K. L., & Griffiths, G. M. (2013). The role of the cytoskeleton at the immunological synapse. Immunological Reviews, 256(1), 107-117. doi:10.1111/imr.12117

Ritter, A. T., Kapnick, S. M., Murugesan, S., Schwartzberg, P. L., Griffiths, G. M., & Lippincott-Schwartz, J. (2017). Cortical actin recovery at the immunological synapse leads to termination of lytic granule secretion in cytotoxic T lymphocytes. Proceedings of the National Academy of Sciences, 114(32), E6585-E6594.

Ritter, Alex T., Asano, Y., Stinchcombe, Jane C., Dieckmann, N. M. G., Chen, B.-C., Gawden-Bone, C., . . . Griffiths, Gillian M. (2015). Actin Depletion Initiates Events Leading to Granule Secretion at the Immunological Synapse. Immunity, 42(5), 864-876.

Ross, S. H., & Cantrell, D. A. (2018). Signaling and Function of Interleukin-2 in T Lymphocytes. Annual review of immunology, 36, 411–433. doi:10.1146/annurev-immunol-042617-053352

Sanui, T., Inayoshi, A., Noda, M., Iwata, E., Oike, M., Sasazuki, T., Fukui, Y. (2003). DOCK2 is essential for antigen-induced translocation of TCR and lipid rafts, but not PKC-theta and LFA-1, in T cells. Immunity, 19: 119–129.

Schroeder CM, & Vale RD. (2016). Assembly and activation of dynein-dynactin by the cargo adaptor protein Hook3. J Cell Biol. 214(3):309-318.

Schürpf, T., & Springer, T. A. (2011). Regulation of integrin affinity on cell surfaces. The EMBO Journal, 30(23), 4712-4727.

Schwindling, C., Quintana, A., Krause, E., & Hoth, M. (2010). Mitochondria Positioning Controls Local Calcium Influx in T Cells. The Journal of Immunology, 184(1), 184-190.

Segal, M., Soifer, I., Petzold, H., Howard, J., Elbaum, M., & Reiner, O. (2012). Ndel1-derived peptides modulate bidirectional transport of injected beads in the squid giant axon. Biology Open, 1(3), 220-231.

Shah, K., & Rossie, S. (2018). Tale of the Good and the Bad Cdk5: Remodeling of the Actin Cytoskeleton in the Brain. Molecular Neurobiology, 55(4), 3426-3438.

Short B, Preisinger C , Schaletzky J , Kopajtich R , & Barr FA. (2002). The Rab6 GTPase regulates recruitment of the dynactin complex to Golgi membranes. Curr Biol. 12(20):1792-1795.

Simões, P. A., Celestino, R., Carvalho, A. X., & Gassmann, R. (). NudE regulates dynein at kinetochores but is dispensable for other dynein functions in the C. elegans early embryo. Journal of cell science, 131(1), jcs212159. doi:10.1242/jcs.212159

Simonson, W. T. N., Franco, S. J., & Huttenlocher, A. (2006). Talin1 Regulates TCR-Mediated LFA-1 Function. The Journal of Immunology, 177(11), 7707-7714.

Skålhegg, B. S., Landmark, B. F., Døskeland, S. O., Hansson, V., Lea, T., & Jahnsen, T. (1992). Cyclic AMP-dependent protein kinase type I mediates the inhibitory effects of 3',5'-cyclic adenosine monophosphate on cell replication in human T lymphocytes. Journal of Biological Chemistry, 267(22), 15707-15714.

Small, J. V., Stradal, T., Vignal, E., & Rottner, K. (2002). The lamellipodium: where motility begins. Trends Cell Biol, 12(3), 112-120. doi:https://doi.org/10.1016/S0962-8924(01)02237-1

Soares, D. C., Carlyle, B. C., Bradshaw, N. J., & Porteous, D. J. (2011). DISC1: Structure, Function, and Therapeutic Potential for Major Mental Illness. ACS chemical neuroscience, 2(11), 609–632. doi:10.1021/cn200062k

Sperner-Unterweger, B., et al., Is schizophrenia linked to alteration in cellular immunity? Schizophr Res, 1989. 2(4-5): p. 417-21.

Steblyanko, M., Au - Anikeeva, N., Au - Buggert, M., Au - Betts, M. R., & Au - Sykulev, Y. (2018). Assessment of the Synaptic Interface of Primary Human T Cells from Peripheral Blood and Lymphoid Tissue. JoVE(137), e58143.

Steinecke, A., Gampe, C., Nitzsche, F., & Bolz, J. (2014). DISC1 knockdown impairs the tangential migration of cortical interneurons by affecting the actin cytoskeleton. Frontiers in Cellular Neuroscience, 8(190).

Stinchcombe, J. C., Majorovits, E., Bossi, G., Fuller, S., & Griffiths, G. M. (2006). Centrosome polarization delivers secretory granules to the immunological synapse. Nature, 443, 462.

Stinchcombe, J. C., Randzavola, L. O., Angus, K. L., Mantell, J. M., Verkade, P., & Griffiths, G. M. (2015). Mother Centriole Distal Appendages Mediate Centrosome Docking at the Immunological Synapse and Reveal Mechanistic Parallels with Ciliogenesis. Current biology: CB, 25(24), 3239-3244.

Stinchcombe, J. C., Salio, M., Cerundolo, V., Pende, D., Arico, M., & Griffiths, G. M. (2011). Centriole polarisation to the immunological synapse directs secretion from cytolytic cells of both the innate and adaptive immune systems. BMC biSuzuki, J., Yamasaki, S., Wu, J., Koretzky, G. A., & Saito, T. (2007). The actin cloud induced by LFA-1–mediated outside-in signals lowers the threshold for T-cell activation. Blood, 109(1), 168-175. Accessed June 13, 2019.ology, 9, 45. doi:10.1186/1741-7007-9-45

Suzuki, J., Yamasaki, S., Wu, J., Koretzky, G. A., & Saito, T. (2007). The actin cloud induced by LFA-1–mediated outside-in signals lowers the threshold for T-cell activation. Blood, 109(1), 168-175. Accessed June 13, 2019.

Tamir, A., & Isakov, N. (1994). Cyclic AMP inhibits phosphatidylinositol-coupled and -uncoupled mitogenic signals in T lymphocytes. Evidence that cAMP alters PKC-induced transcription regulation of members of the jun and fos family of genes. The Journal of Immunology, 152(7), 3391-3399.

Tanaka, T., Narazaki, M., & Kishimoto, T. (). IL-6 in inflammation, immunity, and disease. Cold Spring Harbor perspectives in biology, 6(10), a016295. doi:10.1101/cshperspect.a016295

Tang B. L. (2015). MIRO GTPases in Mitochondrial Transport, Homeostasis and Pathology. Cells, 5(1), 1. doi:10.3390/cells5010001

Tang, W., Zhang, Y., Xu, W., Harden, T. K., Sondek, J., Sun, L., . . . Wu, D. (2011). A PLCβ/PI3Kγ-GSK3 Signaling Pathway Regulates Cofilin Phosphatase Slingshot2 and Neutrophil Polarization and Chemotaxis. Developmental Cell, 21(6), 1038-1050. doi:http://dx.doi.org/10.1016/j.devcel.2011.10.023

Thauland, T. J., & Parker, D. C. (2010). Diversity in immunological synapse structure. Immunology, 131(4), 466-472.

Taya, S., Shinoda, T., Tsuboi, D., Asaki, J., Nagai, K., Hikita, T., . . . Kaibuchi, K. (2007). DISC1 regulates the transport of the NUDEL/LIS1/14-3-3epsilon complex through kinesin-1. J Neurosci, 27(1), 15-26. doi:10.1523/jneurosci.3826-06.2006

Taylor, M. S., Devon, R. S., Millar, J. K., & Porteous, D. J. (2003). Evolutionary constraints on the Disrupted in Schizophrenia locus. Genomics, 81(1), 67-77.

Thurston, S.F., Kulacz, W.A., Shaikh, S., Lee, J.M., & Copeland, J.W. (2012). The ability to induce microtubule acetylation is a general feature of formin proteins. PLoS One, 7(10), e48041.

Topham, N. J., & Hewitt, E. W. (2009). Natural killer cell cytotoxicity: how do they pull the trigger?. Immunology, 128(1), 7–15. doi:10.1111/j.1365-2567.2009.03123.x

Tran, G. T., Wilcox, P. L., Dent, L. A., Robinson, C. M., Carter, N., Verma, N. D., . . . Hodgkinson, S. J. (2017). Interleukin-5 Mediates Parasite-Induced Protection against Experimental Autoimmune Encephalomyelitis: Association with Induction of Antigen-Specific CD4+CD25+ T Regulatory Cells. Frontiers in Immunology, 8(1453).

Tropea, D., Hardingham, N., Millar, K., & Fox, K. (2018). Mechanisms underlying the role of DISC1 in synaptic plasticity. The Journal of physiology, 596(14), 2747-2771.

Tskivitaria-Fuller, I., Seth, A., Mistry, N., Gu, H., Rosen, M.K., & Wulfing, C. (2006). Specific patterns of Cdc42 activity are related to distinct elements of T cell polarization. Journal of immunology, 177(3), 1708-1720.

Tsun A, Qureshi I, Stinchcombe JC, et al. Centrosome docking at the immunological synapse is controlled by Lck signaling. J Cell Biol. 2011;192(4):663-74.

Turner, O. C., Keefe, R. G., Sugawara, I., Yamada, H., & Orme, I. M. (2003). SWR mice are highly susceptible to pulmonary infection with Mycobacterium tuberculosis. Infection and immunity, 71(9), 5266–5272. doi:10.1128/iai.71.9.5266-5272.2003

Ueda, H., Zhou, J., Xie, J., & Davis, M. M. (2015). Distinct Roles of Cytoskeletal Components in Immunological Synapse Formation and Directed Secretion. The Journal of Immunology, 195(9), 4117-4125.

Urlaub, D., Höfer, K., Müller, M.-L., & Watzl, C. (2017). LFA-1 Activation in NK Cells and Their Subsets: Influence of Receptors, Maturation, and Cytokine Stimulation. The Journal of Immunology, 198(5), 1944-1951.

Vallee, R. B., McKenney, R. J., & Ori-McKenney, K. M. (2012). Multiple modes of cytoplasmic dynein regulation. Nature Cell Biology, 14, 224.

van Spronsen, M., Mikhaylova, M., Lipka, J., Schlager, Max A., van den Heuvel, Dave J., Kuijpers, M., . . . Hoogenraad, Casper C. (2013). TRAK/Milton Motor-Adaptor Proteins Steer Mitochondrial Trafficking to Axons and Dendrites. Neuron, 77(3), 485-502.

Venkatesh D. (2017). Primary cilia. Journal of oral and maxillofacial pathology : JOMFP, 21(1), 8-10.

Vivar, O. I., Masi, G., Carpier, J.-M., Magalhaes, J. G., Galgano, D., Pazour, G. J., . . . Baldari, C. T. (2016). IFT20 controls LAT recruitment to the immune synapse and T-cell activation in vivo. Proceedings of the National Academy of Sciences, 113(2), 386-391.

Vogel, S., Pavin, N., Maghelli, N., Julicher, F., & Tolic´-Nørrelykke, I. (2009). Self-organization of dynein motors generates meiotic nuclear oscillations. PLoS Biol. 7: e1000087.

Wang, H., Wei, B., Bismuth, G., & Rudd, C. E. (2009). SLP-76-ADAP adaptor module regulates LFA-1 mediated costimulation and T cell motility. Proceedings of the National Academy of Sciences, 106(30), 12436-12441.

Wang, X., Enomoto, A., Weng, L., Haga, H., Ishida, S., & Takahashi, M. (2018). Abstract 3160: The actin-binding protein Girdin/GIV regulates collective cancer cell migration by controlling cell adhesion and cytoskeletal organization. Cancer Research, 78(13 Supplement), 3160-3160.

Webb, S. R., & Gascoigne, N. R. J. (1994). T-cell activation by superantigens. Current Opinion in Immunology, 6(3), 467-475. doi:https://doi.org/10.1016/0952-7915(94)90129-5

Wehbi, V. L., & Taskén, K. (2016). Molecular Mechanisms for cAMP-Mediated Immunoregulation in T cells - Role of Anchored Protein Kinase A Signaling Units. Frontiers in immunology, 7, 222.

Wi, S. M., Min, Y., & Lee, K.-Y. (2016). Charged MVB protein 5 is involved in T-cell receptor signaling. Experimental &Amp; Molecular Medicine, 48, e206.

Wong, T., Hildebrandt, M. A., Thrasher, S. M., Appleton, J. A., Ahima, R. S., & Wu, G. D. (2007). Divergent Metabolic Adaptations to Intestinal Parasitic Nematode

Infection in Mice Susceptible or Resistant to Obesity. Gastroenterology, 133(6), 1979-1988.

Woods, L.C., Berbusse, G.W., & Naylor, K. (2016). Microtubules Are Essential for Mitochondrial Dynamics–Fission, Fusion, and Motility–in Dictyostelium discoideum. Frontiers in Cell and Developmental Biology, 4(19). doi:10.3389/fcell.2016.00019

Wynshaw-Boris, A. (2007), Lissencephaly and LIS1: insights into the molecular mechanisms of neuronal migration and development. Clinical Genetics, 72: 296-304

Yamamoto, A., West, R., McIntosh, J., & Hiraoka, Y. (1999). A cytoplasmic dynein heavy chain is required for oscillatory nuclear movement of meiotic prophase and efficient meiotic recombination in fission yeast. J. Cell Biol. 145:1233–1249.

Yamamoto, A., C. Tsutsumi, H. Kojima, K. Oiwa, and Y. Hiraoka. 2001. Dynamic behavior of microtubules during dynein-dependent nuclear migrations of meiotic prophase in fission yeast. Mol. Biol. Cell 12: 3933–3946.

Yatim, K. M., & Lakkis, F. G. (2015). A Brief Journey through the Immune System. Clinical Journal of the American Society of Nephrology, 10(7), 1274-1281.

Ye, F., Kang, E., Yu, C., Qian, X., Jacob, F., Yu, C., . . . Zhang, M. (2017). DISC1 Regulates Neurogenesis via Modulating Kinetochore Attachment of Ndel1/Nde1 during Mitosis. Neuron, 96(5), 1041-1054.e1045.

Yeh, E., Skibbens, R., Cheng, J., Salmon, E., & Bloom, K. (1995). Spindle dynamics and cell cycle regulation of dynein in the budding yeast, Saccharomyces cerevisiae. J. Cell Biol. 130: 687–700.

Yi, J., Wu, X. S., Crites, T., & Hammer, J. A. (2012). Actin retrograde flow and actomyosin II arc contraction drive receptor cluster dynamics at the immunological synapse in Jurkat T cells. Molecular Biology of the Cell, 23(5), 834-852.

Zhu, J., Yamane, H., & Paul, W. E. (2010). Differentiation of effector CD4 T cell populations (*). Annual review of immunology, 28, 445–489. doi:10.1146/annurev-immunol-030409-101212